14-10

RTD-TDR-63-4044
PART I

PRESSURE MEASUREMENTS FOR MACH 8 FLOWS OVER EXPANSION CORNERS AND RAMPS ON AN INTERNALLY COOLED MODEL

PART I: EXPANSION CORNER FLOWS
Part of an Investigation of Hypersonic Flow Separation and Control Characteristics

TECHNICAL DOCUMENTARY REPORT No. RTD-TDR-63-4044, PART I

OCTOBER 1963

FLIGHT CONTROL DIVISION
AIR FORCE FLIGHT DYNAMICS LABORATORY
RESEARCH AND TECHNOLOGY DIVISION
AIR FORCE SYSTEMS COMMAND
WRIGHT-PATTERSON AIR FORCE BASE, OHIO

Project No. 8219, Task No. 821902

(Prepared under Contract No. AF 33(616)-8130 by the Research Department of Grumann Aircraft Engineering Corporation, Bethpage, New York
Author: Louis G. Kaufman II)

431280

NOTICES

When Government drawings, specifications, or other data are used for any purpose other than in connection with a definitely related Government procurement operation, the United States Government thereby incurs no responsibility nor any obligation whatsoever; and the fact that the Government may have formulated furnished, or in any way supplied the said drawings, specifications, or other data, is not to be regarded by implication or otherwise as in any manner licensing the holder or any other person or corporation, or conveying any rights or permission to manufacture, use, or sell any patented invention that may in any way be related thereto.

Qualified requsters may obtain copies of this report from the Defense Documentation Center (DDC), (formerly ASTIA), Cameron Station, Bldg. 5, 5010 Duke Street, Alexandria, Virginia, 22314.

This report has been released to the Office of Technical Services, U.S. Department of Commerce, Washington 25, D. C., for sale to the general public.

Copies of this report should not be returned to the Research and Technology Division, Wright-Patterson Air Force Base, Ohio, unless return is required by security considerations, contractual obligations, or notice on a specific document.

500 - February 1964 - 162-26-478

FOREWORD

This entire report, written in three parts under separate covers, presents the results of a portion of the experimental program for the investigation of hypersonic flow separation and control characteristics being conducted by the Research Department of Grumman Aircraft Engineering Corporation, Bethpage, New York. Mr. Donald E. Hoak of the Air Force Flight Dynamics Laboratory, Research and Technology Division, located at Wright-Patterson Air Force Base, Ohio, is the Air Force Project Engineer for the program, which is being supported primarily under Contract AF33(616)-8130, Air Force Task 821902.

The author wishes to dedicate this to the memory of his beloved Grandmother: MARY SOMERVILLE WELCH. He also wishes to express his appreciation to the staff of the von Karman Facility for their helpfulness in conducting the tests, and particularly to Messrs. Schueler and Baer for providing the machine plotted graphs of the experimental data included in this report. Ozalid reproducible copies of the tabulated data are available on loan from the Air Force Flight Dynamics Laboratory.

The parts which constitute a complete report for this segment of the over-all program are:

Part I: Expansion Corner Flows

Part II: Flows Over a Flat Plate with and without a Partial Span Ramp

Part III: Flows Over Full Span Ramps Mounted on a Flat Plate

ABSTRACT

Pressure distributions were obtained for Mach 8 flows over a sharp 40 degree expansion corner and ahead of ramps on an internally cooled model. Full and partial span ramps, having wedge angles up to 30 degrees, were tested at model angles of attack from -45 to +10 degrees for Reynolds numbers ranging from 1.1 to 3.3 million. The model wall temperature was maintained at fairly constant levels ranging from 450 to 1150 degrees Rankine.

PUBLICATION REVIEW

This report has been reviewed and is approved.

FOR THE COMMANDER:

Charles B. Westbrook

CHARLES B. WESTBROOK
Chief, Control Criteria Branch
Flight Control Division

TABLE OF CONTENTS

LIST OF ILLUSTRATIONS

---

*See Table II, page 8 , for figure numbers corresponding to particular test conditions.

LIST OF SYMBOLS

C_p	pressure coefficient, $C_p \equiv (p-p_\infty)/q_\infty$
M_∞	free stream Mach number
p	pressure (psia)
p_o	stagnation pressure (psia)
p_∞	free stream static pressure (psia)
q_∞	free stream dynamic pressure (psia)
Re_∞/ft	Reynolds number per foot, $Re_\infty/ft \equiv \rho_\infty U_\infty/\mu_\infty$
T_{aw}	adiabatic wall temperature (°R)
T_o	stagnation temperature (°R)
T_w	wall temperature (°R)
T_∞	free stream static temperature (°R)
U_∞	free stream velocity (ft/sec)
α	angle of attack of model (deg.)
μ_∞	viscosity of air in the free stream (slugs/ft sec)
ρ_∞	density of air in the free stream (slugs/ft^3)

INTRODUCTION

The experimental data generated for an investigation of hypersonic flow separation and aerodynamic control characteristics are presented in a series of reports, of which this is one. Pressure, heat transfer, and force data are being obtained for hypersonic flows over "basic geometries," such as a wedge mounted on a flat plate, and for "typical" hypersonic flight configurations with aerodynamic control surfaces. The experimental portion of the program required a total of eleven models (see Fig. 1, page 9); eight for tests in the von Karman Facility of the Arnold Engineering Development Center and three for tests in the Grumman Hypersonic Shock Tunnel (Refs. 1 and 2). The data obtained from AEDC tests of one of the models are given in this three-volume report (see Foreword).

Pressure distributions were obtained over a sharp expansion corner and ahead of wedge shaped ramps mounted on an internally cooled flat plate. The data obtained are to be used in investigating the effects of wall temperature on the pressure distribution and region of separated flow ahead of ramps. These effects must be clearly understood before comprehensive conclusions can be drawn from earlier tests during which aerodynamic heating data were obtained on "cold" models and pressure data were obtained on the same models after they had reached their equilibrium temperatures. The data presented herein were obtained in the AEDC 50-inch Mach 8 Tunnel (Ref. 3). Geometrically similar models, without internal cooling but with both heat transfer and pressure instrumentation, were tested in the AEDC 40-inch and 50-inch tunnels and in the Grumman Hypersonic Shock Tunnel (see Fig. 1).

Manuscript released by author in Aug. 1963 for publication as an ASD Technical Documentary Report.

This report (Part I) presents data obtained on the lower surfaces of the model. These surfaces, which were not internally cooled, form a sharp expansion corner.

MODEL

Photographs of the lower surfaces of the model, installed in the AEDC 50-inch Mach 8 Tunnel, are shown in Figs. 2 and 3. The model has a nominally sharp leading edge and a twelve inch square planform. The lower surfaces of the model form a sharp, 40 degree, expansion corner; the upper surface of the model is a flat plate to which various ramps were added. The lower face of the model intersects the upper surface at 35 degrees. This, coupled with the 40 degree expansion corner, causes the downstream lower surface to be "hidden" from the free stream flow for model angles of attack less than 5 degrees. At $\alpha = +5°$, the leading edge shock is attached and the lower surface, downstream of the expansion corner, is parallel to the free stream flow.

Coolant exhaust fairings, attached to the trailing edge of the model, are shown in Fig. 2. The fairings were designed to prevent possible "pluming" of the coolant (a mixture of cold nitrogen and oxygen), exhausting into the tunnel stream air from the base of the model.

Although it had been desired to cool the entire model, the necessary mass flow rate would have exfeeded that readily available at the test facility. Thus, only the upper surface of the model was cooled directly. The coolant was then allowed to expand within the model before exhausting into the tunnel air stream (see Parts II and III for a more complete description of the cooling system).

Detailed pressure distributions were afforded by closely spaced pressure taps on the lower surfaces of the model in the vicinity of the expansion corner and along the model centerline (see Fig. 4). Five static pressure taps were positioned just upstream of the expansion corner; 10 downstream of the corner; and one directly in the corner, bisecting

the angle. Also, as shown in Fig. 4, there are three pairs of total pressure Stanton tubes mounted downstream of the expansion corner. Each pair consists of one forward and one rearward facing tube with their orifices at the same "X" station and at the same distance below the surface. Thus, as shown in Fig. 4, tubes no. 17 and no. 18 have their openings $\frac{1}{4}$ inch downstream of the corner and their centerlines are 0.010 inches below the surface.

TEST CONDITIONS

Pressure data and wall temperature distributions were obtained at $M_\infty = 8$ for free stream Reynolds numbers per foot of 1.1, 2.2, and 3.3 million. The tunnel conditions corresponding to the different Reynolds numbers are shown in Table I.

The model was pitched from 43 degrees nose down to 10 degrees nose up. These model angles of attack are referenced to the flat plate upper surface of the model. Thus the lower surface, downstream of the expansion corner, is parallel to the free stream at $\alpha = +5°$; the corresponding wedge angle of the surface upstream of the corner is 40 degrees with respect to the free stream (see Fig. 4). The model angles of attack and free stream Reynolds numbers are indicated in Table II.

The coolant flow rate is also indicated in Table II; although the coolant was used for the upper portion of the model and is not expected to affect the pressure distributions for the expansion corner flows. The coolant flow rate was adjusted to yield three different temperature levels for the upper, flat plate, surface of the model. The minimum temperature (maximum cooling) was just sufficient to avoid condensation and icing on the model; the maximum temperature was essentially the equilibrium wall temperature for the upper surface of the model with no cooling.

DATA REDUCTION AND ACCURACY

All pressure data, including the Stanton tube total pressures, were reduced to standard pressure coefficient form:

$$C_p = \frac{p - p_\infty}{q_\infty}$$

where p is the measured pressure, p_∞ is the free stream static pressure, and q_∞ is the free stream dynamic pressure. The inaccuracy in the measured pressure varies from ±0.003 psia for pressures below 0.40 psia, to 0.026 psia for pressures greater than 15 psia. Pressure coefficient uncertainties vary, for example, from 0.004 for $C_p < 0.3$ and Re_∞/ft = 1.1 million, to 0.013 for C_p = 2.0 and Re_∞/ft = 3.3 million. At the higher pressure coefficients, the greatest part of the inaccuracy is due to the deviations in the Mach 8 free stream dynamic pressure (Ref. 5).

The automatic plotting machines, used in presenting the data herein, introduce another source of possible error. The discrepancy in the plotted pressure coefficients due to this machine error should not exceed ±0.01. Nevertheless, there is always the rare possibility that a point will be completely misplotted. Each graph has been inspected and questionable points checked with the tabulated pressure coefficients.

RESULTS

Table II summarizes the data obtained on the lower surfaces of the model and indicates the corresponding figure numbers where the sets of data are presented. The AEDC group

number is presented in the last column. This number indicates the order in which the data were obtained and is to be used when referring to the tabulated data.

Shadowgraph flow photographs were obtained for the conditions indicated in Table II. These photographs show just the expansion corner flow region. Photographs of the flow over the upper portion of the model are given in Parts II and III of this report. In order to include the entire expansion corner flow in just one photograph, the camera was rotated in several instances (as apparent from the orientation of the model and the test conditions indicated on the flow photographs.

Pressure coefficients are plotted versus X, streamwise surface distance measured from the apex of the expansion corner. As indicated in Fig. 4, pressure taps no. 13, no. 14, and no. 15 are all at $X = 1.75$ inches, (in order to observe any spanwise effects), but the C_p values for taps no. 13 and no. 15 are plotted at $X = 1.70$ and 1.80 inches, respectively. Total pressures, measured by the Stanton tubes, are plotted in coefficient form for each pair of forward and rearward facing tubes. The total pressures measured by the forward facing tubes are plotted just to the left of the three vertical lines delineating the three pairs of tubes; the total pressures measured by the rearward facing tubes are plotted just to the right of the lines. As shown in Fig. 4, and indicated in the pressure plots, the openings of the first pair of tubes are at $X = \frac{1}{4}$ inch, the lines of the first two pairs are 0.010 inch away from the model surface, the centerlines of the third pair of tubes are 0.060 inch away from the surface.

Although the accuracy of the plotted data should suffice for engineering purposes, ozalid reproducible copies of the tabulated data are available on loan (see Foreword). The plotted data may be read accurately using standard 20/inch grid, tracing graph paper overlays.

REFERENCES

1. Kaufman, Louis G. II, et al., A Review of Hypersonic Flow Separation and Control Characteristics, ASD-TDR-62-168, March 1962.

2. Evans, William J. and Kaufman, Louis G. II, Pretest Report on Hypersonic Flow Separation and Control Models for AEDC Tunnels A, B, Hotshot 2 and Grumman Hypersonic Shock Tunnel, Grumman Research Department Memorandum RM-209, July 1962.

3. Arnold Center, Test Facilities Handbook, Arnold Air Force Station, January 1961.

4. Kaufman, Louis G. II, Pressure and Heat Transfer Measurements for Hypersonic Flows Over Expansion Corners and Ahead of Ramps, (4 parts), to be published as an ASD Technical Documentary Report.

5. Kaufman, Louis G. II and Meckler, Lawrence, Pressure and Heat Transfer Measurements at Mach 5 and 8 for a Fin - Flat Plate Model, ASD-TDR-63-235, February 1963.

6. Kaufman, Louis G. II, Pressure Measurements and Oil Film Photographs for Mach 5 Flows Past Fins Mounted on a Flat Plate, to be published as an ASD Technical Documentary Report.

7. Hartofilis, Stavros A., Pressure Measurements at Mach 19 for a Winged Re-entry Configuration, ASD-TDR-63-319, March 1963.

8. Meckler, Lawrence, Static Aerodynamic Characteristics at Mach 5 and 8 of an Aerodynamically Controlable Winged Re-entry Configuration, to be published as an ASD Technical Documentary Report.

9. Kaufman, Louis G. II, Pressure and Heat Transfer Measurements for Hypersonic Flows Over a Blunt Pyramidal Configuration with Aerodynamic Controls, to be published as an ASD Technical Documentary Report.

TABLE I

TUNNEL CONDITIONS

$\frac{Re_\infty}{10^6 ft}$	1.1	2.2	3.3
M_∞	8.04	8.08	8.09
p_∞ (psia)	0.025	0.049	0.074
q_∞ (psia)	1.13	2.24	3.37
p_o (psia)	252	510	770
T_o (°R)	1,350	1,350	1,350

TABLE II

TEST CONDITIONS

Coolant Flow Rate*	Re_∞ / 10^6 ft	α (deg.)	Figure Nos. Photo†	Figure Nos. C_p	AEDC Group Nos.
OFF	1.1	-43		12	131
"	2.2	"		13	125
"	3.3	"		14	121
MAXIMUM	"	"		15	122
OFF	1.1	-40		16	130
"	3.3	"		17	120
"	1.1	-35		18	129
"	3.3	"		19	119
OFF	1.1	-30		20	128
"	2.2	"		21	124
"	3.3	"		22	118
MAXIMUM	"	"		23	123
OFF	1.1	-25		24	127
"	3.3	"		25	117
"	1.1	-20		26	126
"	3.3	"		27	116
OFF	1.1	-15		28	43
MAXIMUM	"	"	5a	29	45
OFF	3.3	"		30	20
MEDIUM	"	"		31	29
MAXIMUM	"	"	5b	32	34
OFF	1.1	-10		33	42
MAXIMUM	"	"	6a	34	46
OFF	3.3	"		35	21
MAXIMUM	"	"	6b	36	33
OFF	1.1	-5		37	41
MAXIMUM	"	"	7a	38	47
OFF	3.3	"		39	22
MEDIUM	"	"		40	28
MAXIMUM	"	"	7b	41	32
OFF	1.1	0		42	40
MAXIMUM	"	"	8a	43	48
OFF	2.2	"		44	36
MAXIMUM	"	"	8b	45	38
OFF	3.3	0		46	23
MEDIUM	"	"		47	26
MAXIMUM	"	"	9	48	31
OFF	1.1	+5		49	39
MAXIMUM	"	"	10a	50	49
OFF	3.3	"		51	24
MAXIMUM	"	"	10b	52	30
OFF	1.1	+10		53	44
MAXIMUM	"	"		54	50
OFF	2.2	"		55	37
OFF	3.3	+10		56	25
MEDIUM	"	"		57	27
MAXIMUM	"	"	11	58	35

*Coolant flow rate adjusted such that the upper surface wall temperature was approximately 450°R for maximum cooling, 800°R for medium cooling, and 1150°R without cooling (see Test Condition).

†Shadowgraph flow photographs.

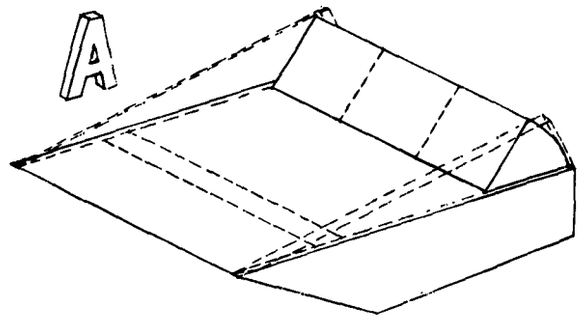

Separated Flows ahead of a Ramp
Fore and aft flaps, end plates
3 separate models:

1) Pressure and heat transfer, AEDC Tunnels A & B, M = 5 & 8, Results in Ref. 4.

2) Controlled wall temperature, pressure, AEDC Tunnel B, M = 8, Results herein.

3) Pressure and heat transfer, Grumman Shock Tunnel, M ≈ 13 & 19, Results not yet available.

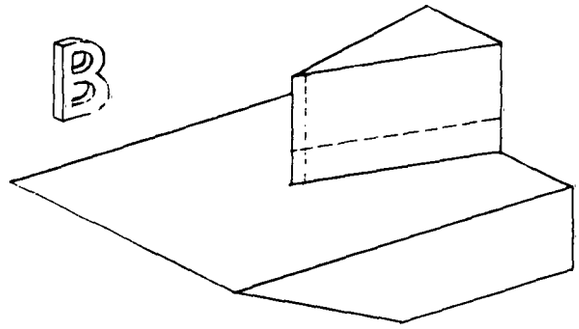

Wedge - Plate Interaction
Small and large fins with sharp and blunt leading edges
2 separate models:

1) Pressure and heat transfer, AEDC Tunnels A & B, M = 5 & 8, Results in Ref. 5 and 6.

2) Pressure and heat transfer, Grumman Shock Tunnel, M ≈ 13 & 19, Results not yet available.

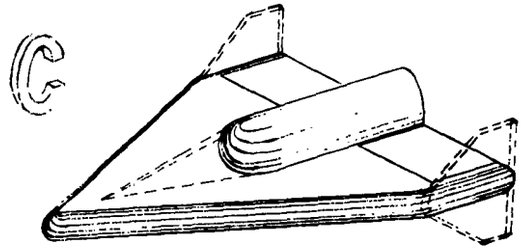

Clipped Delta, Blunt L.E.
Center body, T.E. flaps, drooped nose, spoiler, tip fins
3 separate models:

1) Pressure and heat transfer, AEDC Tunnels A & B, M = 5 & 8, Results not yet available.

2) Pressure, AEDC Hotshot 2, M ≈ 19, Results in Ref. 7.

3) Six component force, AEDC Tunnels A & B, M = 5 & 8, Results in Ref. 8.

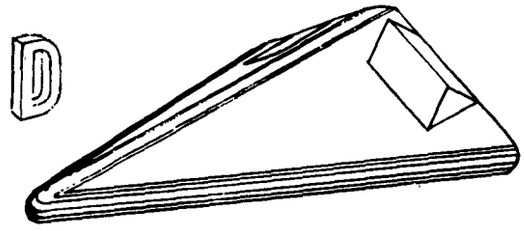

Delta, Blunt L.E., Dihedral
T.E. flaps, canard, ventral fin
3 separate models:

1) Pressure and heat transfer, AEDC Tunnels A & B, M = 5 & 8, Results in Ref. 9.

2) Pressure and heat transfer, Grumman Shock Tunnel, M 19, Results not yet available.

3) Six component force, AEDC Tunnels A & B, M = 5 & 8. Results not yet available.

Fig. 1 General Outline of Models and Remarks for Over-all Program

Fig. 2 Photograph of Lower Surface of Model, with Coolant Exhaust Fairings, Installed in the AEDC 50-inch Mach 8 Tunnel

Fig. 3 Photograph of Lower Surface of Model without Coolant Exhaust Fairings

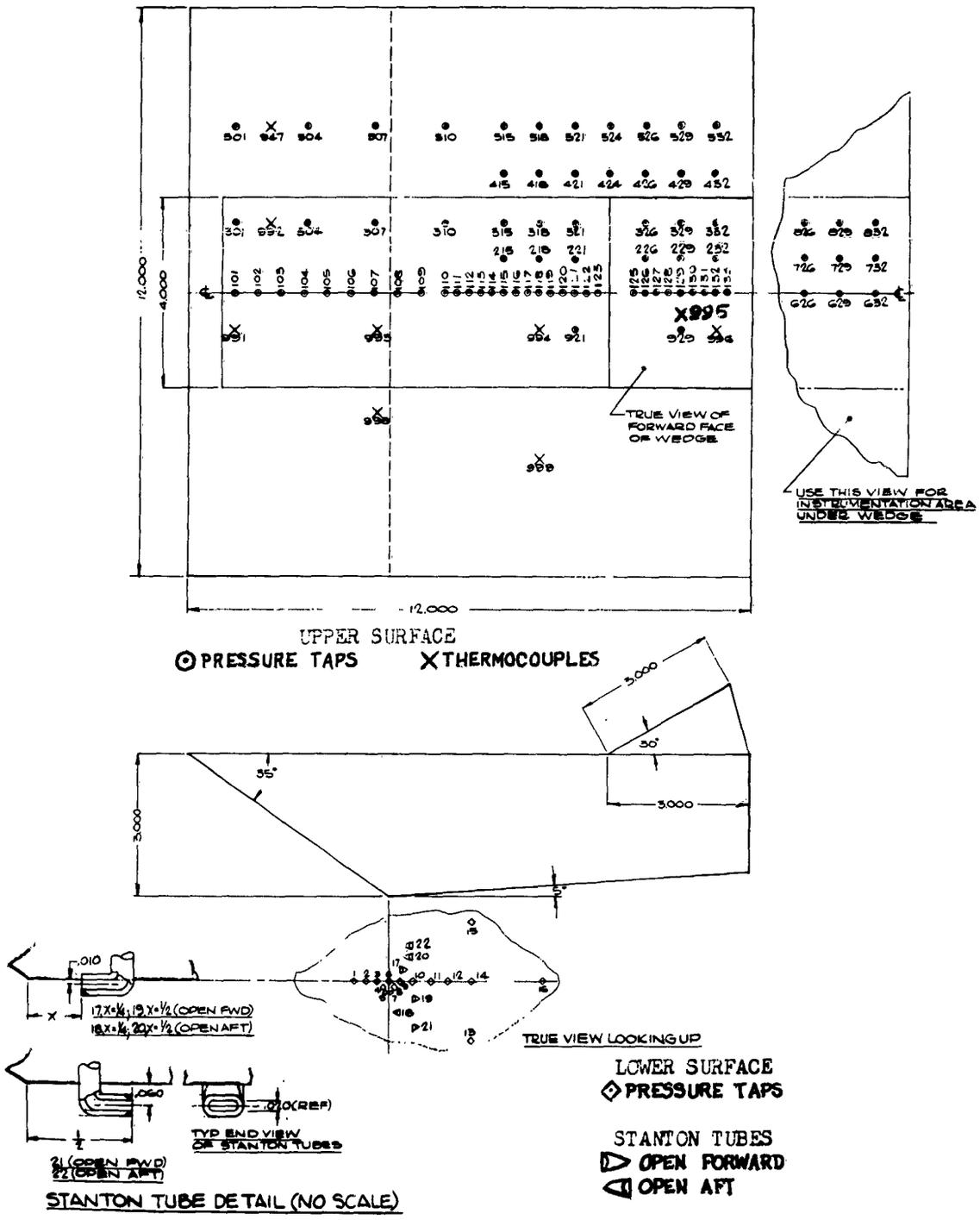

Fig. 4 Model Instrumentation

a)

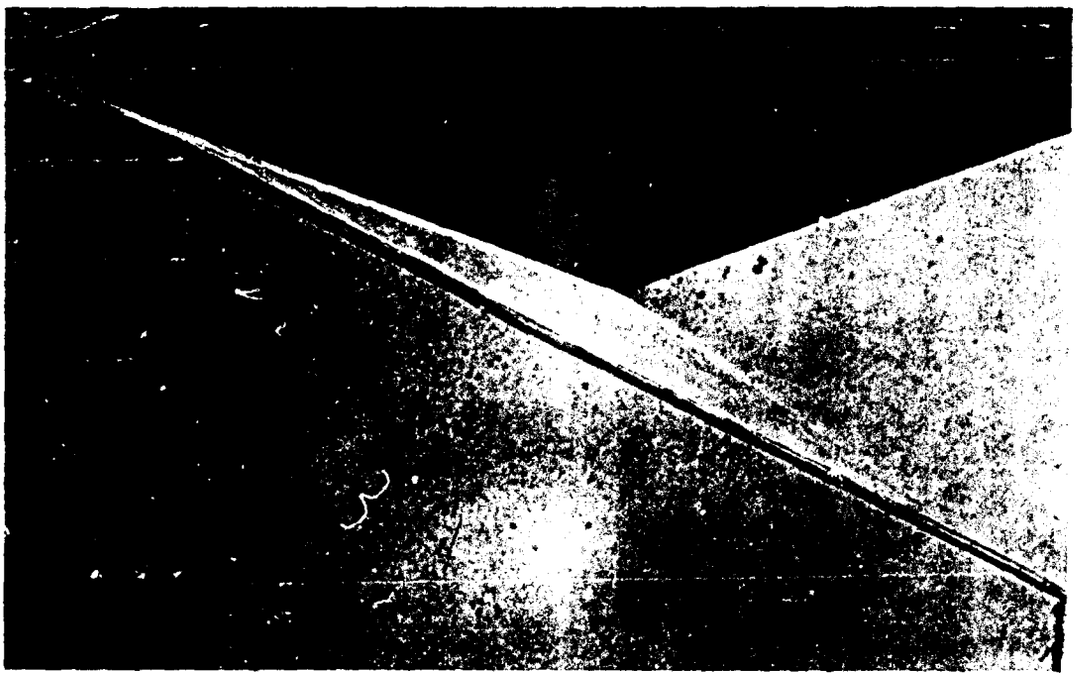

b)

Fig. 5 Shadowgraph Flow Photographs, α = -15°
a) Re_∞/ft = 1,100,000
b) Re_∞/ft = 3,300,000

a)

b)

Fig. 6 Shadowgraph Flow Photographs, $\alpha = -10°$
a) Re_∞/ft = 1,100,000
b) Re_∞/ft = 3,300,000

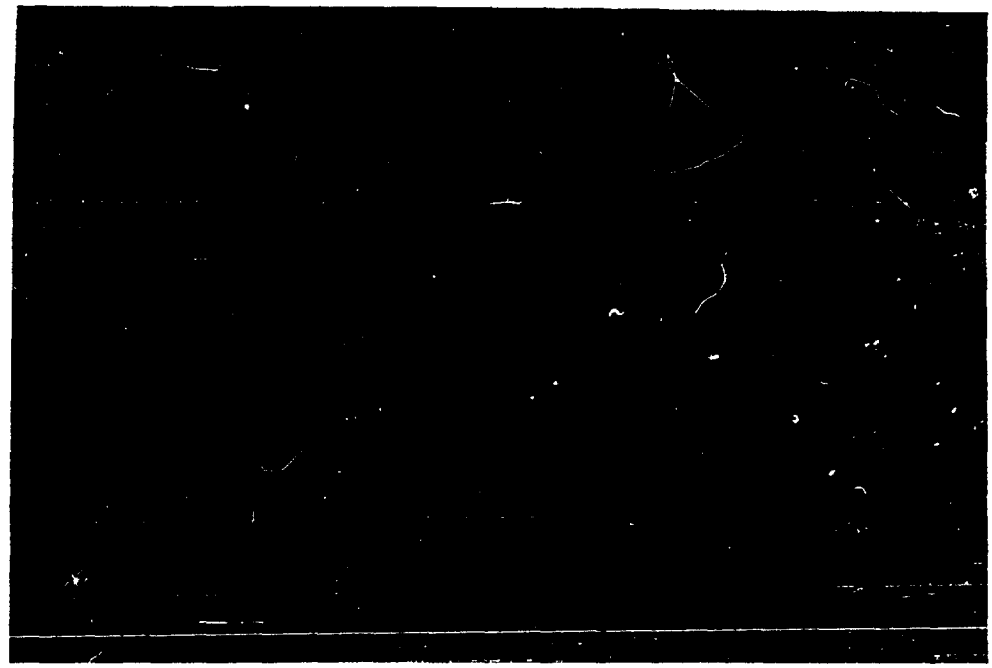

a)

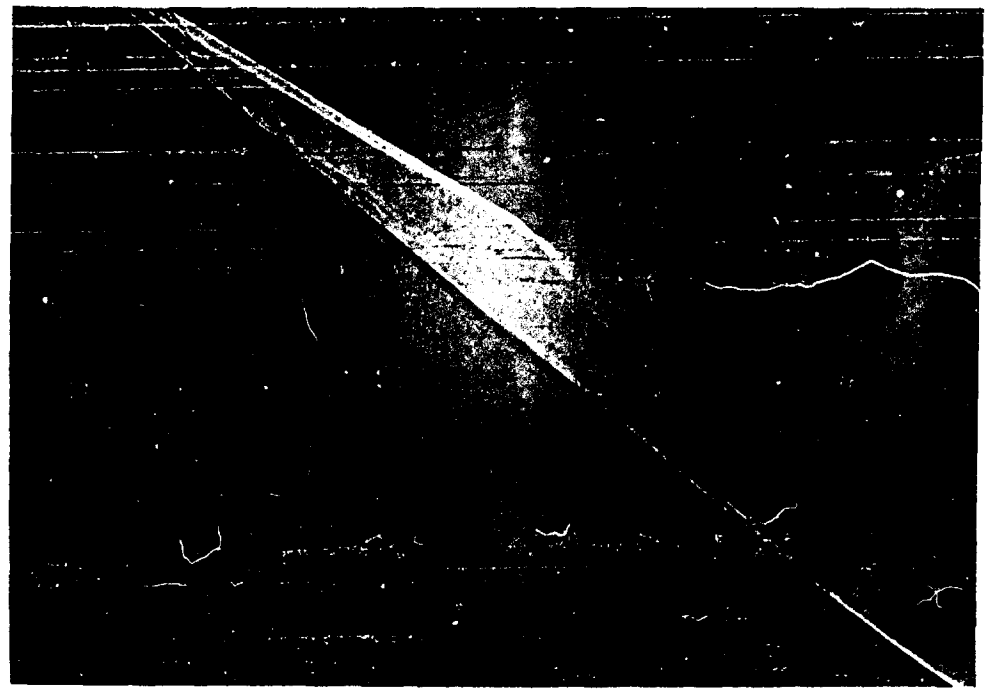

b)

Fig. 7 Shadowgraph Flow Photographs, $\alpha = -5°$
a) Re_∞/ft = 1,100,000
b) Re_∞/ft = 3,300,000

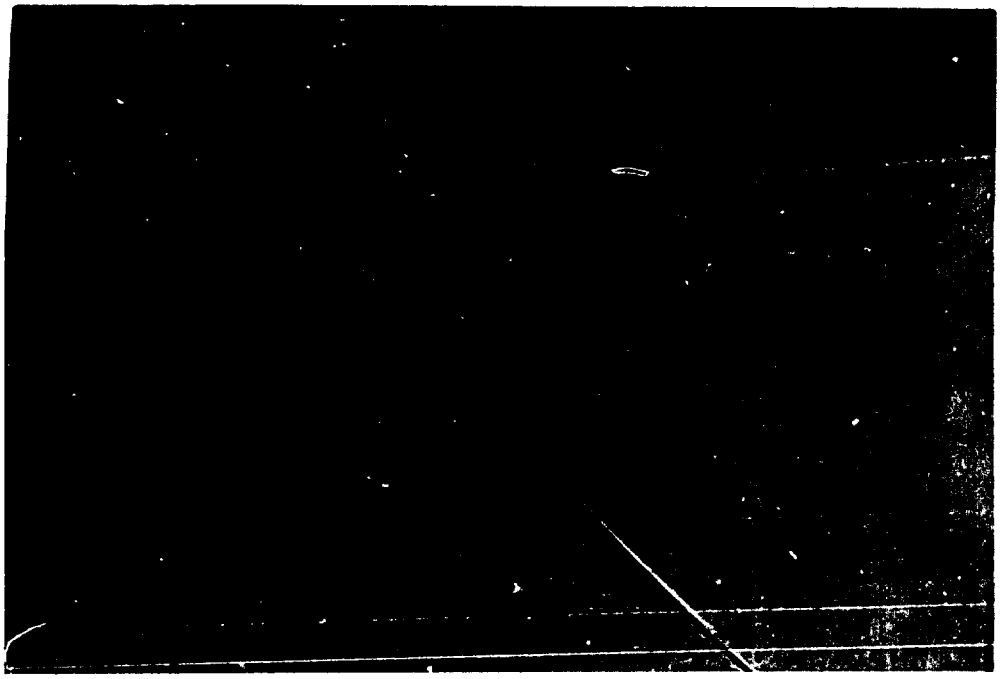

a)

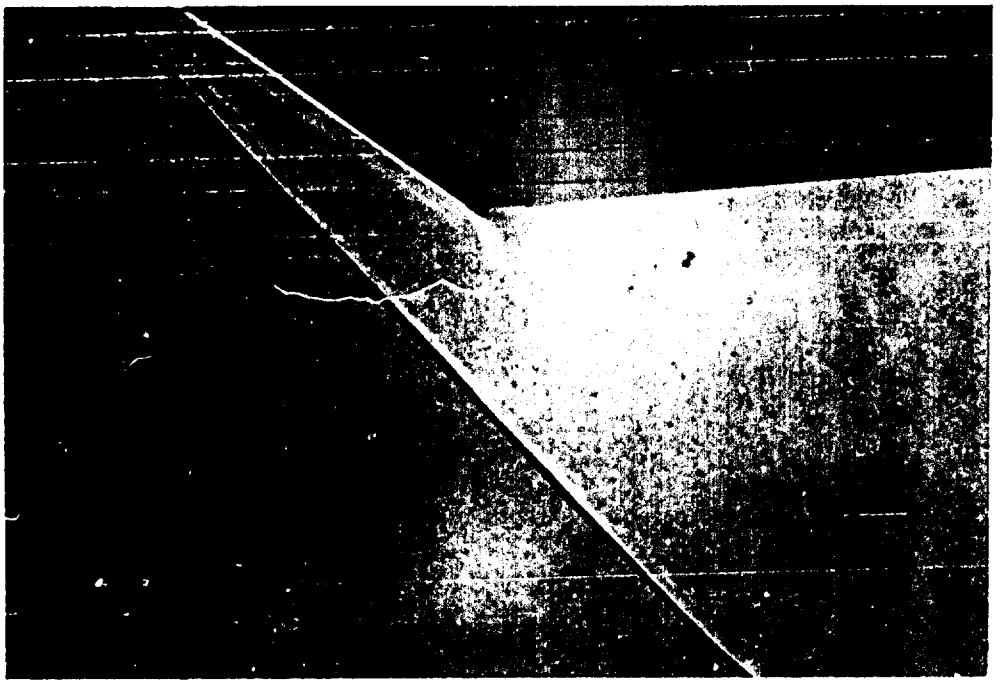

b)

Fig. 8 Shadowgraph Flow Photographs, $\alpha = 0$
a) Re_∞/ft = 1,100,000
b) Re_∞/ft = 2,200,000

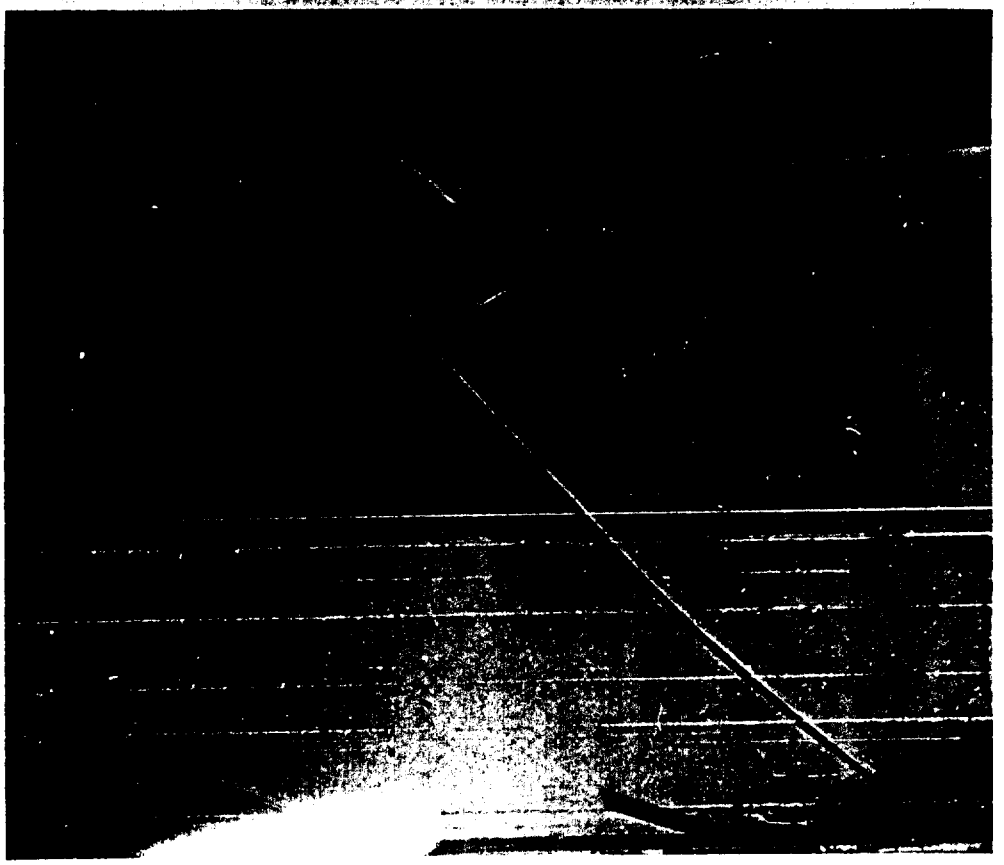

Fig. 9 Shadowgraph Flow Photograph $\alpha = 0$ and $Re_\infty/ft = 3,300,000$

a)

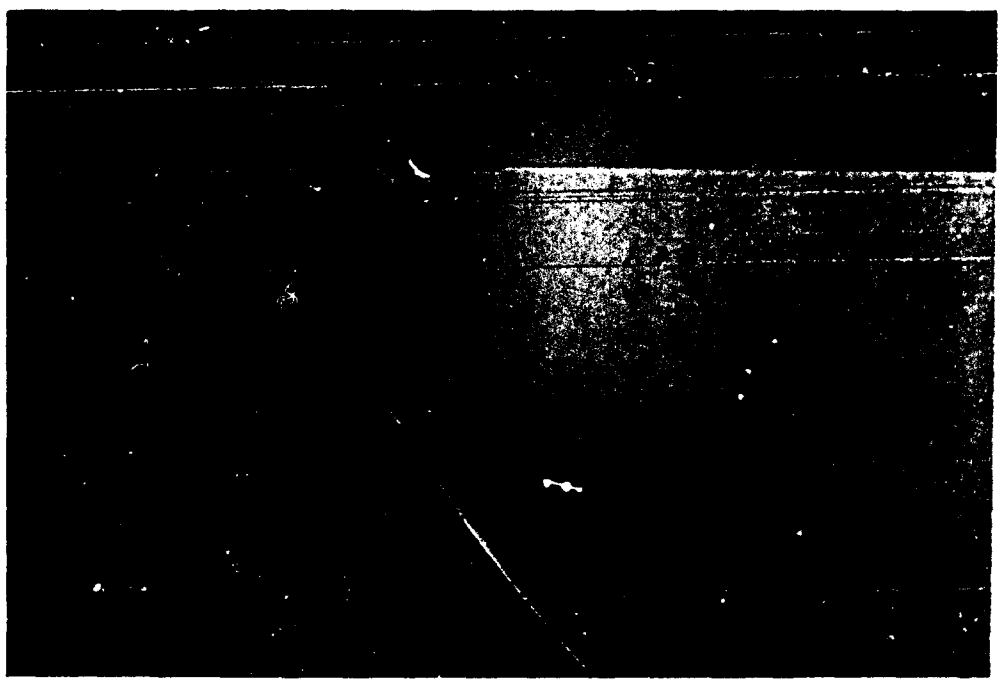

b)

Fig. 10 Shadowgraph Flow Photographs, $\alpha = +5°$
a) Re_∞/ft = 1,100,000
b) Re_∞/ft = 3,300,000

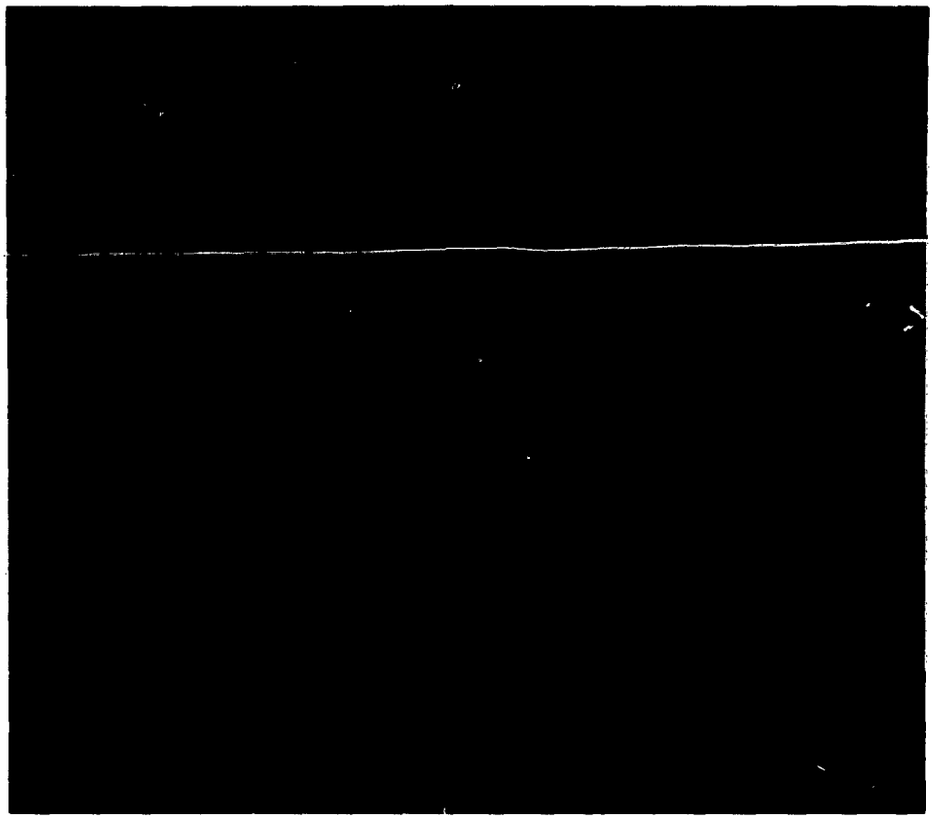

Fig. 11 Shadowgraph Flow Photograph $\alpha = +10°$ and $Re_\infty/ft = 3{,}300{,}000$

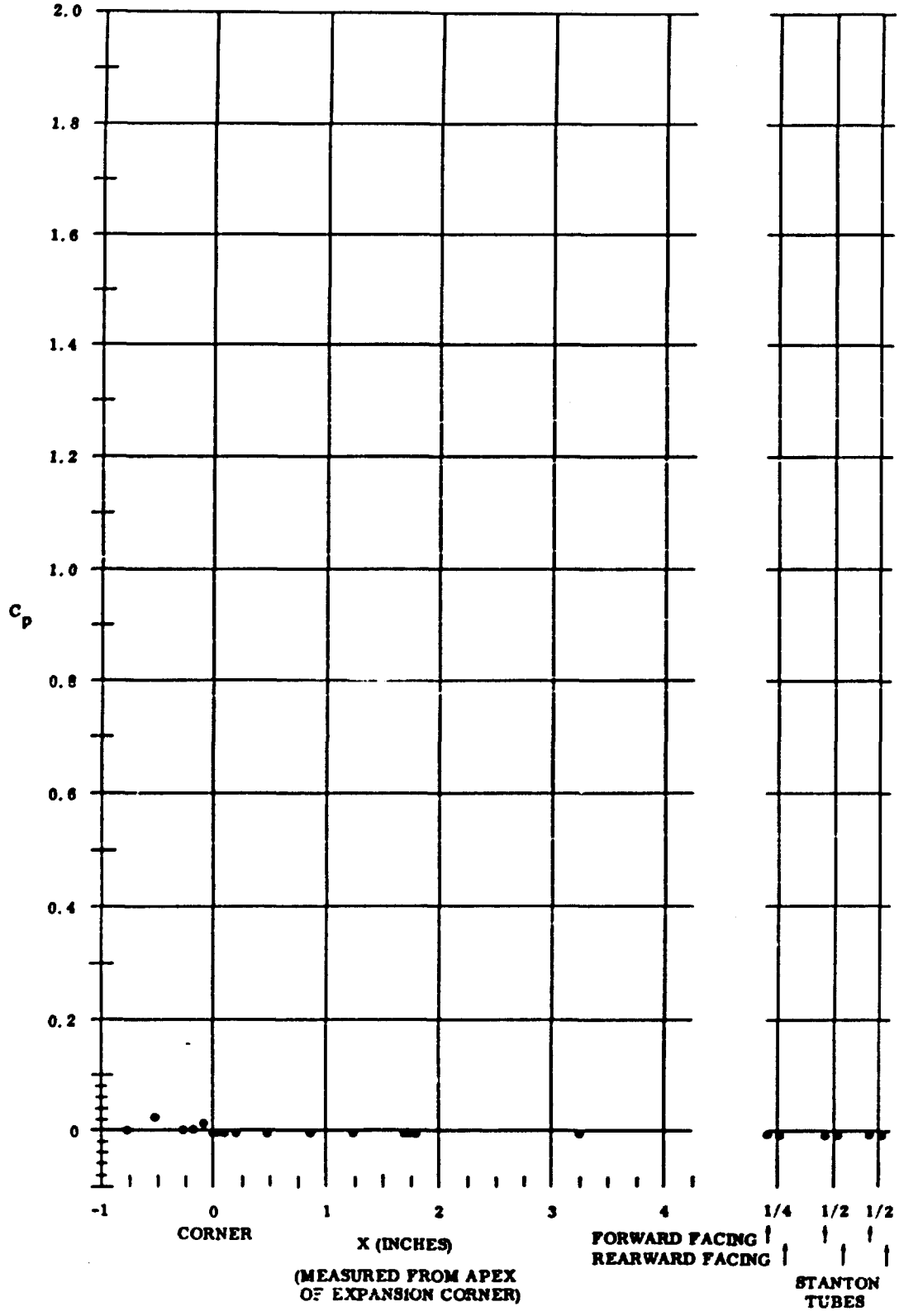

Fig. 12 Pressure Coefficient Data Plots (no coolant flow for upper surface); $\alpha = -43°$ and $Re_\infty/ft = 1{,}100{,}000$

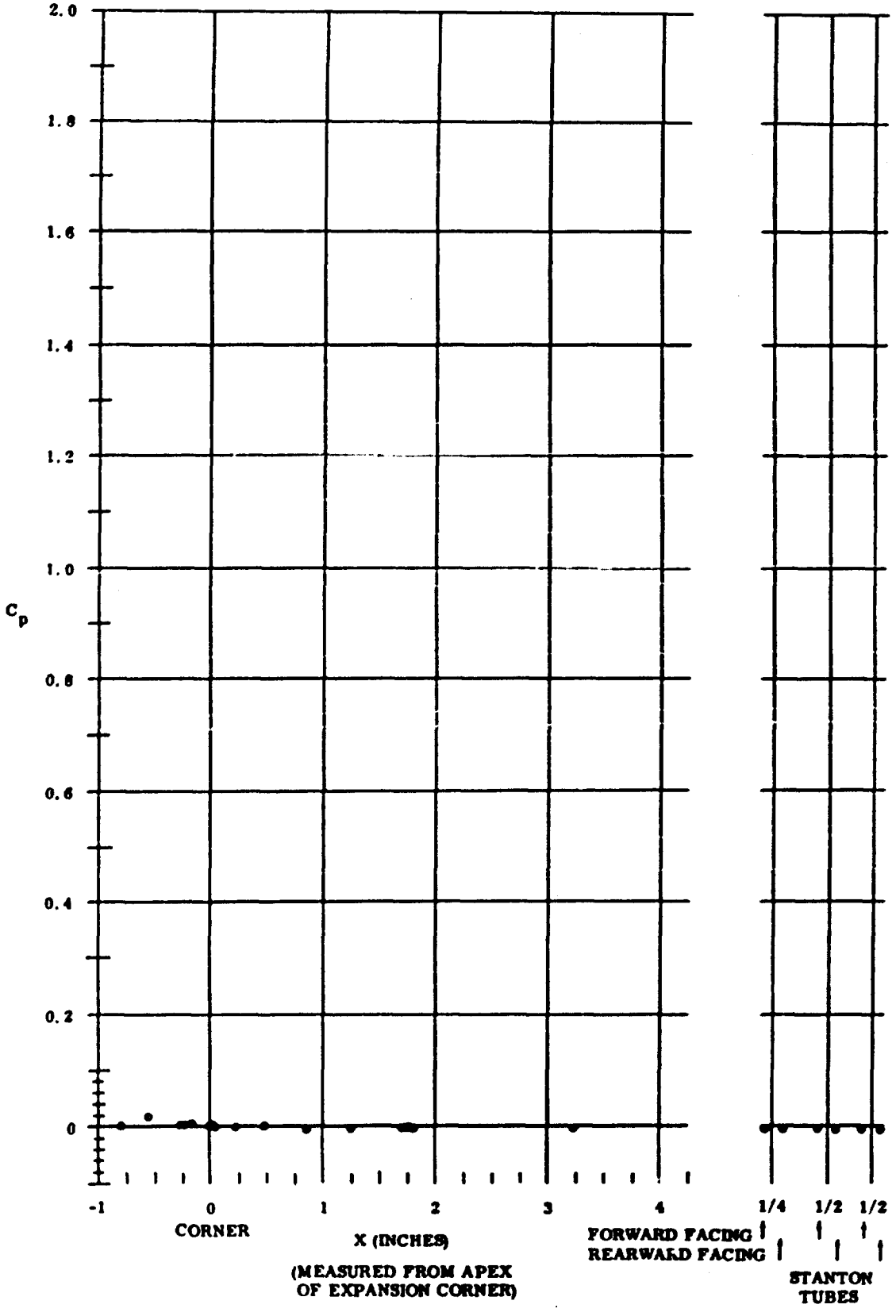

Fig. 13 Pressure Coefficient Data Plots (no coolant flow for upper surface); $\alpha = -43°$ and $Re_\infty/ft = 2{,}200{,}000$

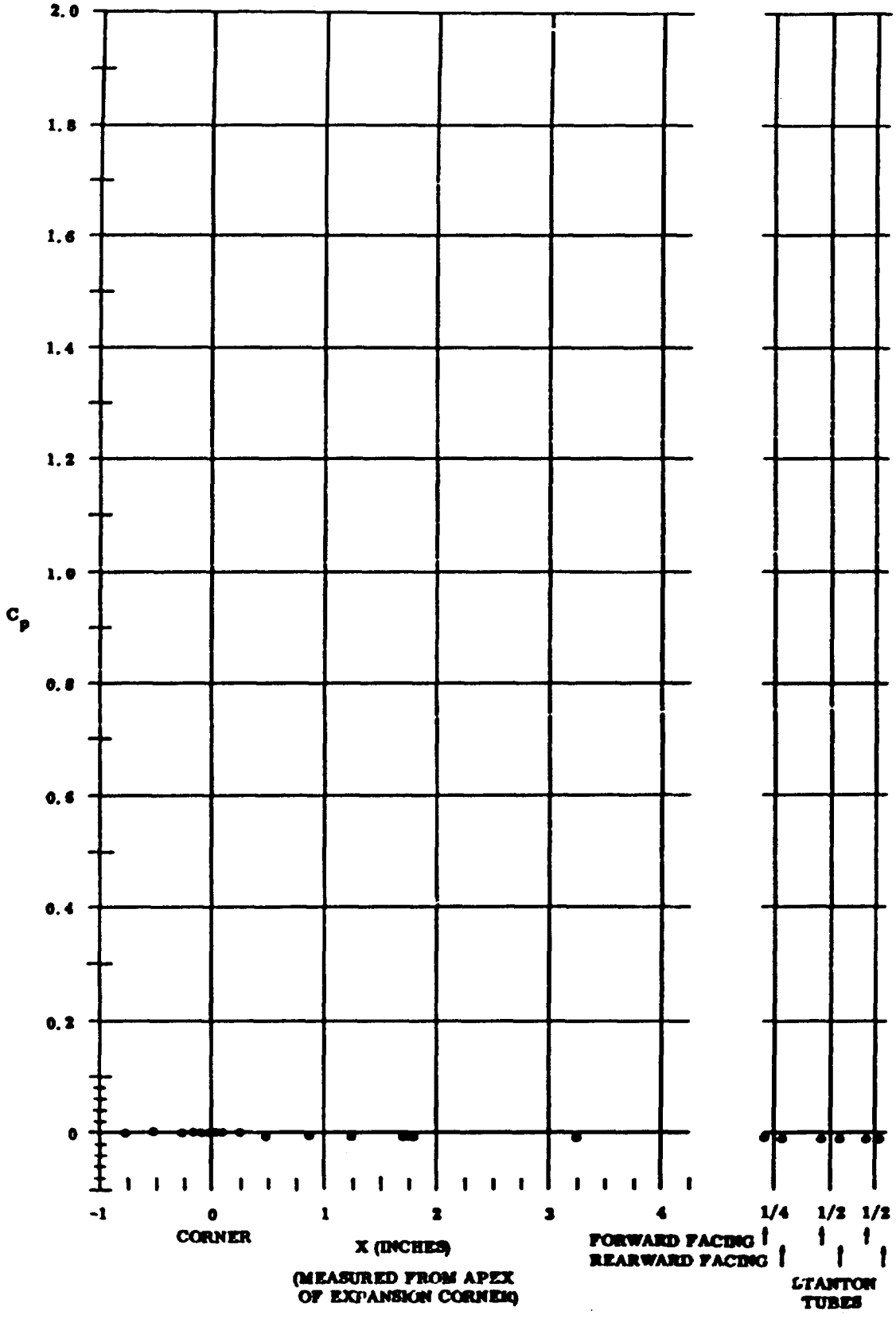

Fig. 14 Pressure Coefficient Data Plots (no coolant flow for upper surface); $\alpha = -43°$ and $Re_\infty/ft = 3{,}300{,}000$

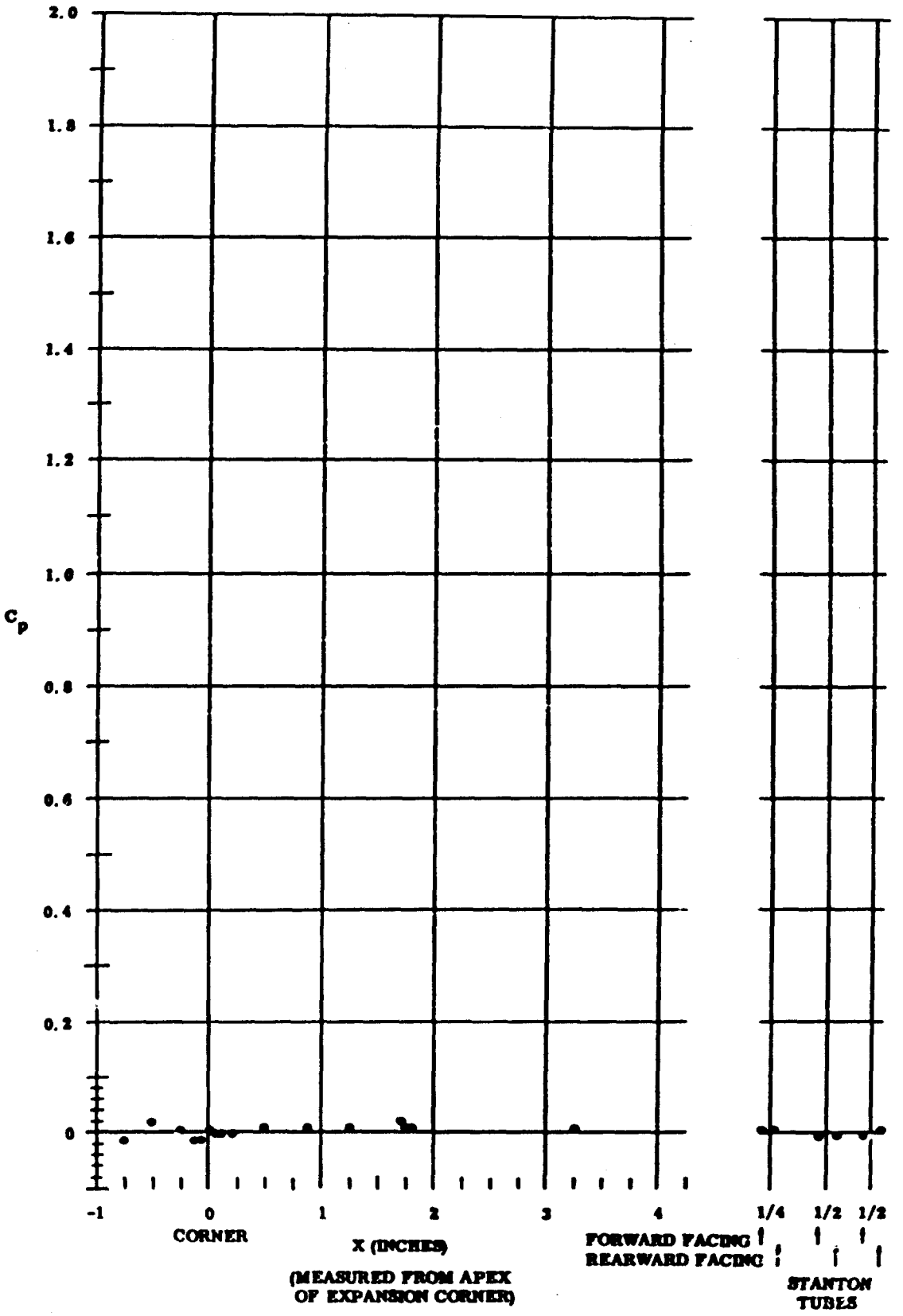

Fig. 15 Pressure Coefficient Data Plots (maximum coolant flow rate for upper surface); $\alpha = -43°$ and $Re_\infty/ft = 3{,}300{,}000$

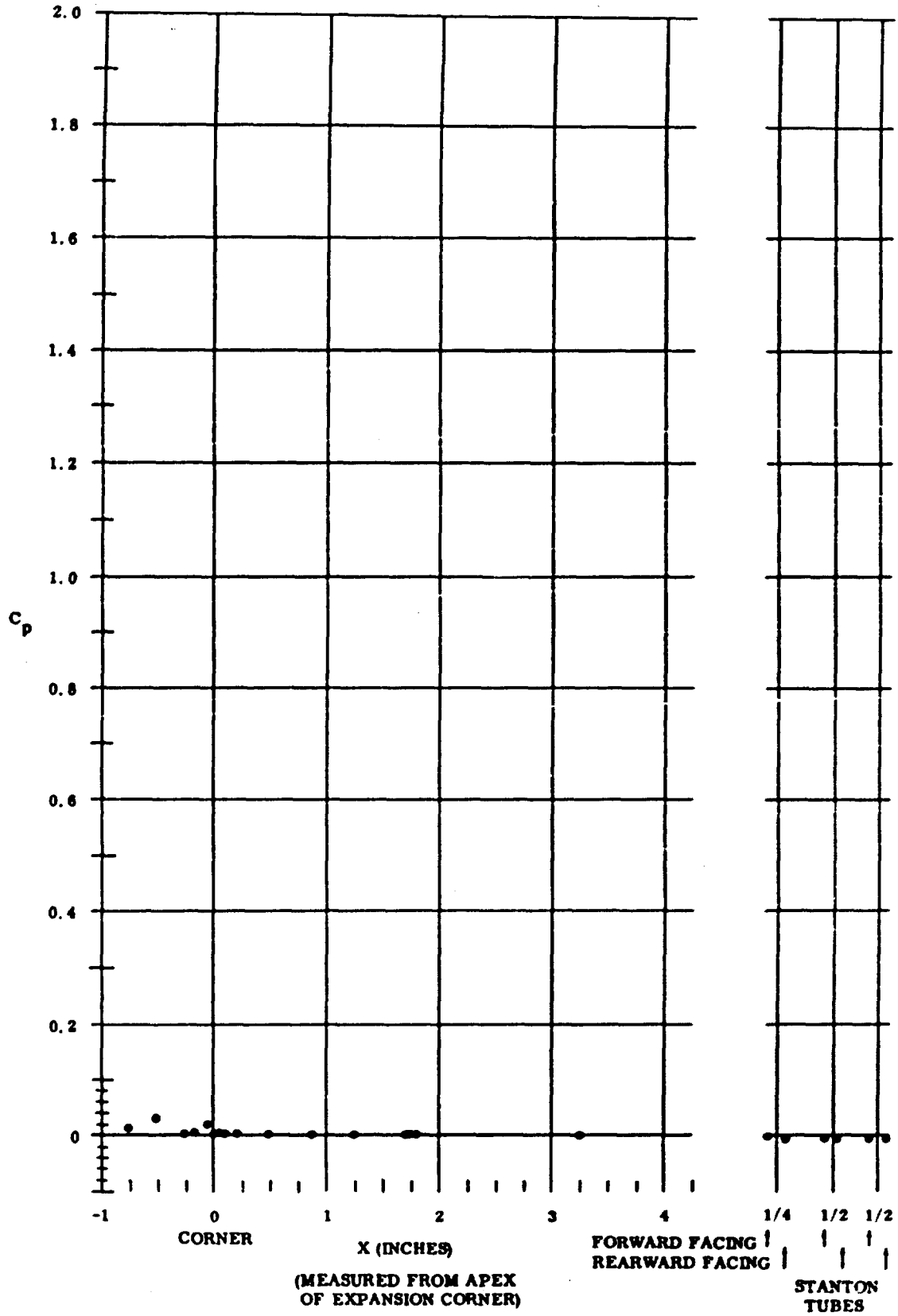

Fig. 16 Pressure Coefficient Data Plots (no coolant flow for upper surface); $\alpha = -40°$ and $Re_\infty/ft = 1{,}100{,}000$

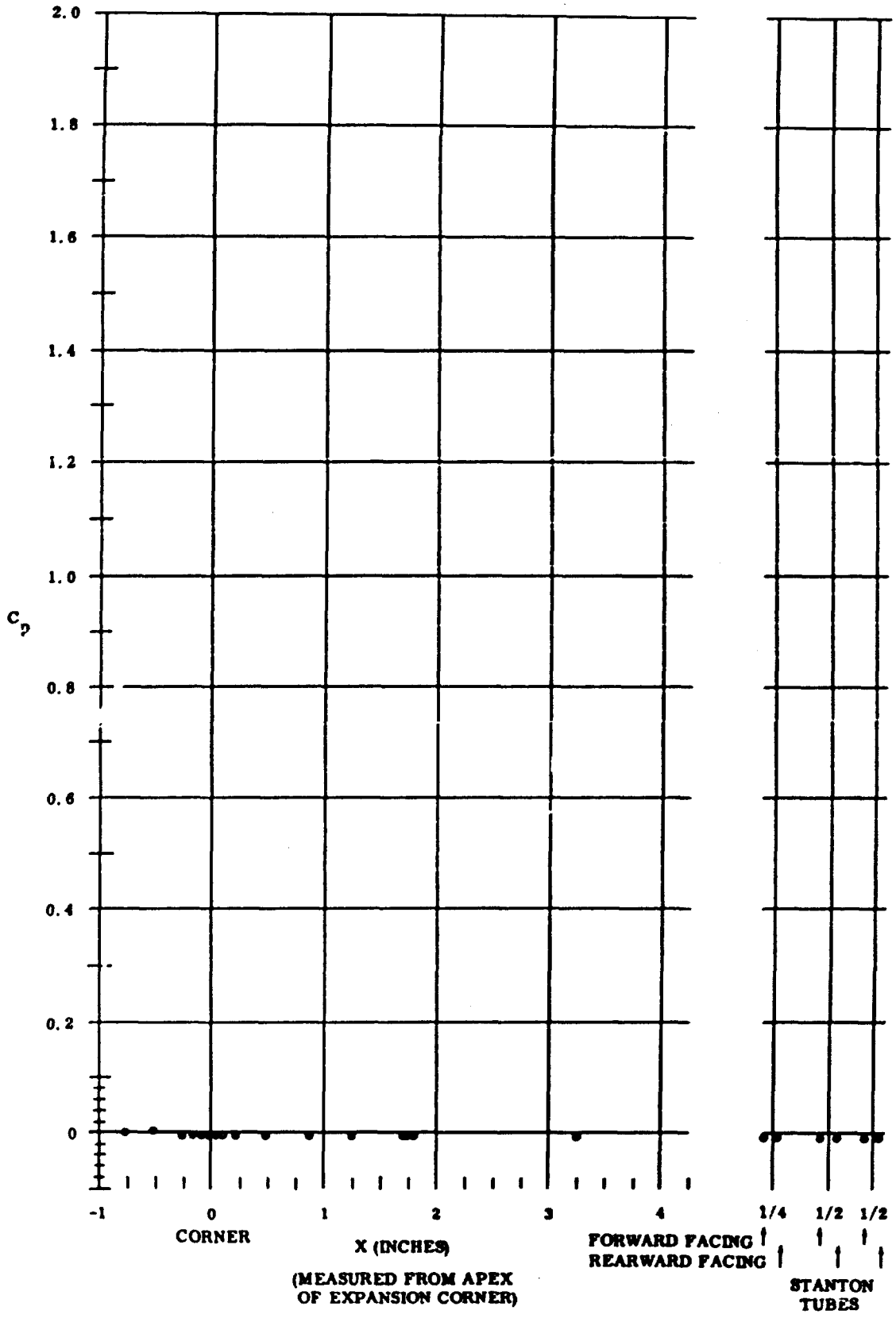

Fig. 17 Pressure Coefficient Data Plots (no coolant flow for upper surface); $\alpha = -40°$ and $Re_\infty/ft = 3{,}300{,}000$

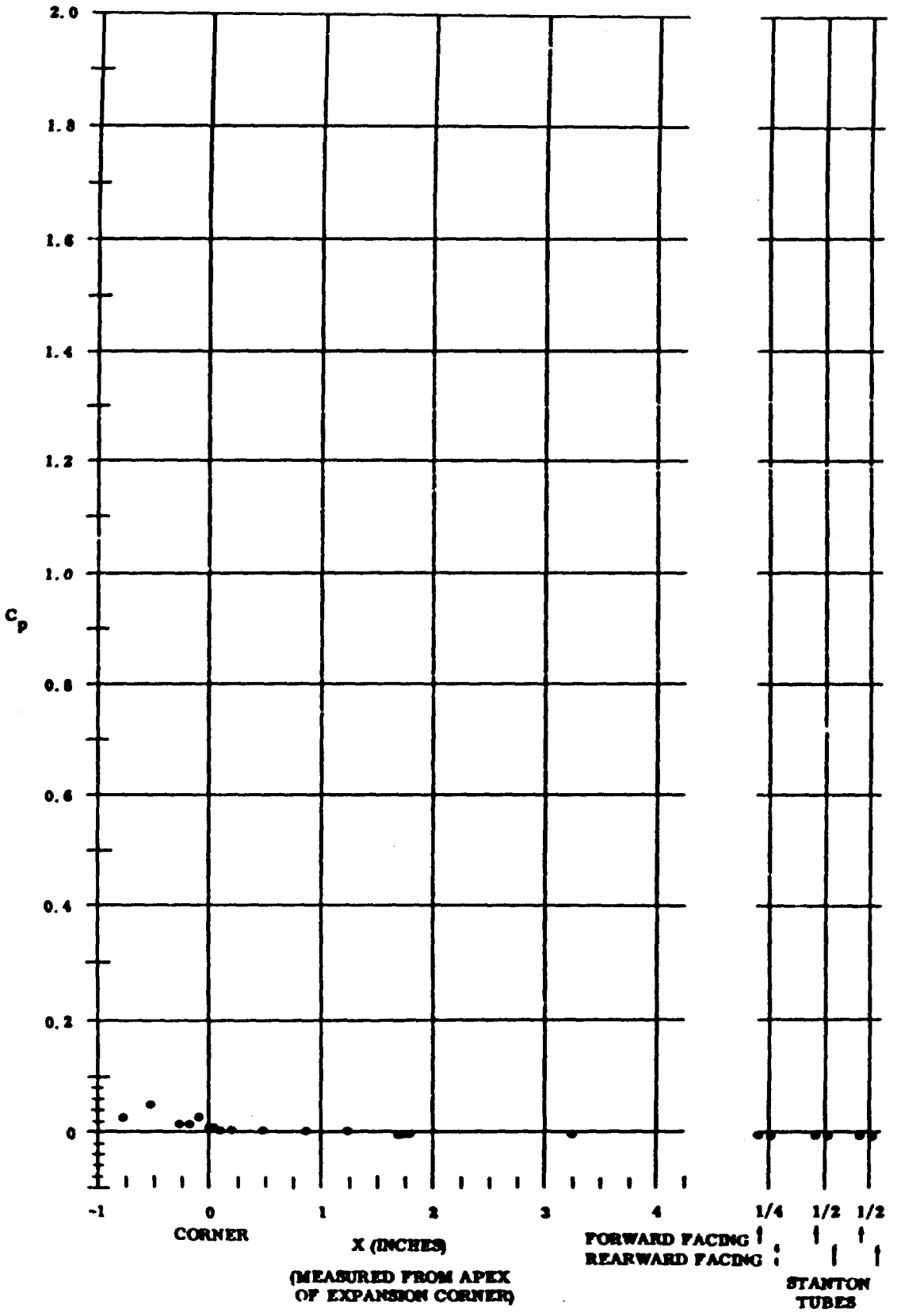

Fig. 18 Pressure Coefficient Data Plots (no coolant flow for upper surface); $\alpha = -35°$ and $Re_{\infty}/ft = 1{,}100{,}000$

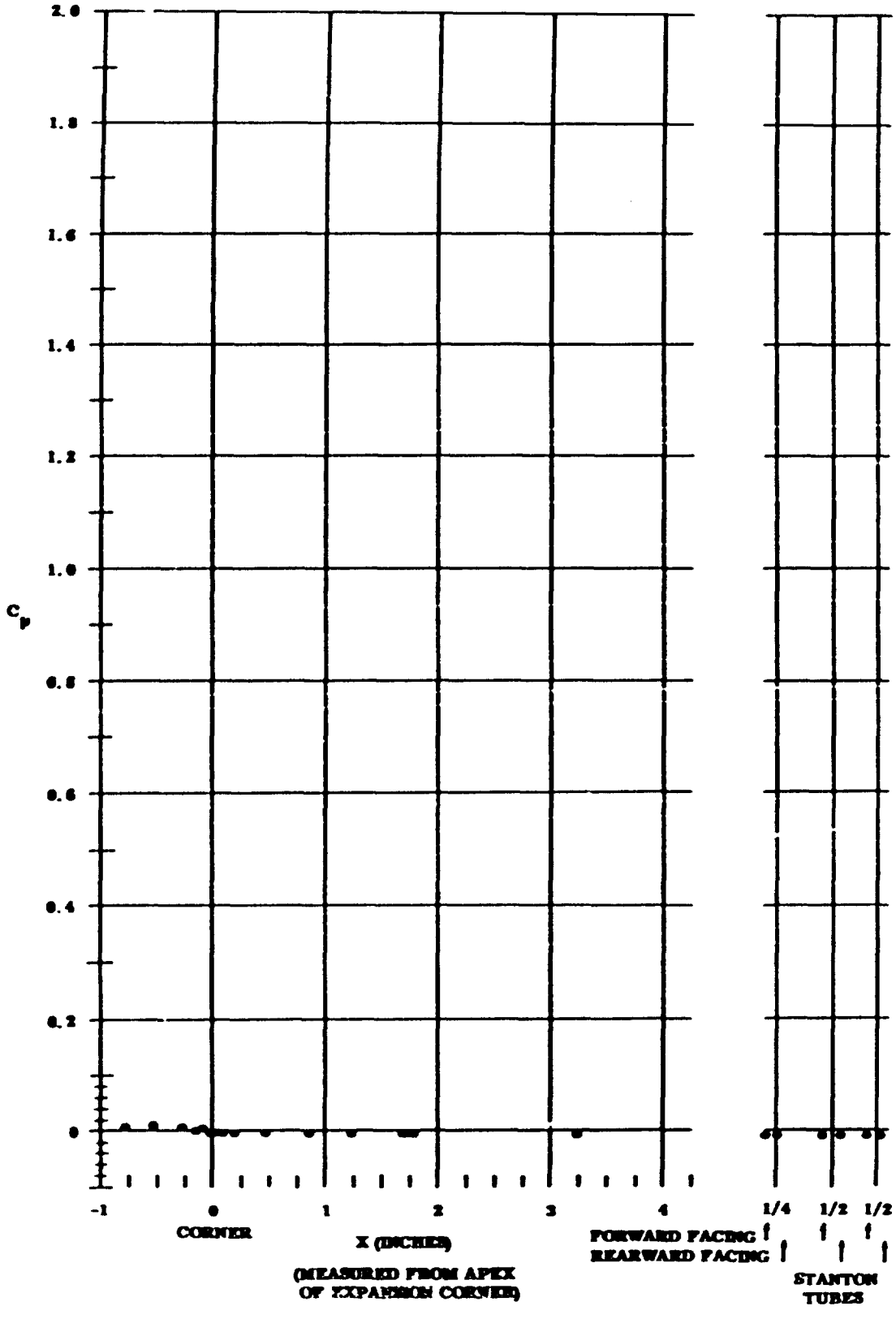

Fig. 19 Pressure Coefficient Data Plots (no coolant flow for upper surface); α = -35° and Re_∞/ft = 3,300,000

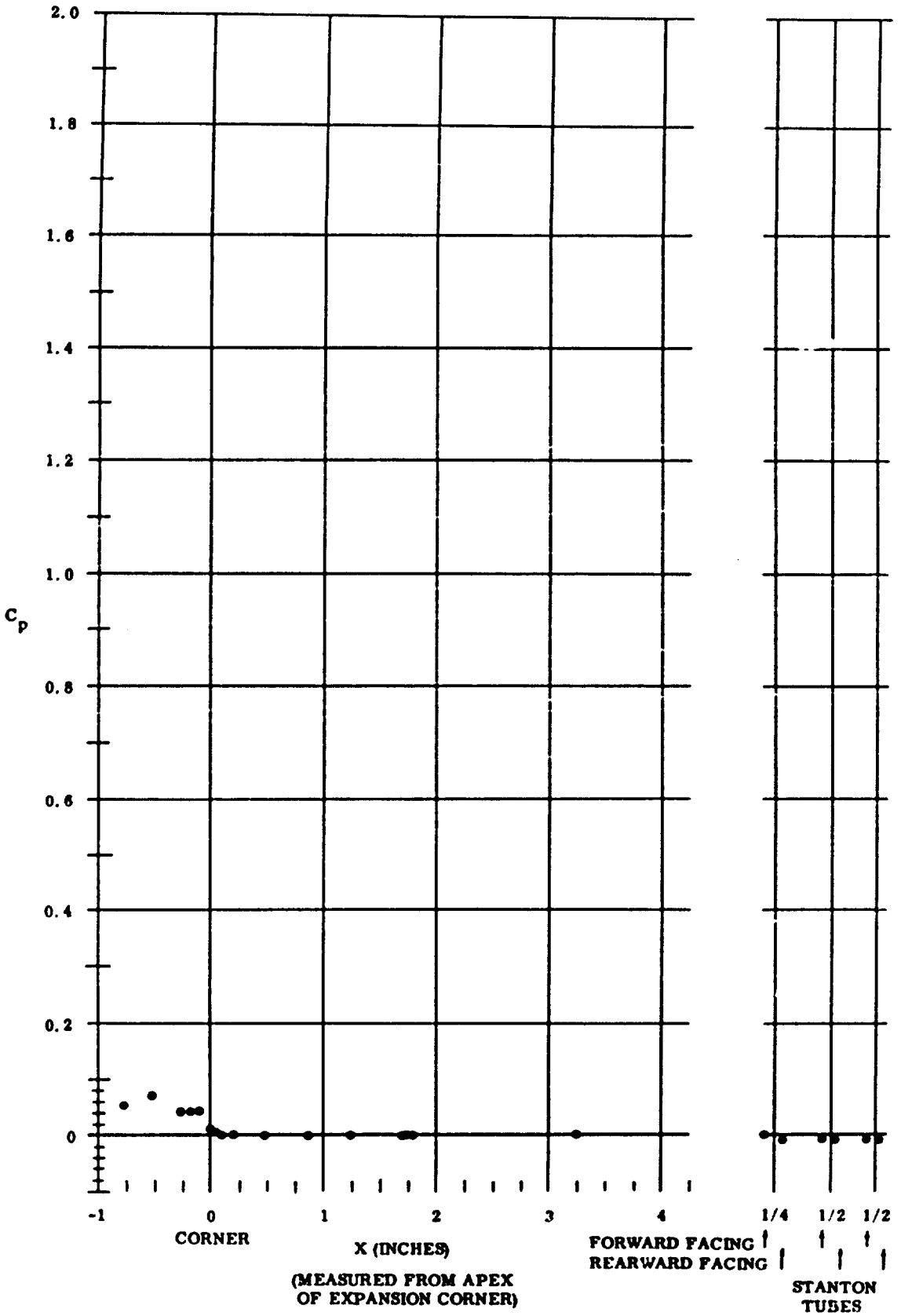

Fig. 20 Pressure Coefficient Data Plots (no coolant flow for upper surface); $\alpha = -30°$ and $Re_\infty/ft = 1{,}100{,}000$

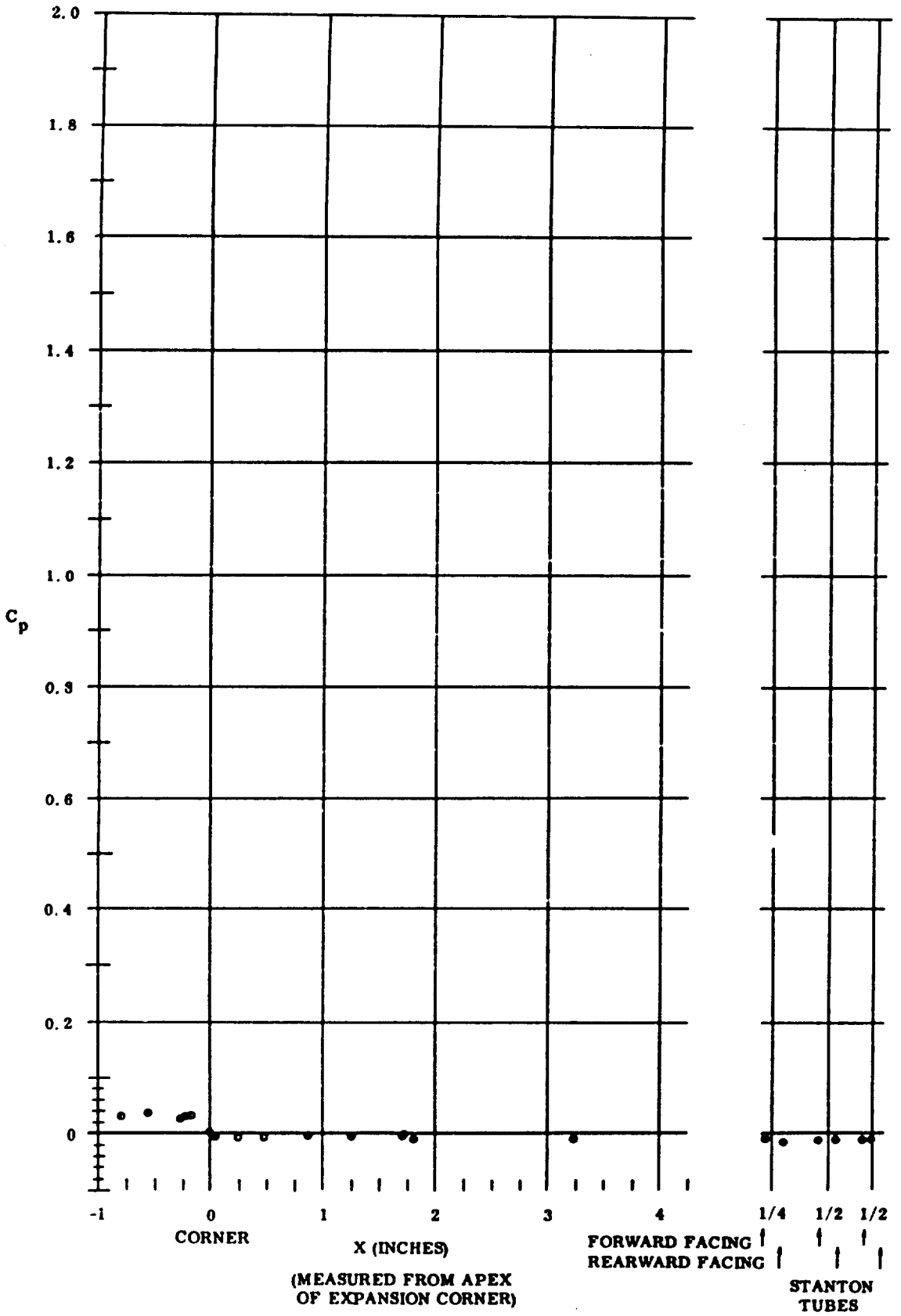

Fig. 21 Pressure Coefficient Data Plots (no coolant flow for upper surface); α = -30° and Re_∞/ft = 2,200,000

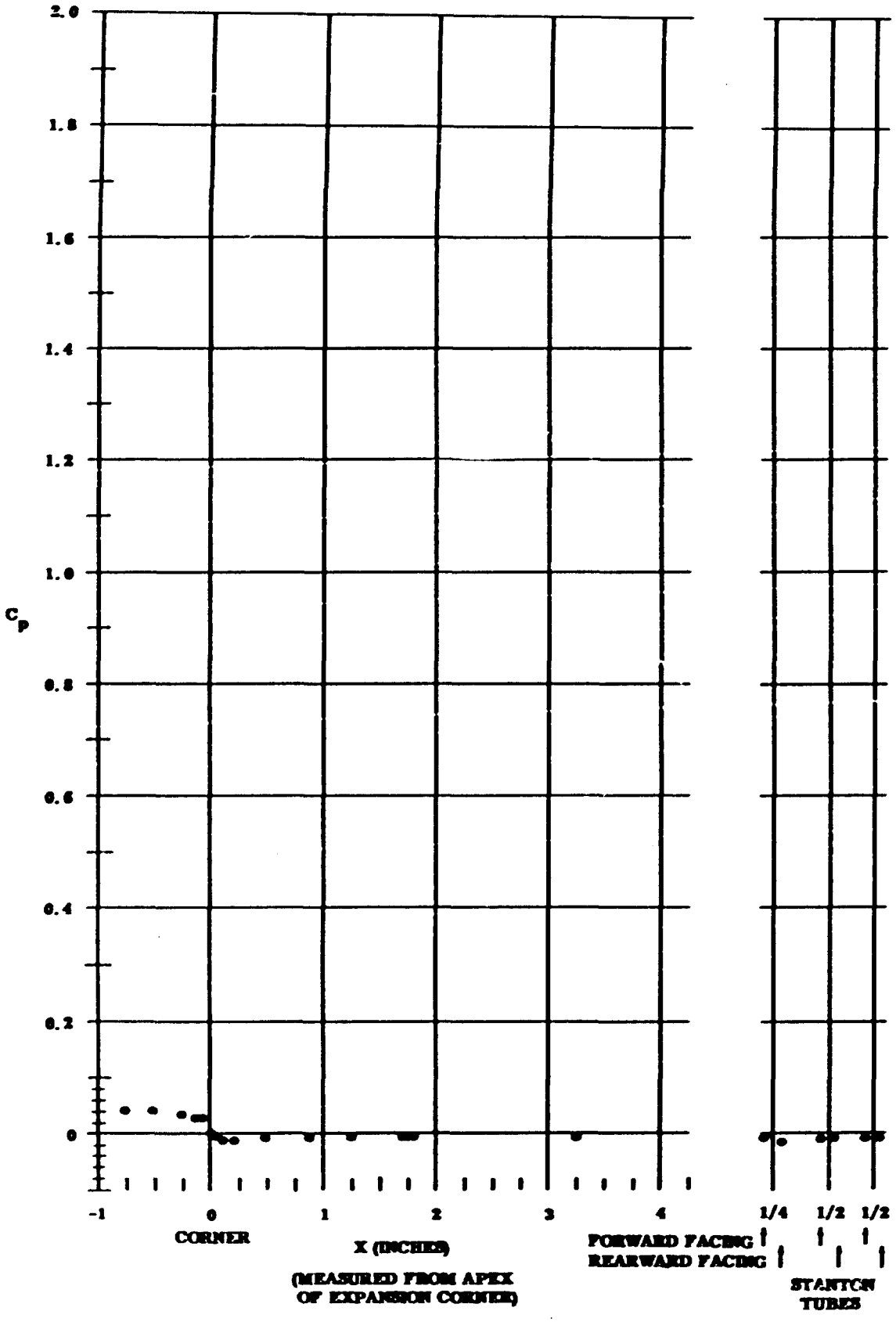

Fig. 22 Pressure Coefficient Data Plots (no coolant flow for upper surface); $\alpha = -30°$ and $Re_\infty/ft = 3{,}300{,}000$

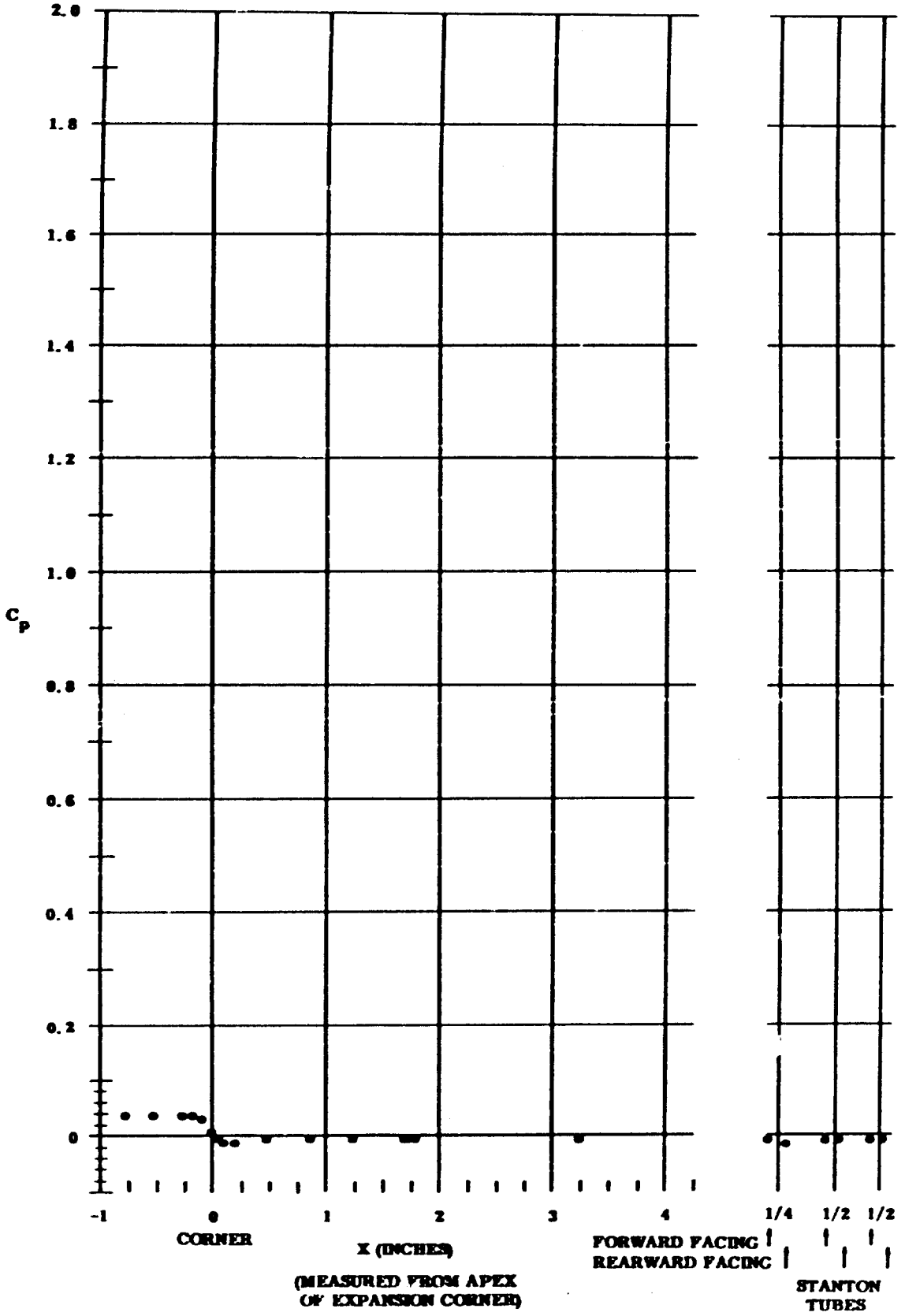

Fig. 23 Pressure Coefficient Data Plots (maximum coolant flow rate for upper surface); α = -30° and Re_{∞}/ft = 3,300,000

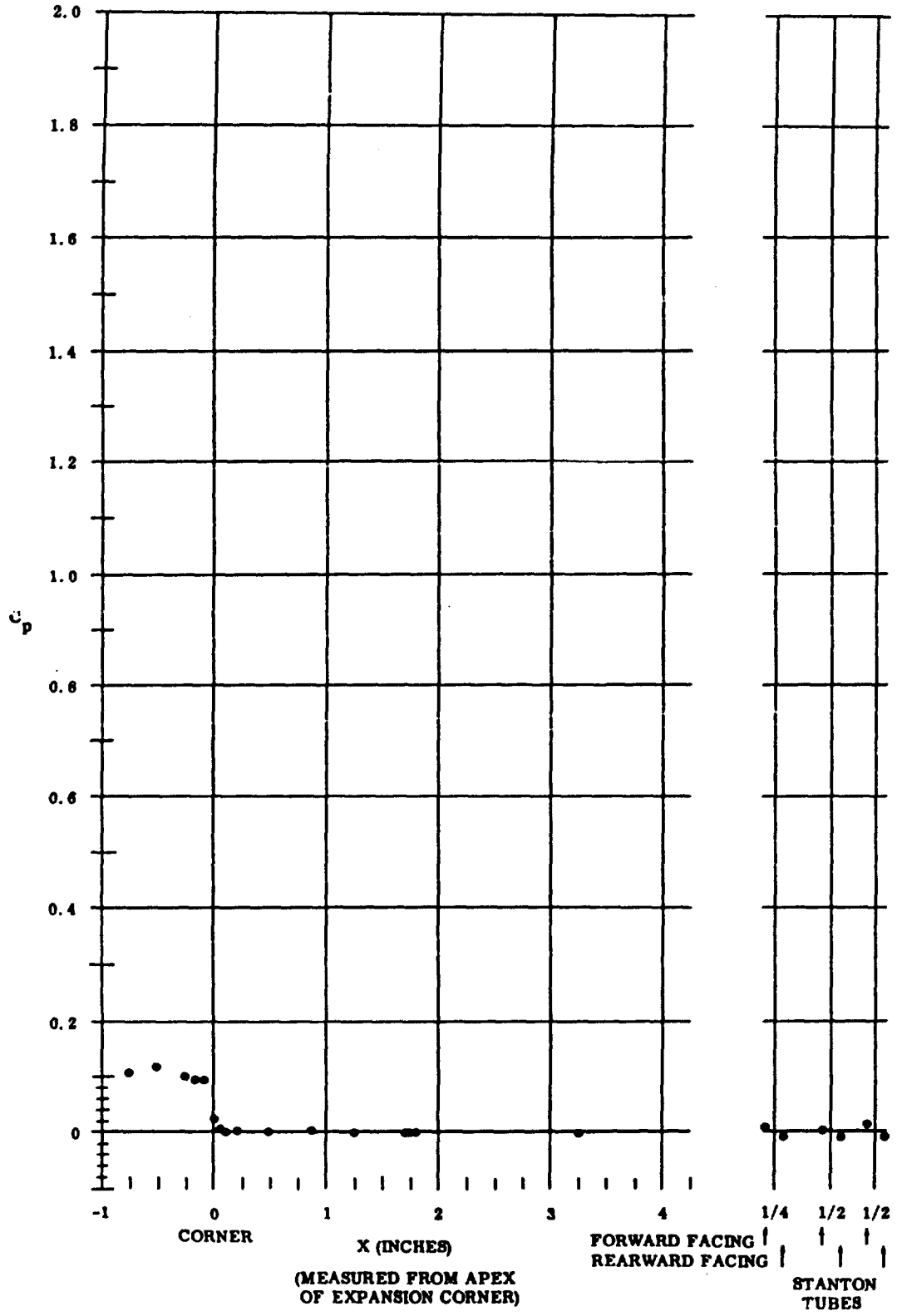

Fig. 24 Pressure Coefficient Data Plots (no coolant flow for upper surface); $\alpha = -25°$ and $Re_\infty/ft = 1{,}100{,}000$

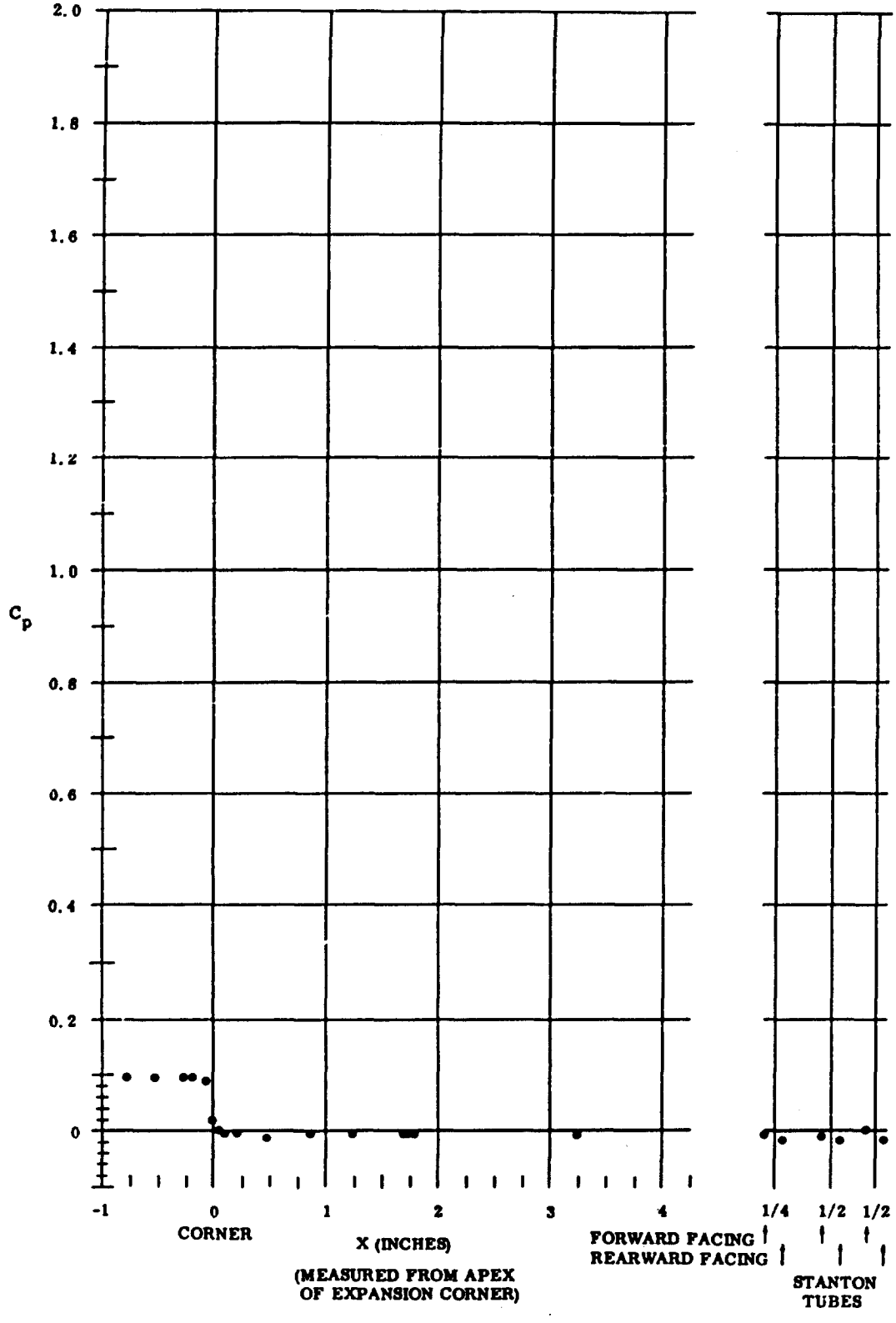

Fig. 25 Pressure Coefficient Data Plots (no coolant flow for upper surface); $\alpha = -25°$ and $Re_\infty/ft = 3,300,000$

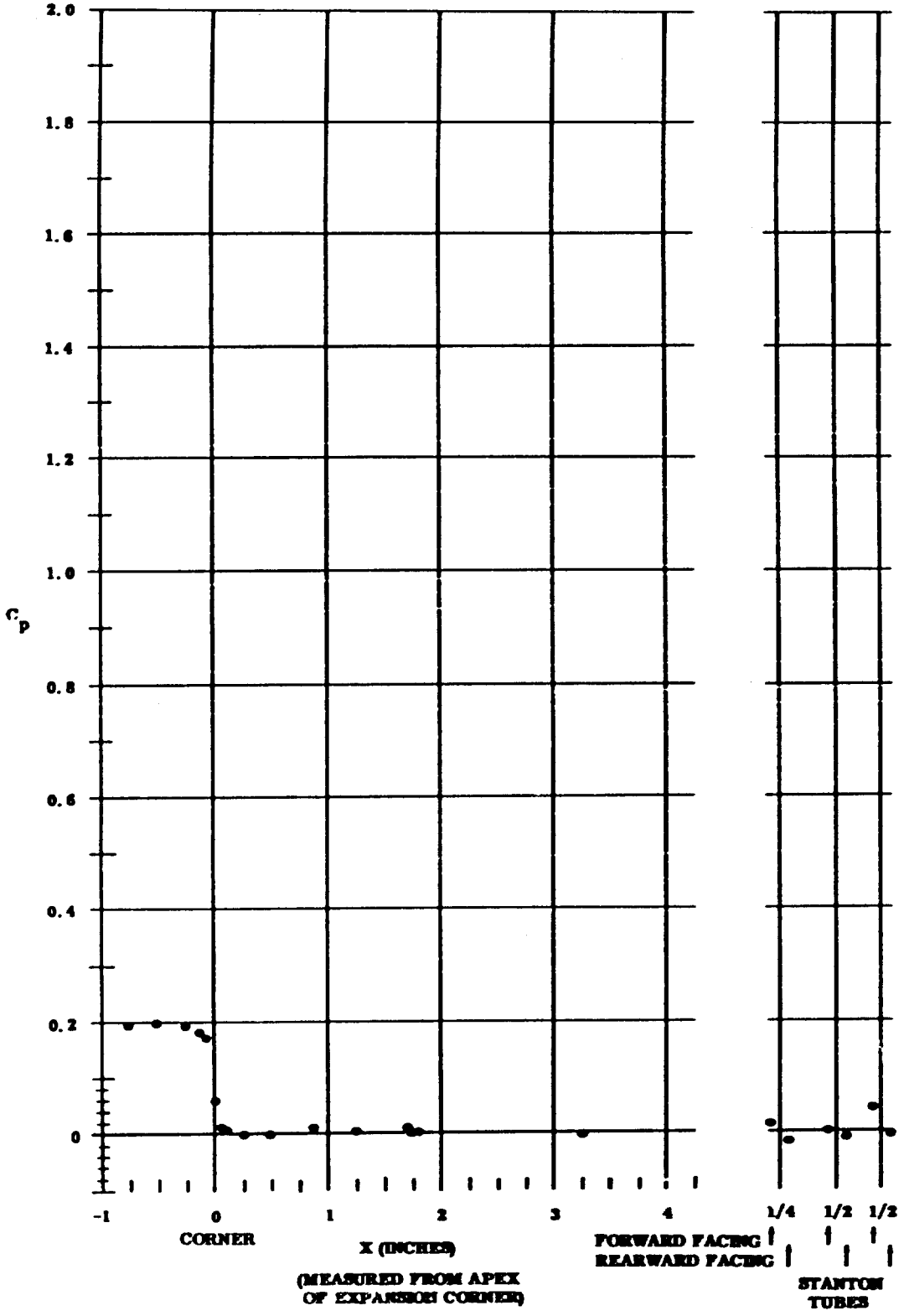

Fig. 26 Pressure Coefficient Data Plots (no coolant flow for upper surface); α = -20° and Re_∞/ft = 1,100,000

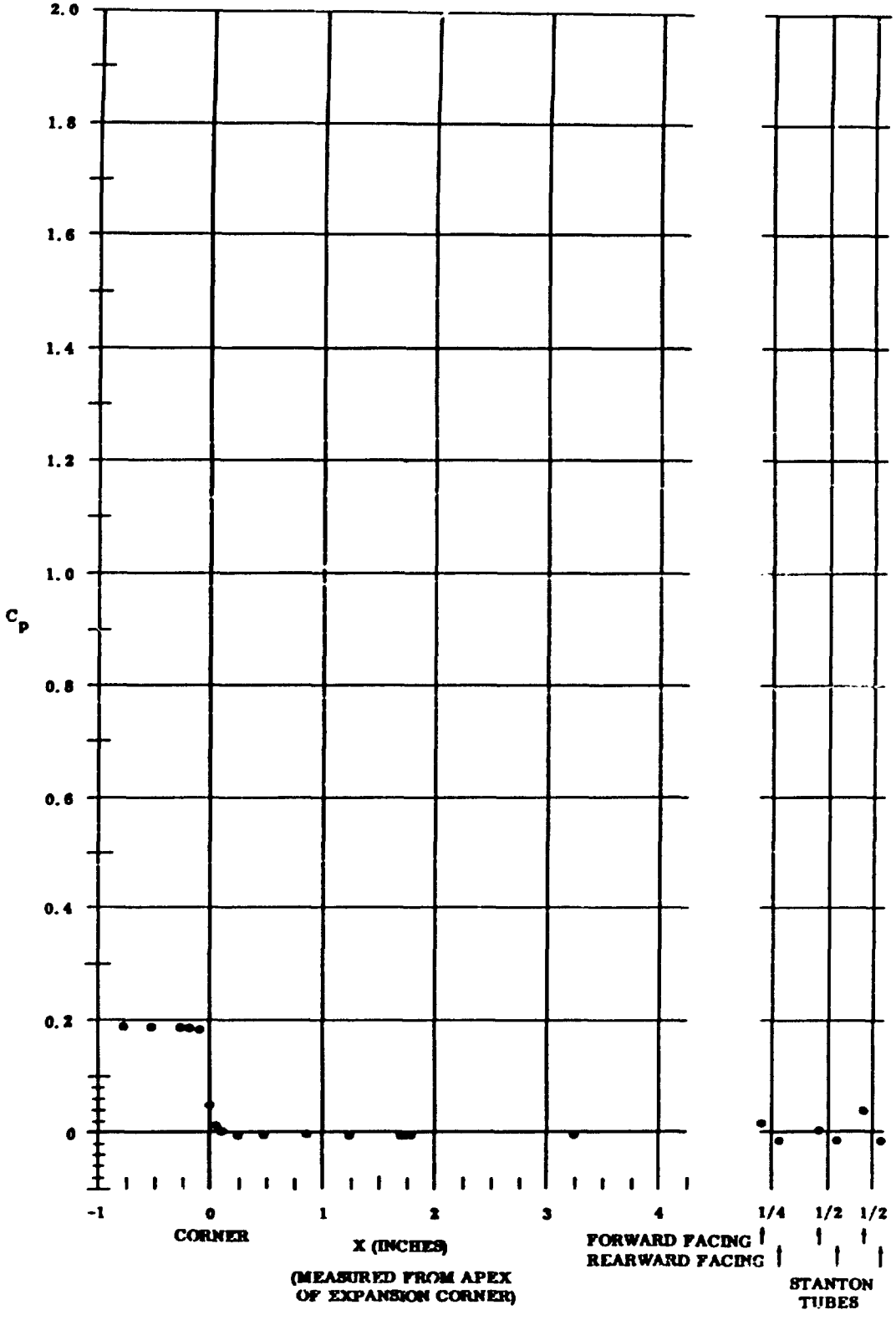

Fig. 27 Pressure Coefficient Data Plots (no coolant flow for upper surface); $\alpha = -20°$ and $Re_\infty/ft = 3,300,000$

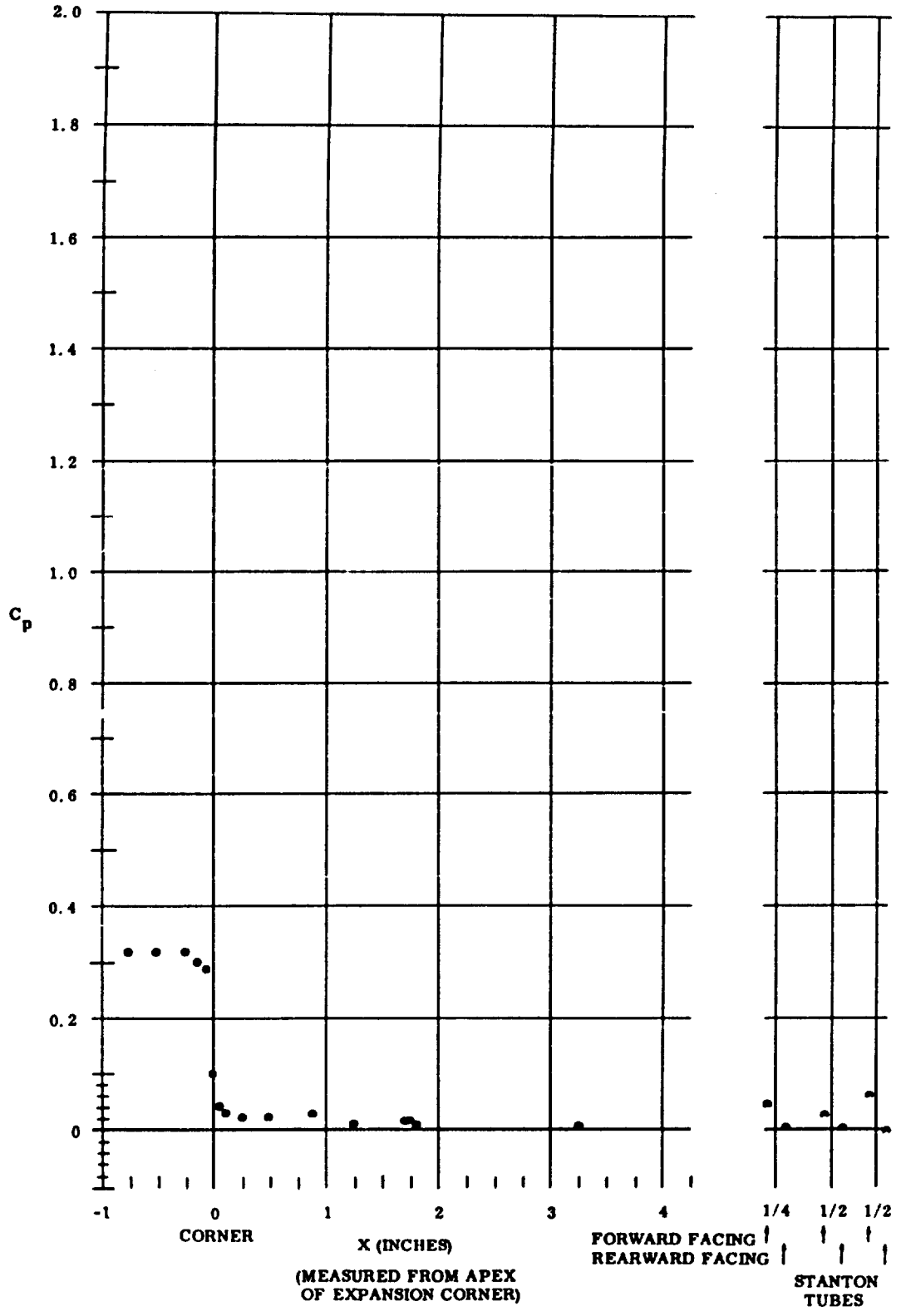

Fig. 28 Pressure Coefficient Data Plots (no coolant flow for upper surface); $\alpha = -15°$ and $Re_\omega/ft = 1{,}100{,}000$

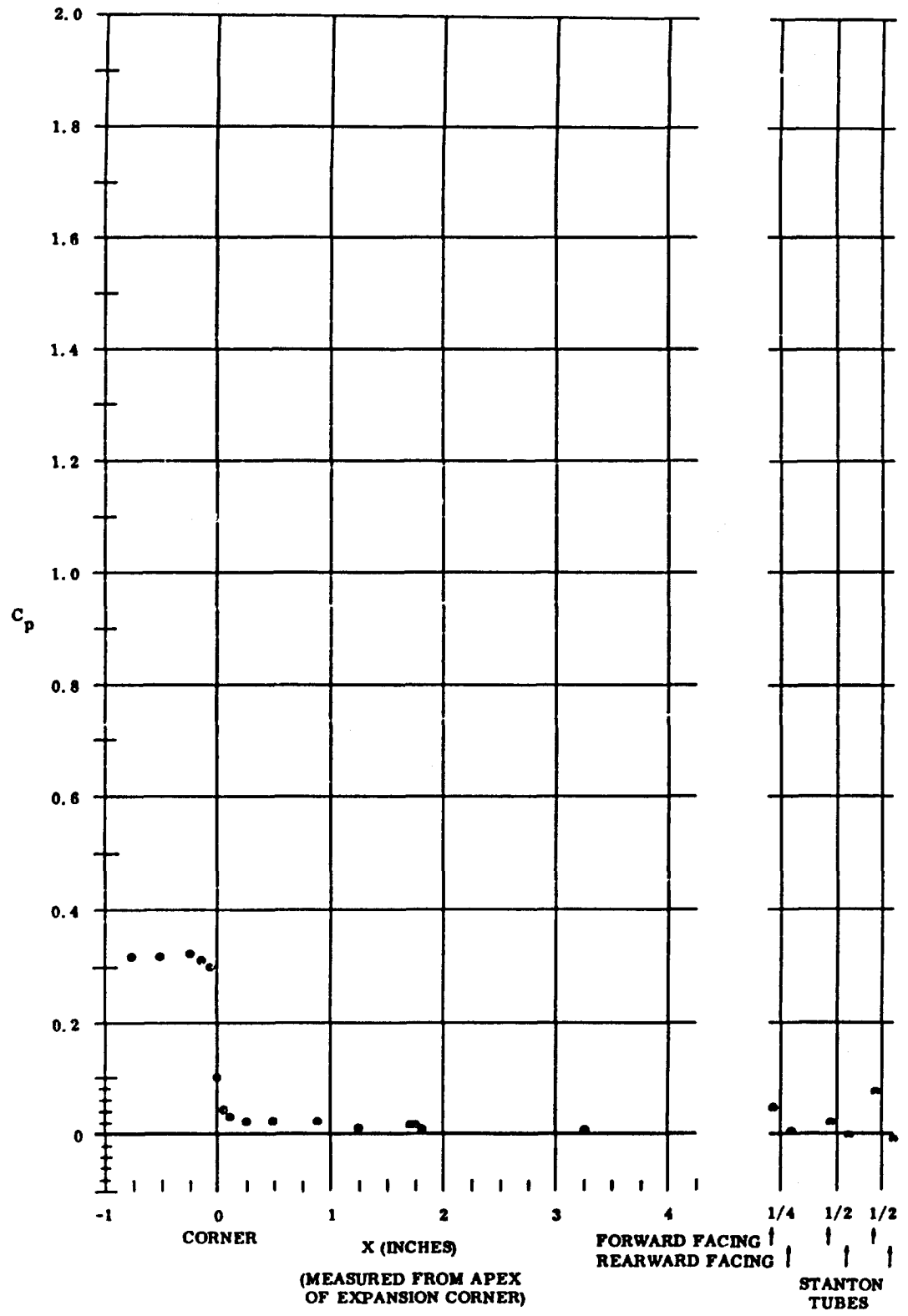

Fig. 29 Pressure Coefficient Data Plots (maximum coolant flow rate for upper surface); α = -15° and Re_∞/ft = 1,100,000

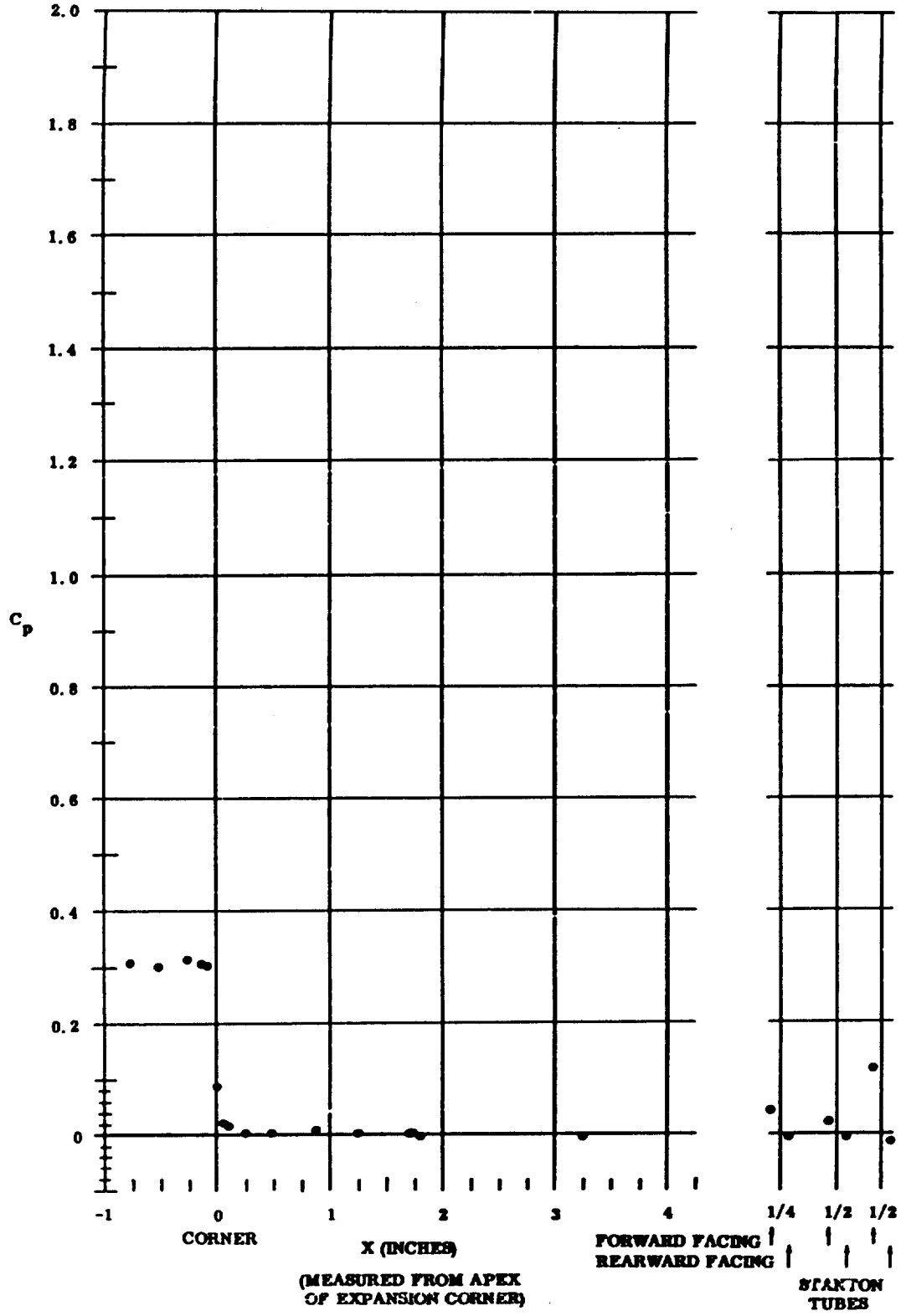

Fig. 30 Pressure Coefficient Data Plots (no coolant flow for upper surface); $\alpha = -15°$ and $Re_\infty/ft = 3{,}300{,}000$

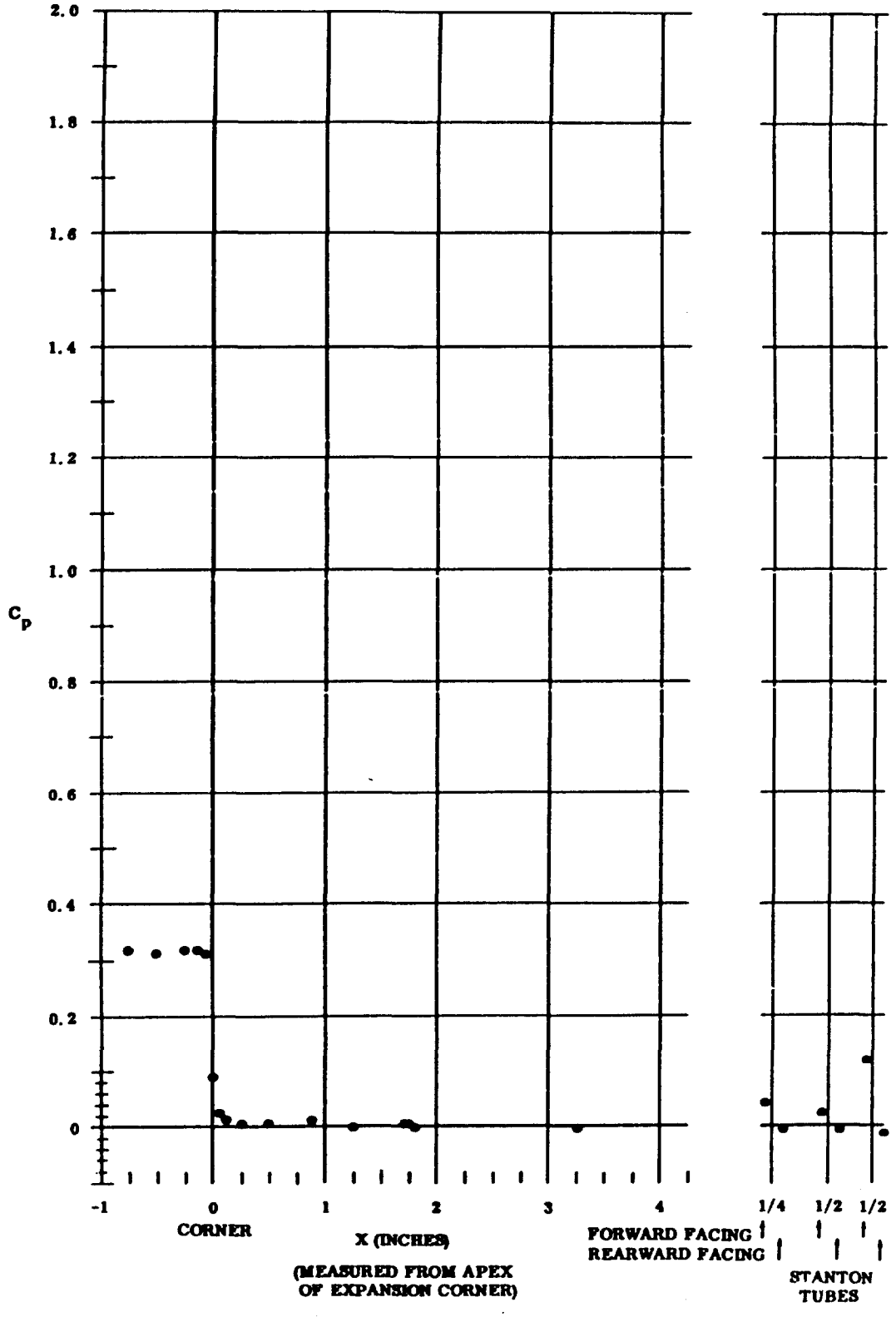

Fig. 31 Pressure Coefficient Data Plots (medium coolant flow rate for upper surface); $\alpha = -15°$ and $Re_\infty/ft = 3{,}300{,}000$

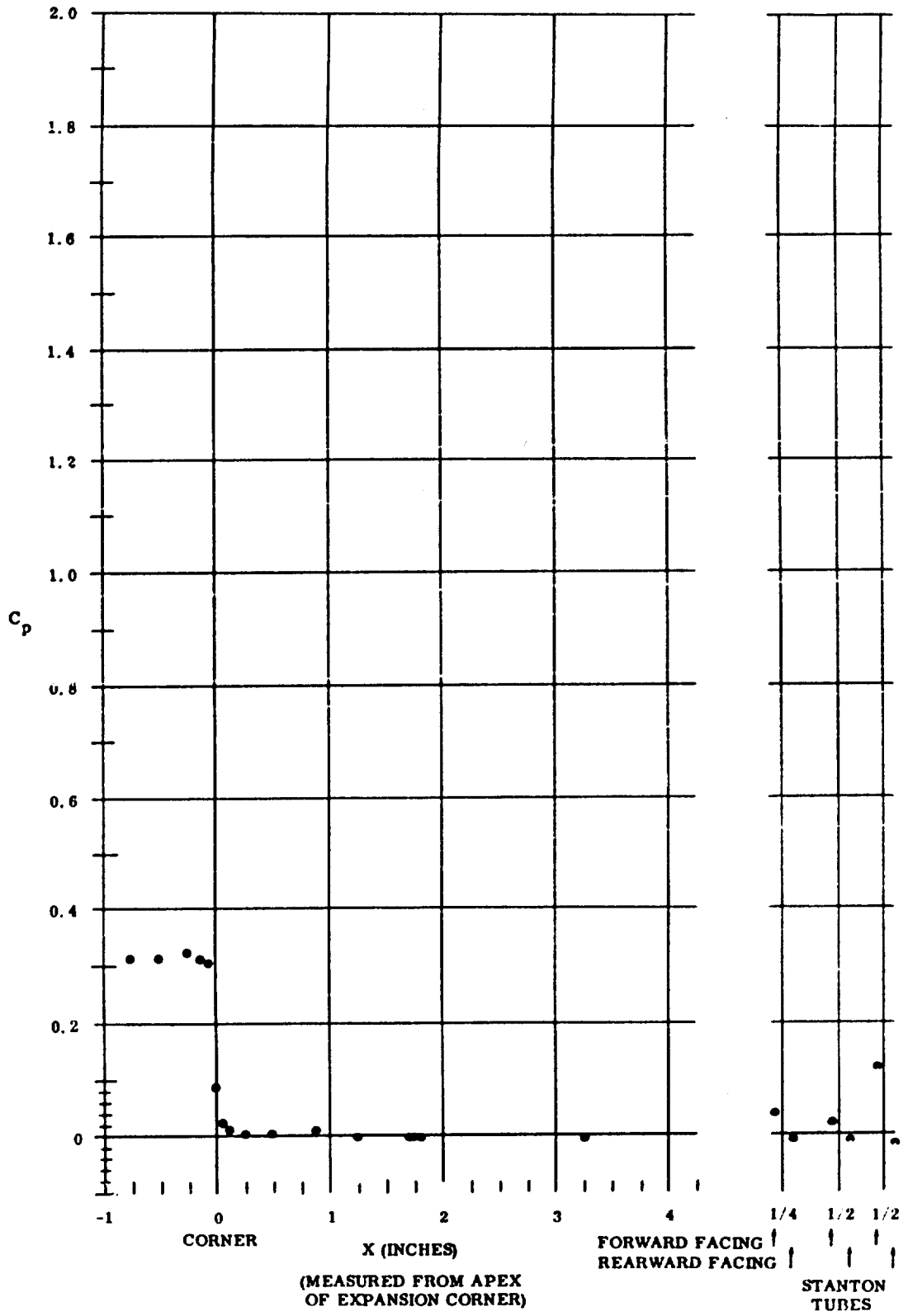

Fig. 32 Pressure Coefficient Data Plots (maximum coolant flow rate for upper surface); $\alpha = -15°$ and $Re_\infty/ft = 3{,}300{,}000$

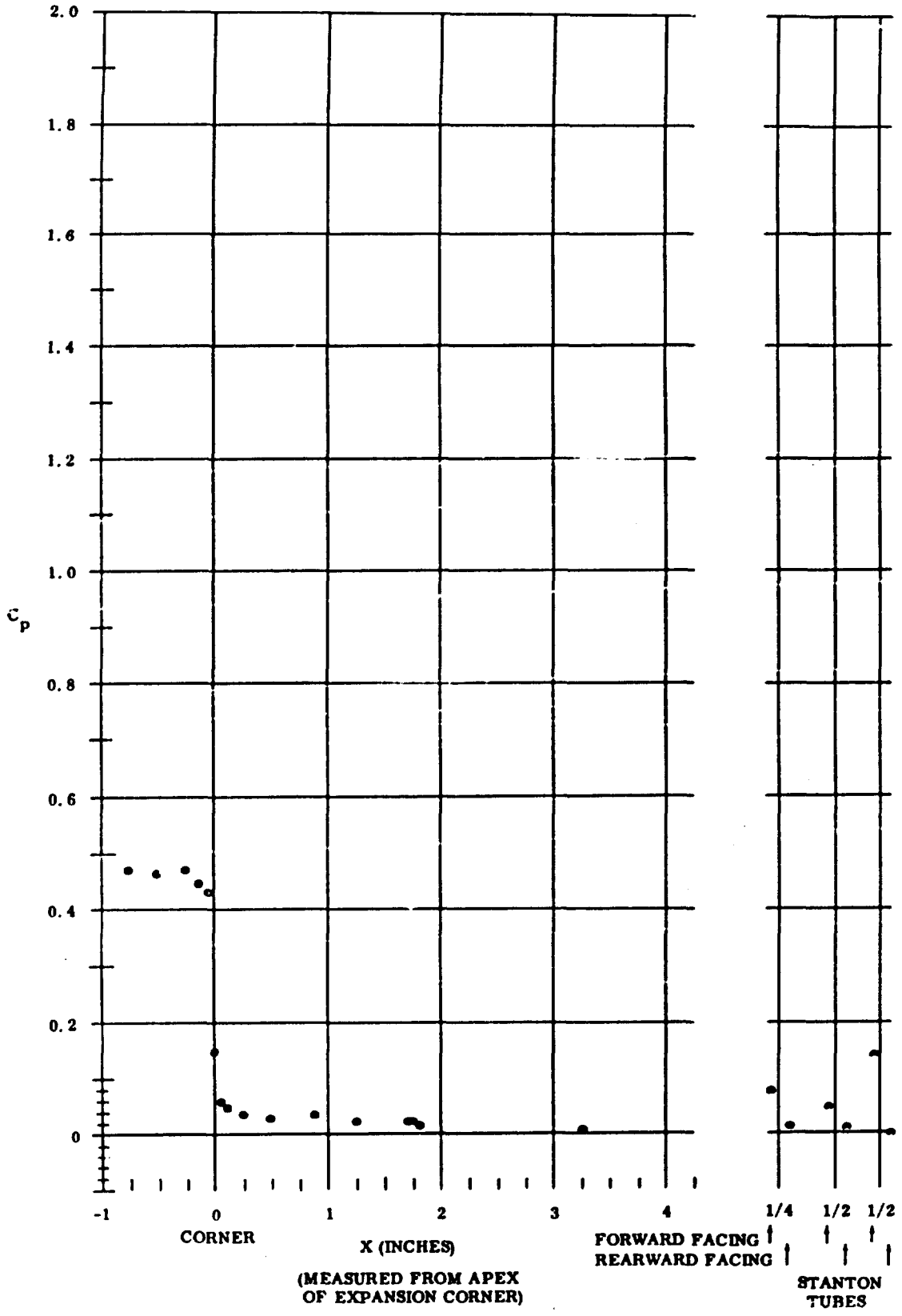

Fig. 33 Pressure Coefficient Data Plots (no coolant flow for upper surface); $\alpha = -10°$ and $Re_\infty/ft = 1{,}100{,}000$

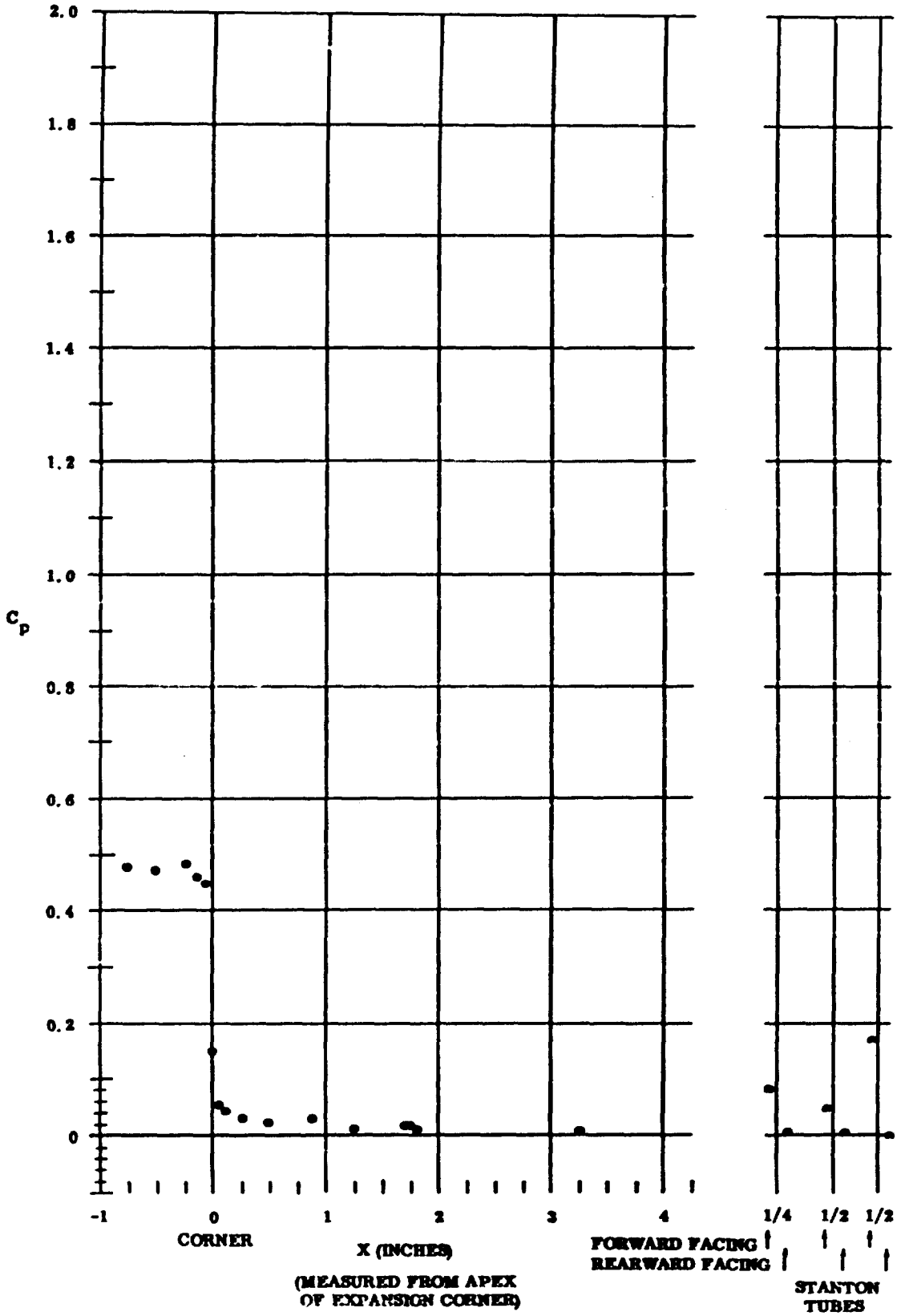

Fig. 34 Pressure Coefficient Data Plots (maximum coolant flow rate for upper surface); $\alpha = -10°$ and $Re_\infty/ft = 1{,}100{,}000$

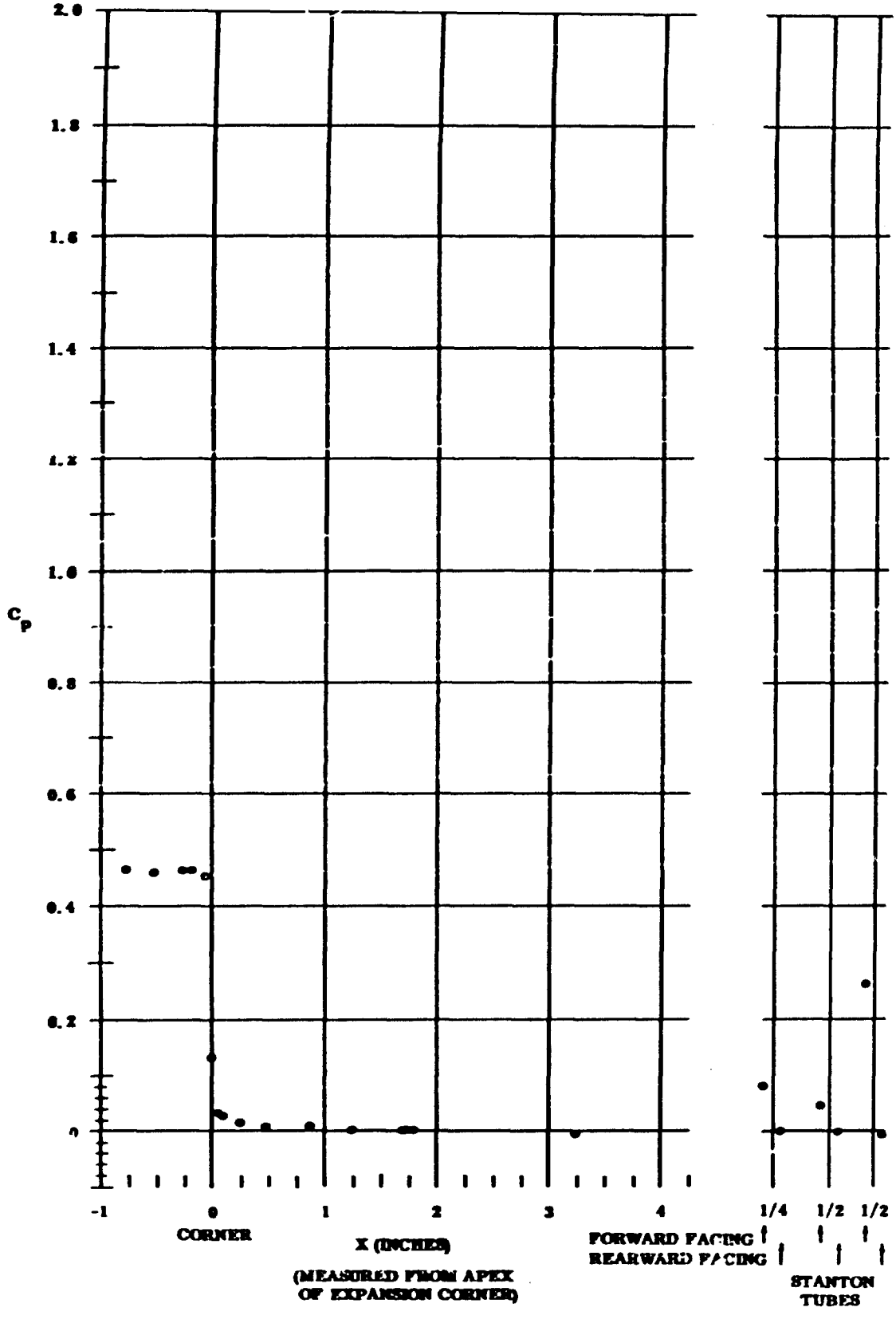

Fig. 35 Pressure Coefficient Data Plots (no coolant flow for upper surface); $\alpha = -10°$ and $Re_\infty/ft = 3{,}300{,}000$

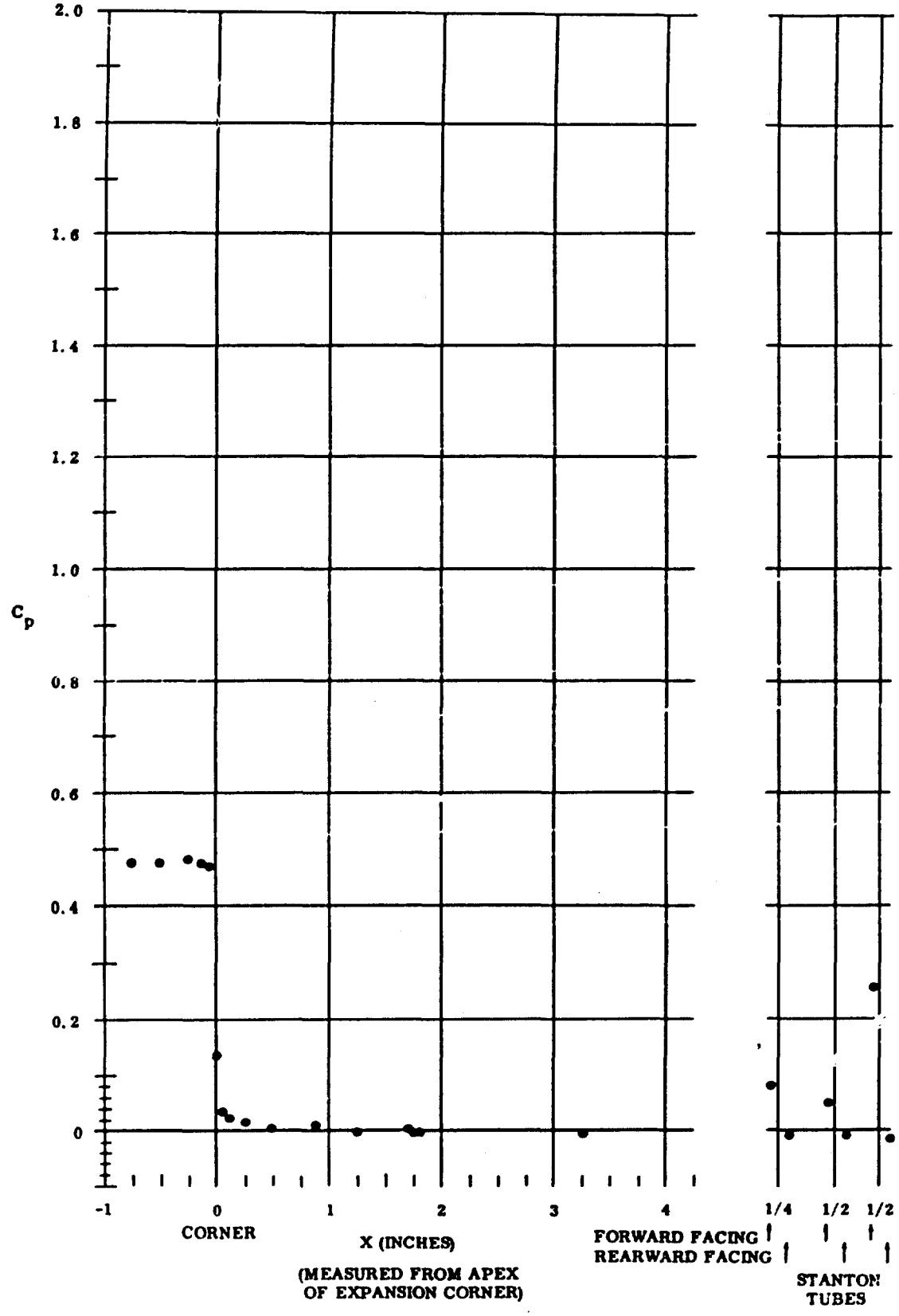

Fig. 36 Pressure Coefficient Data Plots (maximum coolant flow rate for upper surface); $\alpha = -10°$ and $Re_\infty/ft = 3{,}300{,}000$

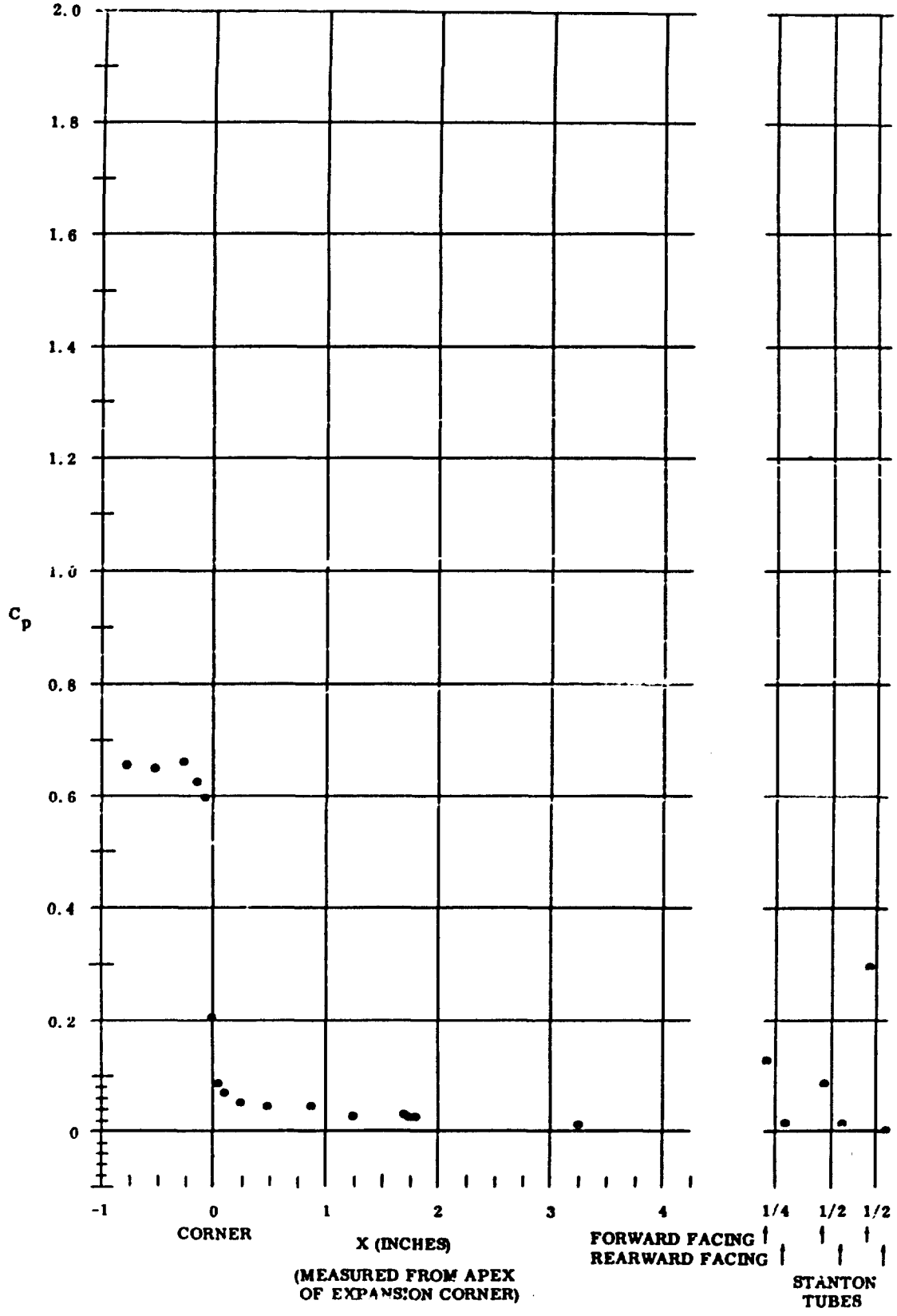

Fig. 37 Pressure Coefficient Data Plots (no coolant flow for upper surface); $\alpha = -5°$ and $Re_\infty/ft = 1{,}100{,}000$

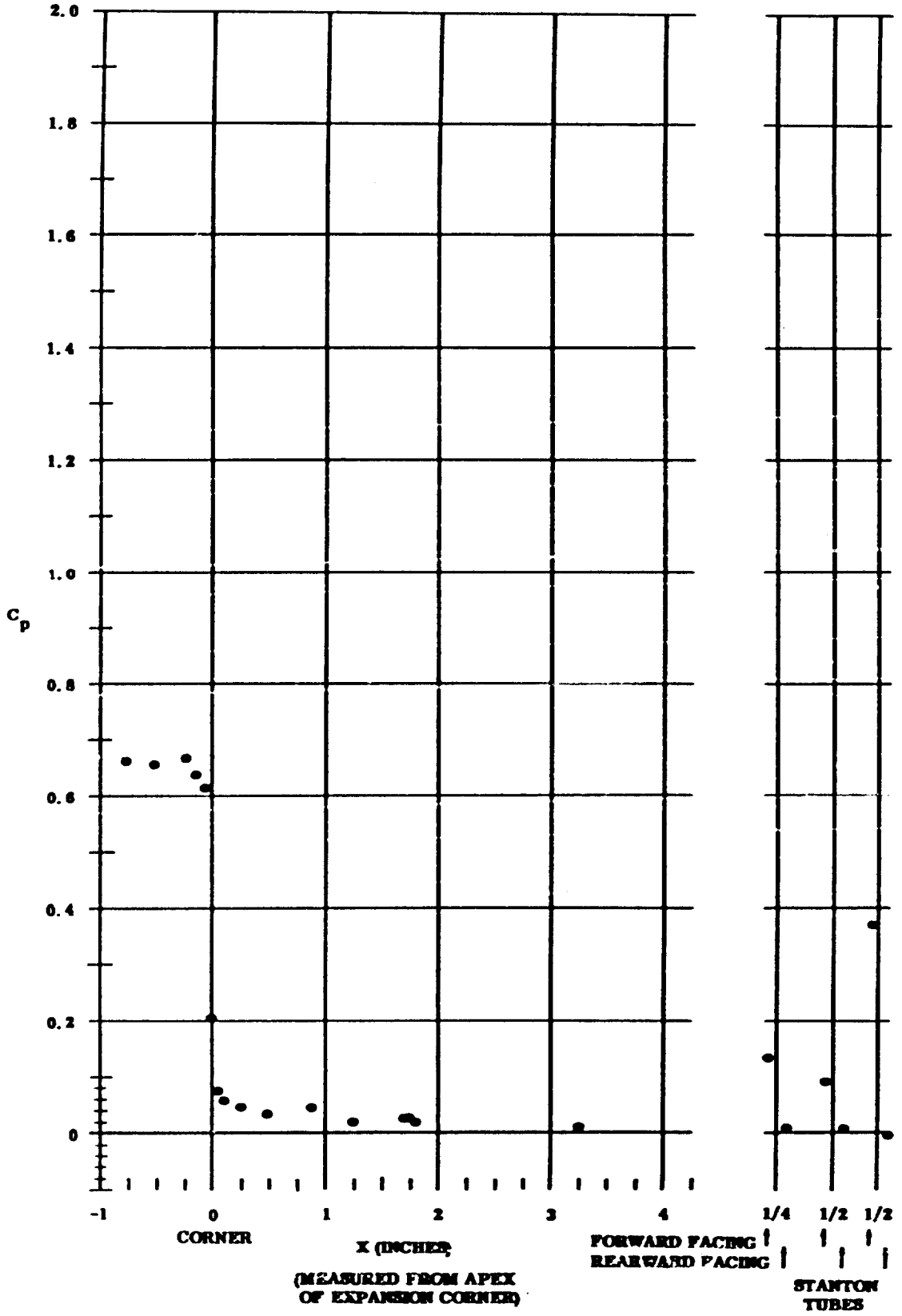

Fig. 38 Pressure Coefficient Data Plots (maximum coolant flow rate for upper surface); $\alpha = -5°$ and $Re_{\infty}/ft = 1{,}100{,}000$

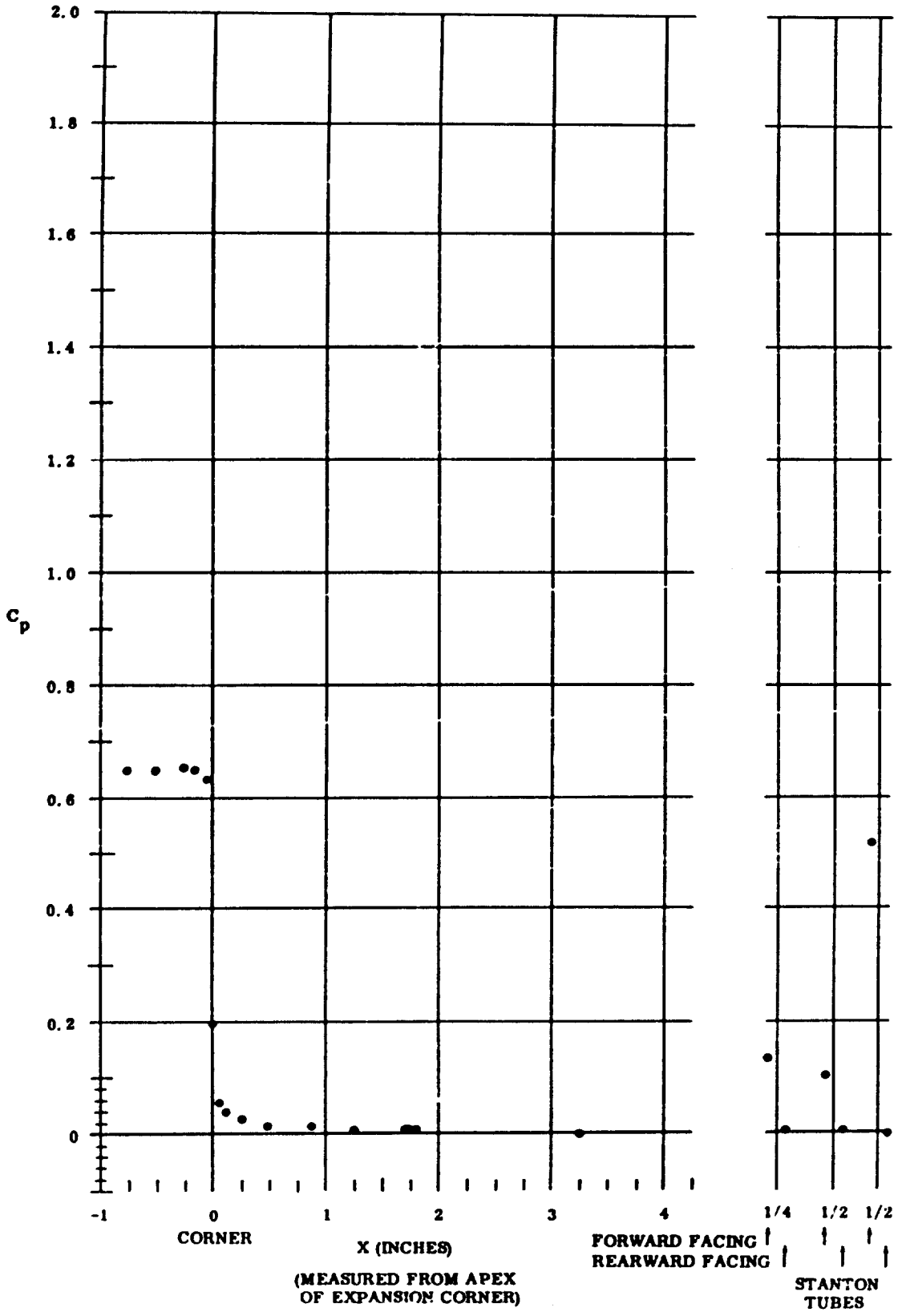

Fig. 39 Pressure Coefficient Data Plots (no coolant flow for upper surface); $\alpha = -5°$ and $Re_\infty/ft = 3{,}300{,}000$

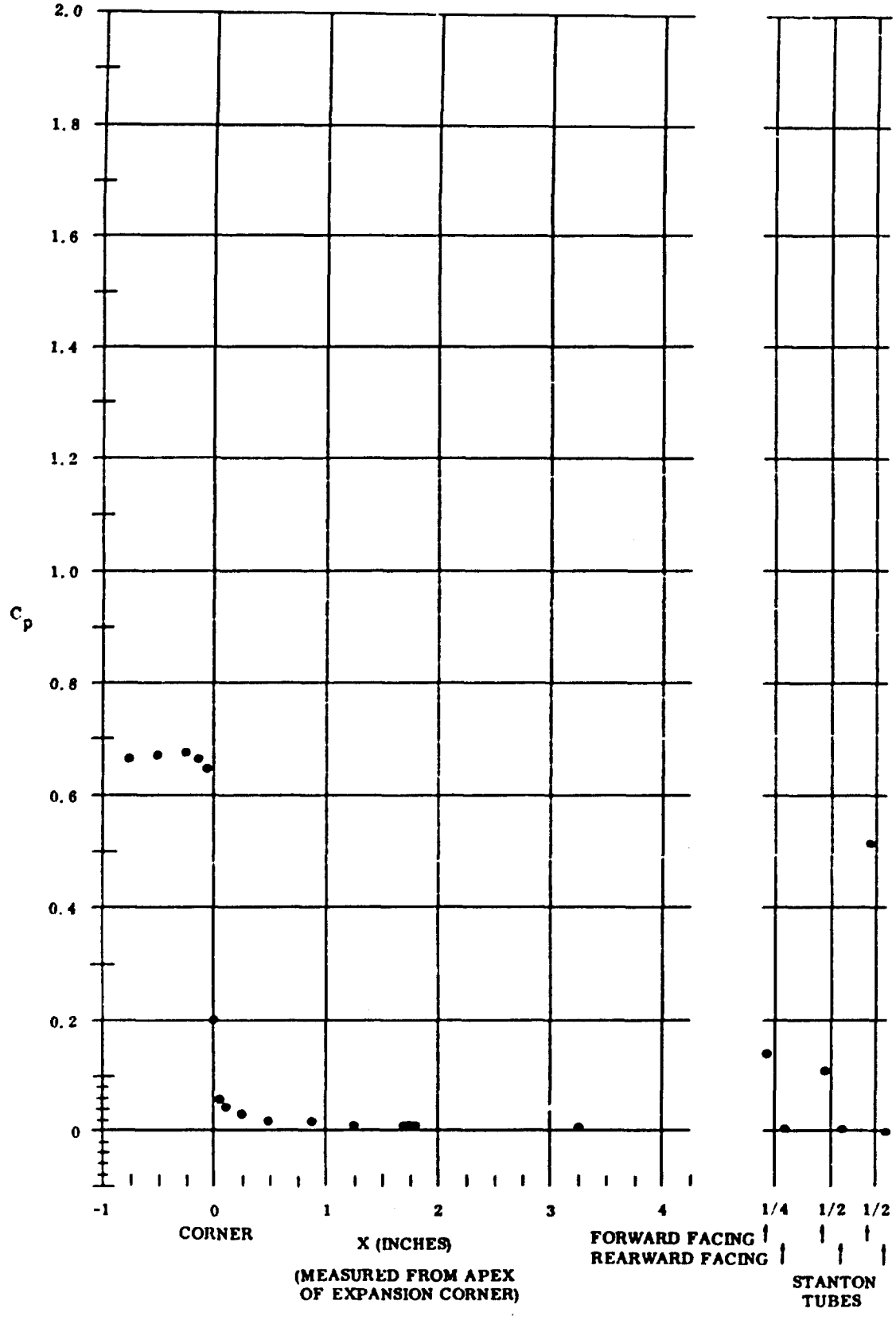

Fig. 40 Pressure Coefficient Data Plots (medium coolant flow rate for upper surface); α = -5° and Re_∞/ft = 3,300,000

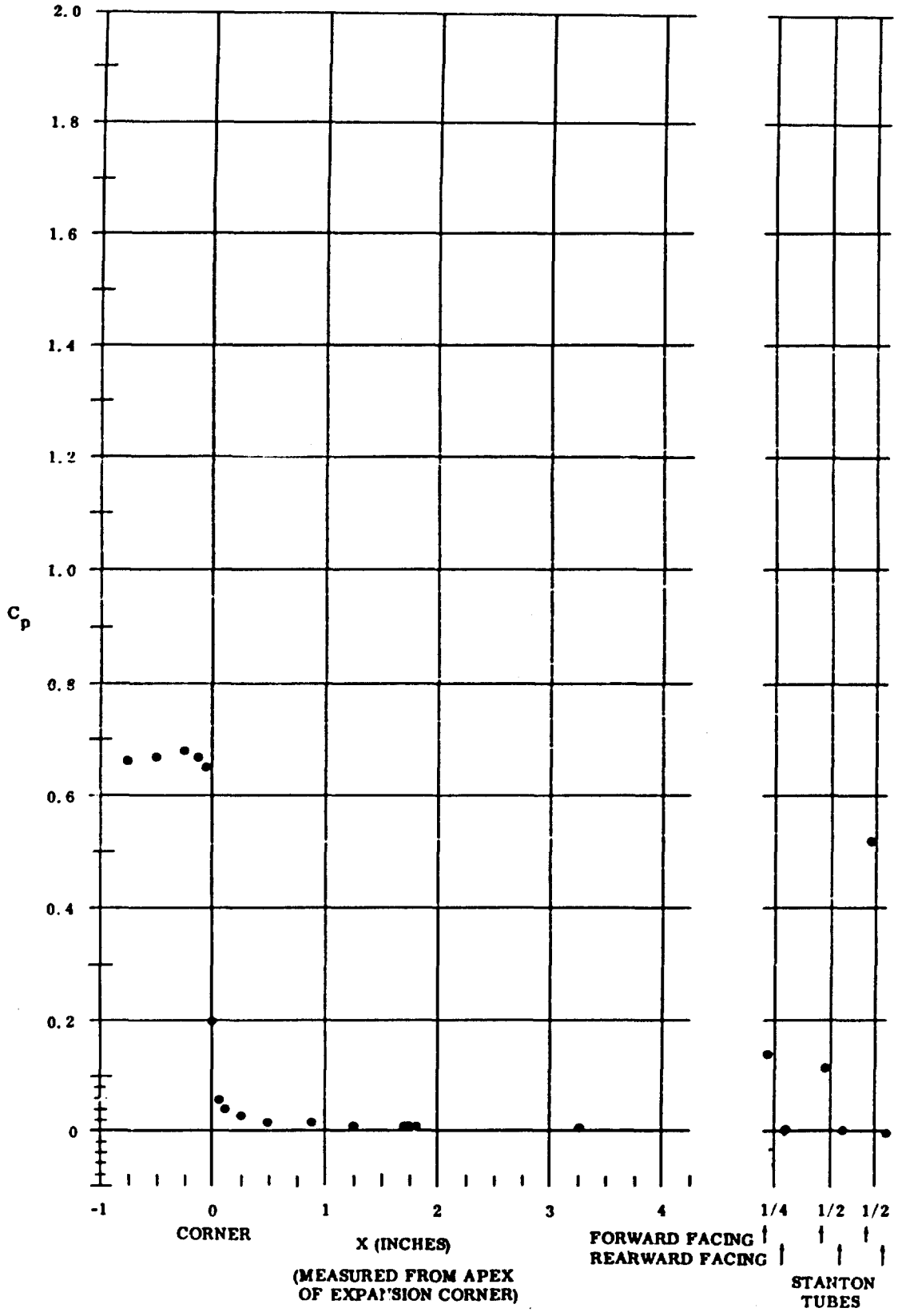

Fig. 41 Pressure Coefficient Data Plots (maximum coolant flow rate for upper surface); $\alpha = -5°$ and $Re_\infty/ft = 3{,}300{,}000$

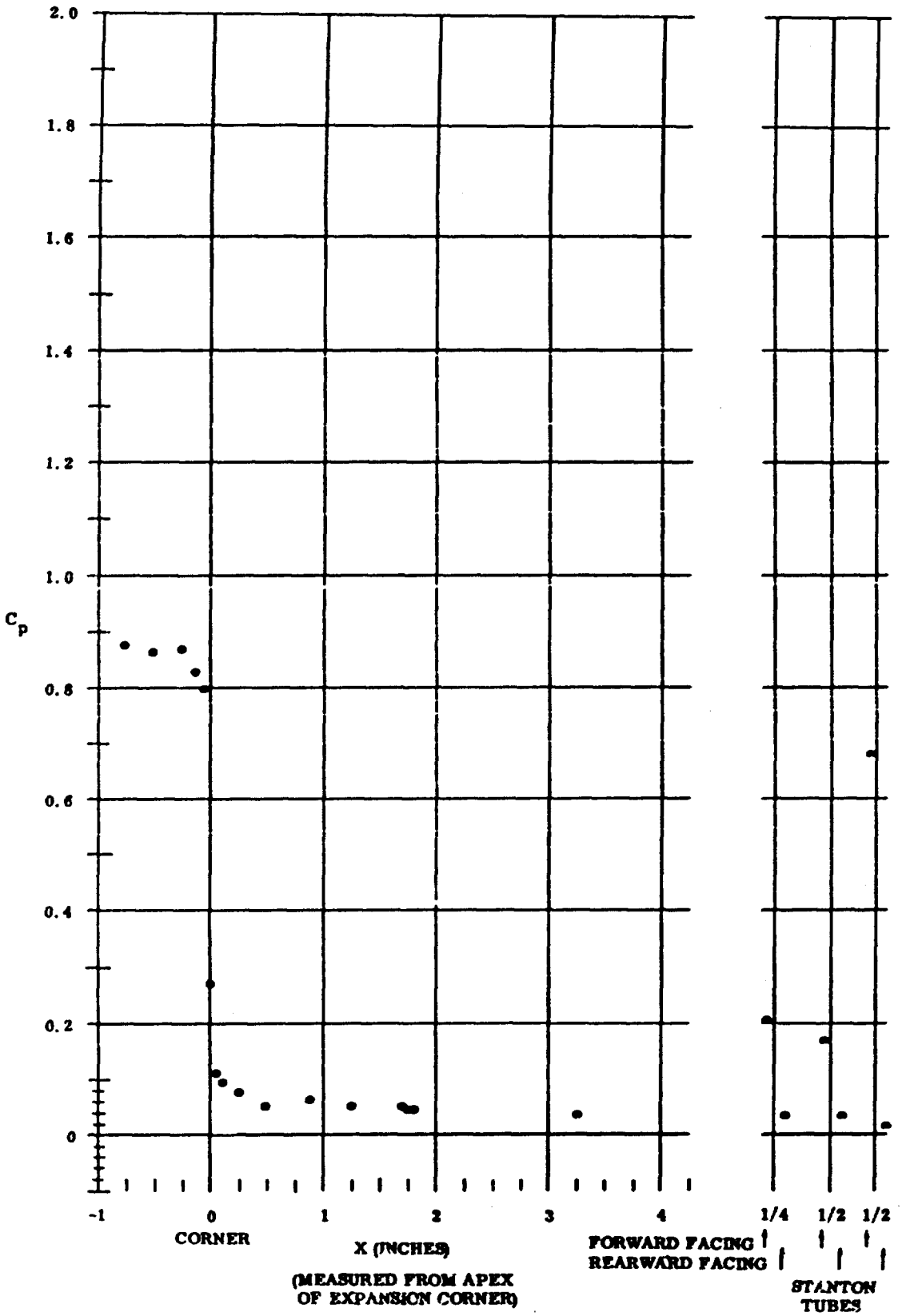

Fig. 42 Pressure Coefficient Data Plots (no coolant flow for upper surface); $\alpha = 0°$ and $Re_\infty/ft = 1{,}100{,}000$

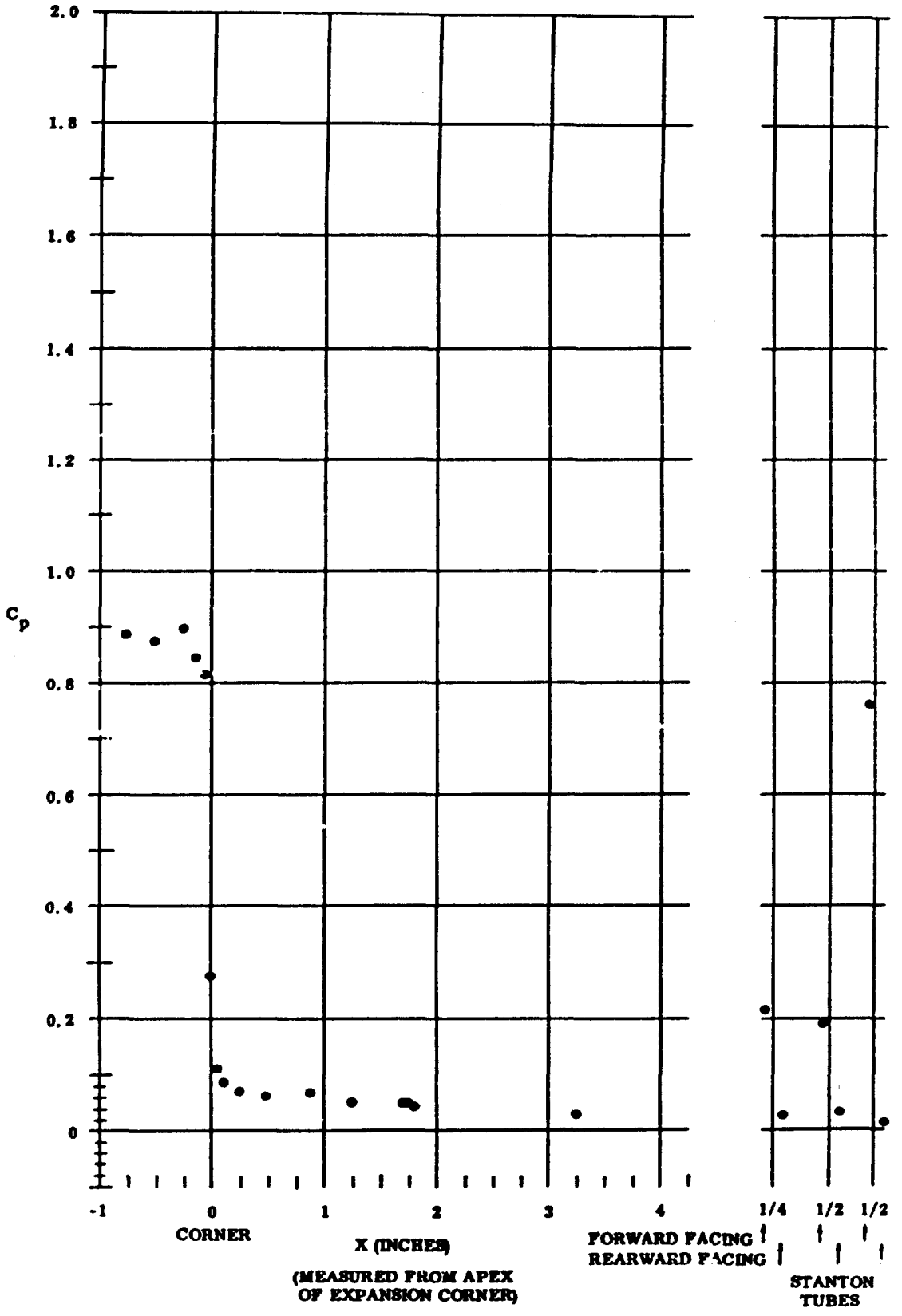

Fig. 43 Pressure Coefficient Data Plots (maximum coolant flow rate for upper surface); $\alpha = 0°$ and $Re_\infty/ft = 1{,}100{,}000$

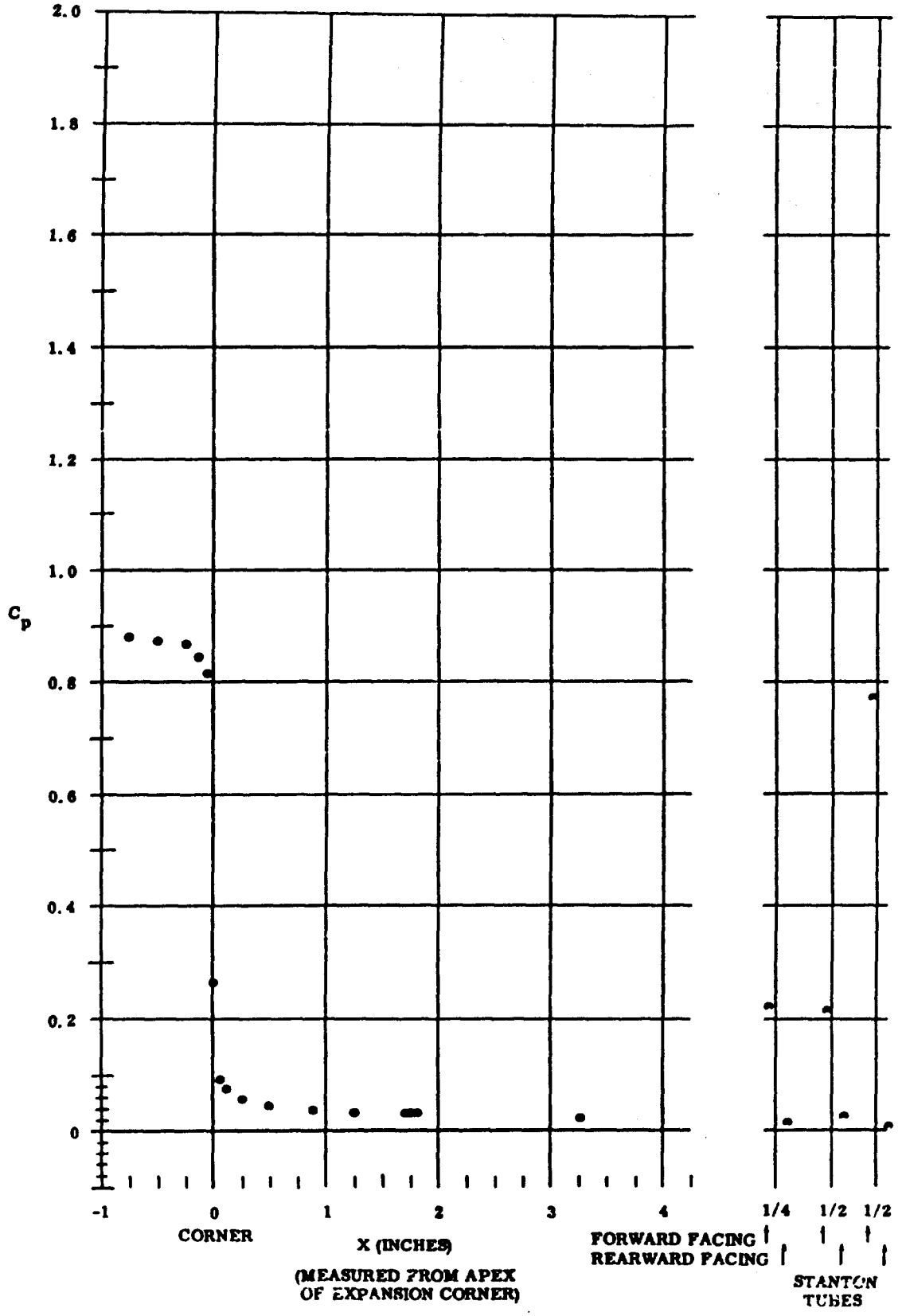

Fig. 44 Pressure Coefficient Data Plots (no coolant flow for upper surface); $\alpha = 0°$ and $Re_\infty/ft = 2{,}200{,}000$

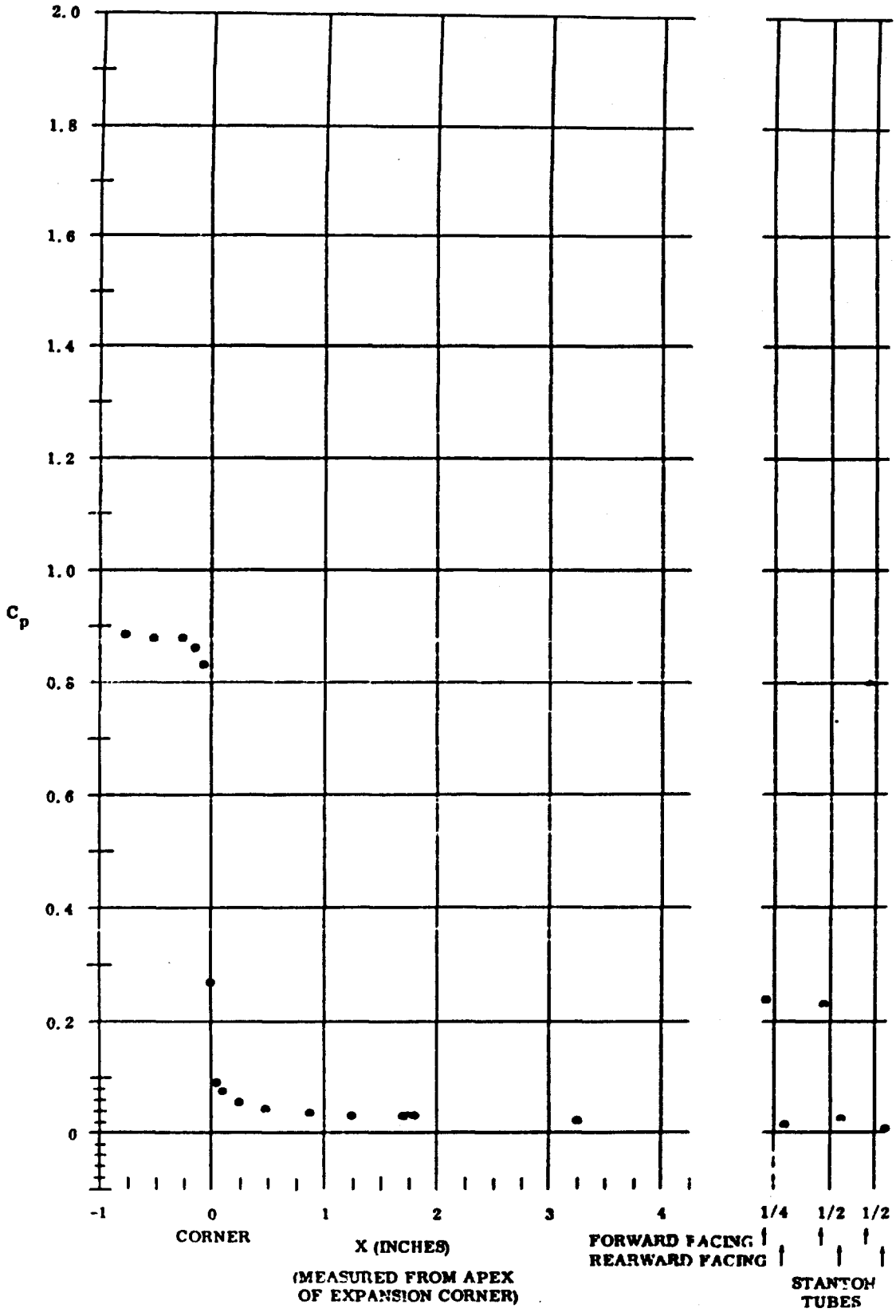

Fig. 45 Pressure Coefficient Data Plots (maximum coolant flow rate for upper surface); $\alpha = 0°$ and $Re_\infty/ft = 2{,}200{,}000$

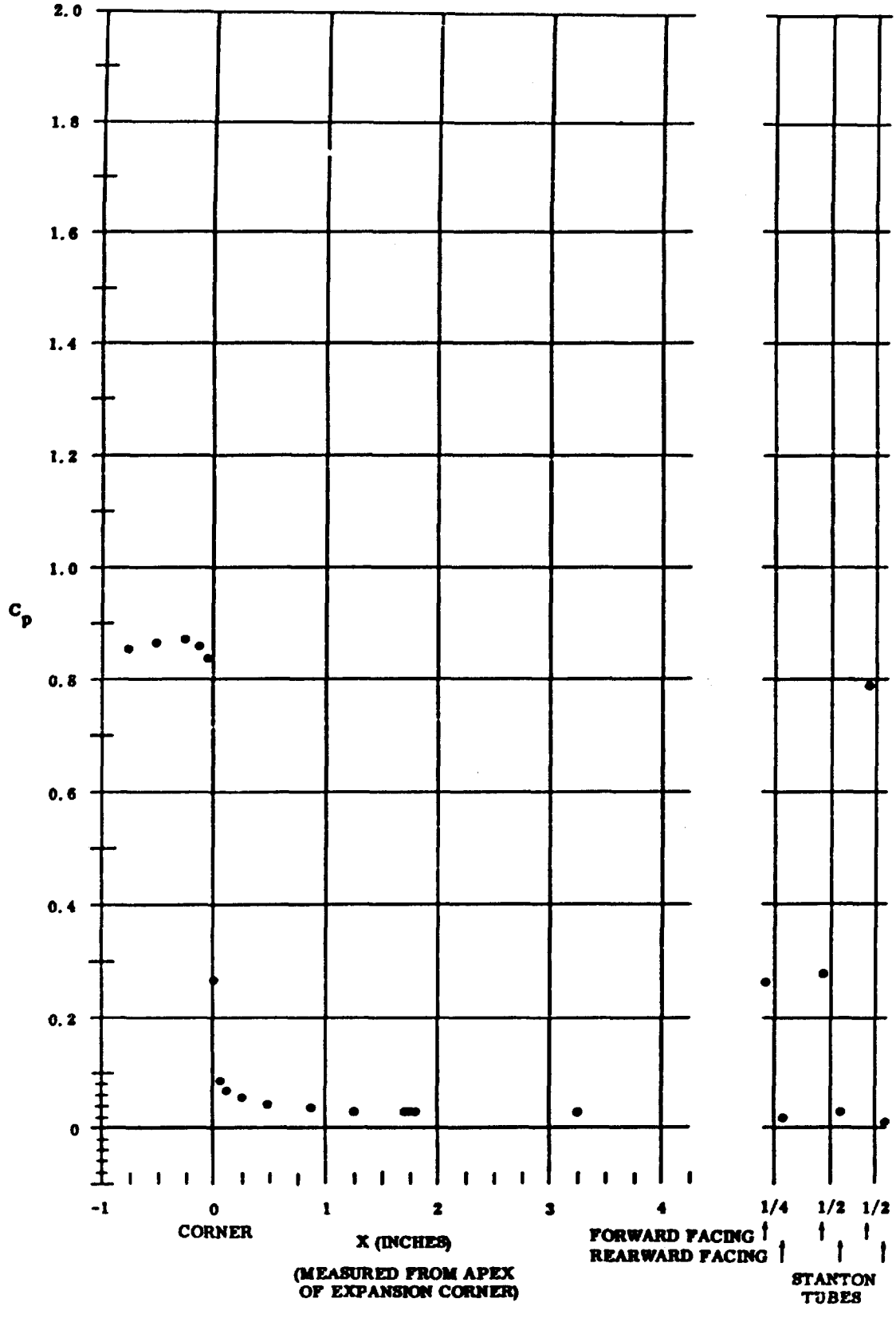

Fig. 46 Pressure Coefficient Data Plots (no coolant flow for upper surface); $\alpha = 0°$ and $Re_\infty/ft = 3{,}300{,}000$

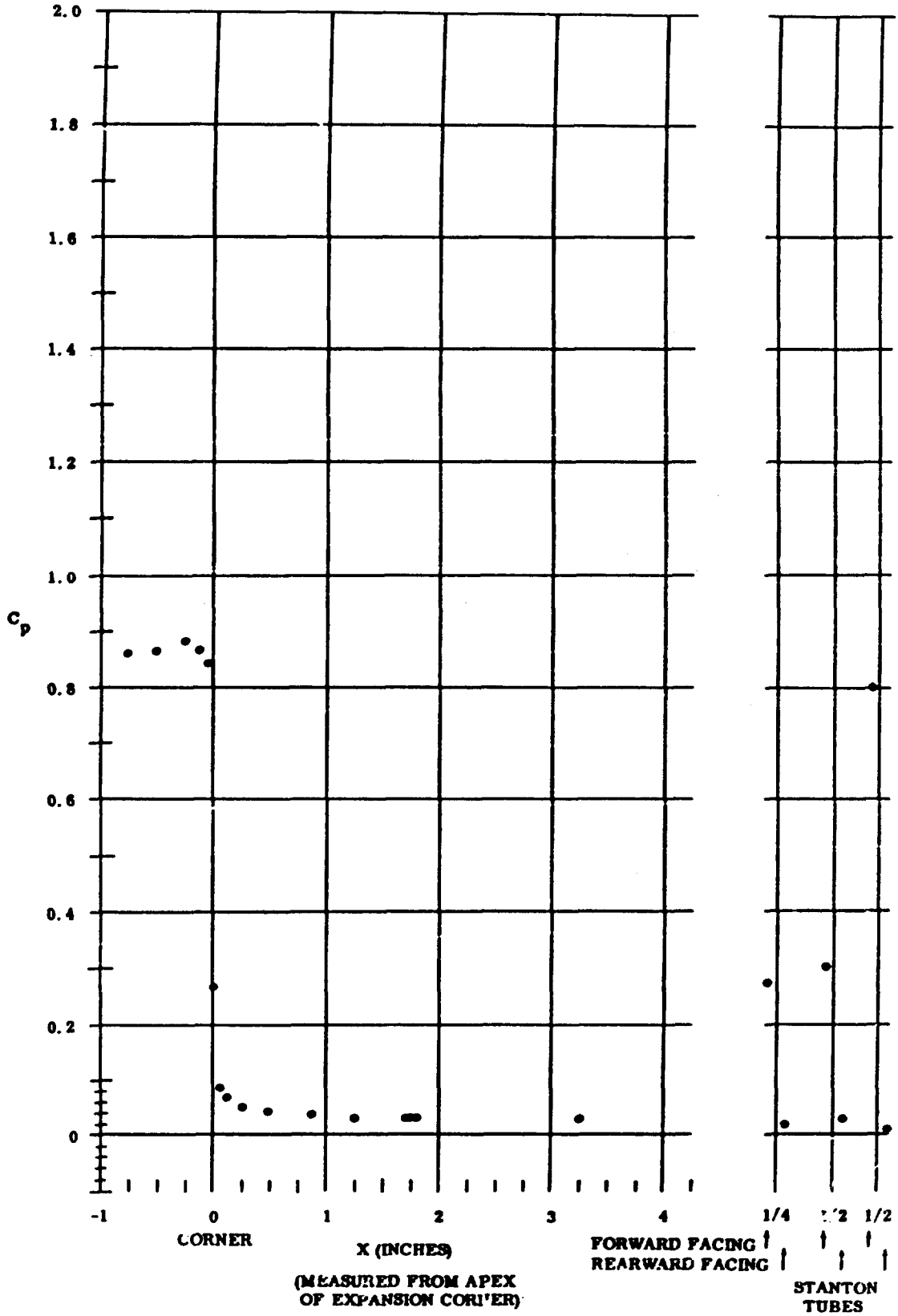

Fig. 47 Pressure Coefficient Data Plots (medium coolant flow rate for upper surface); $\alpha = 0°$ and $Re_\infty/ft = 3{,}300{,}000$

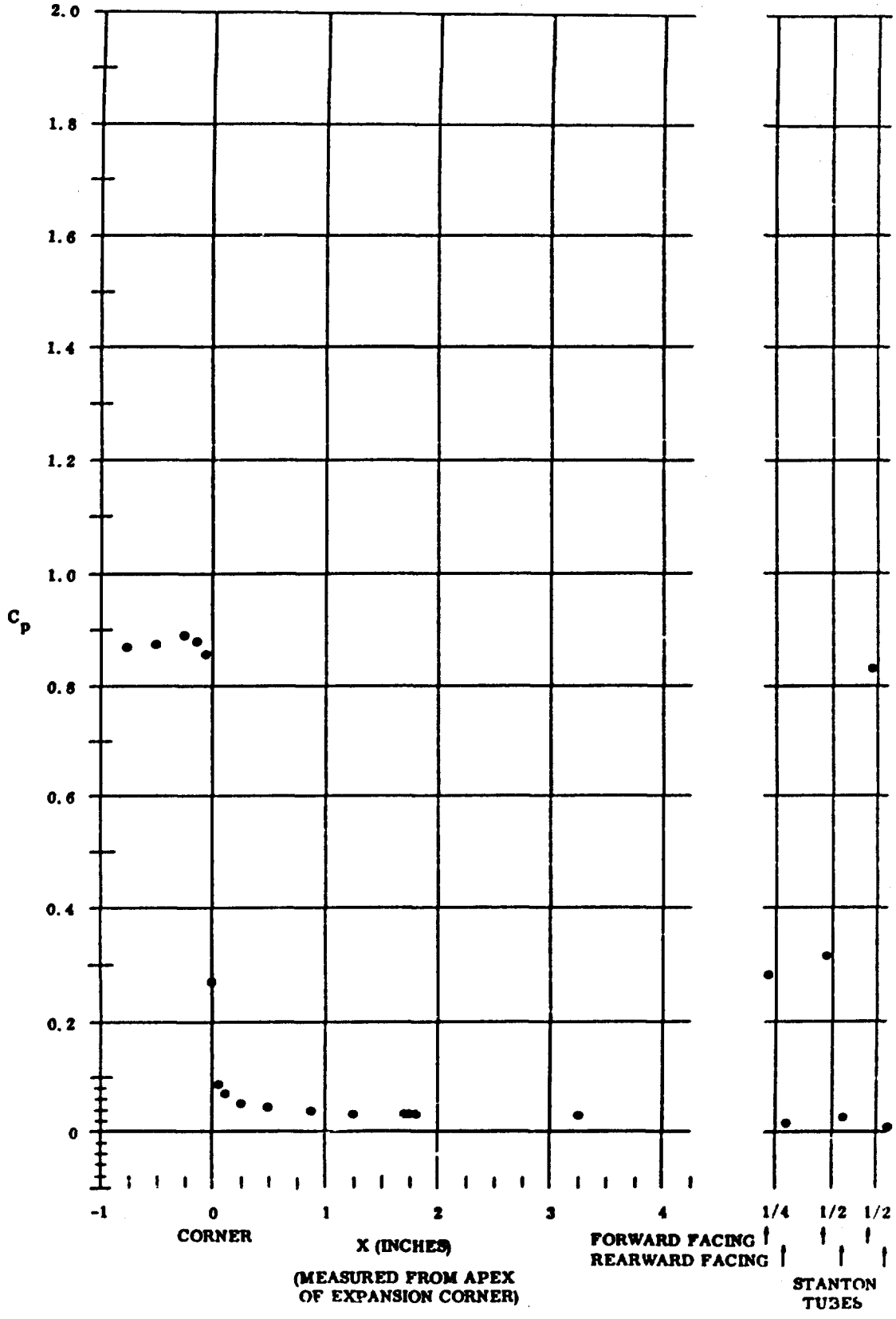

Fig. 48 Pressure Coefficient Data Plots (maximum coolant flow rate for upper surface); $\alpha = 0°$ and $Re_\infty/ft = 3{,}300{,}000$

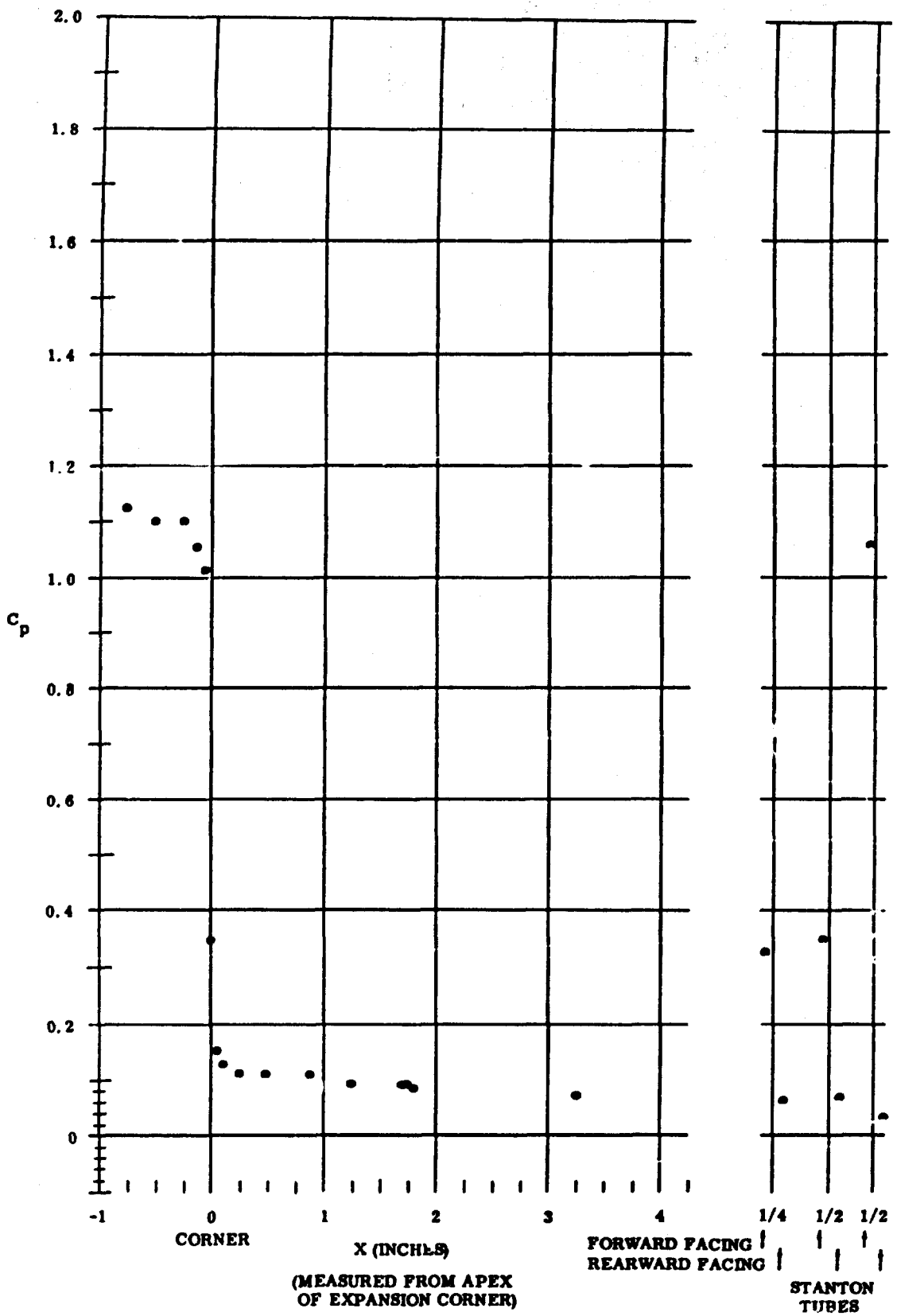

Fig. 49 Pressure Coefficient Data Plots (no coolant flow for upper surface); $\alpha = +5°$ and $Re_\infty/ft = 1{,}100{,}000$

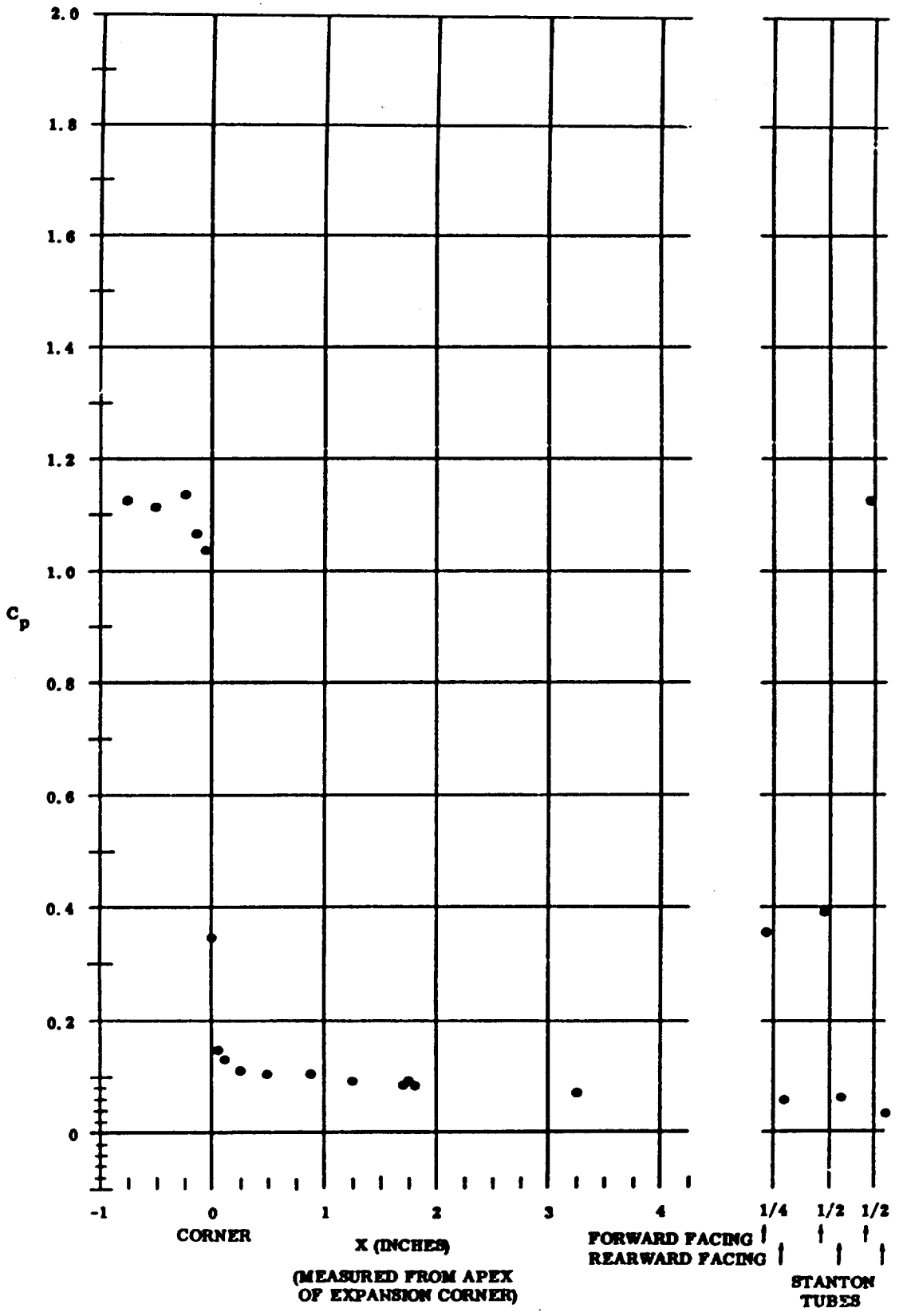

Fig. 50 Pressure Coefficient Data Plots (maximum coolant flow rate for upper surface); $\alpha = +5°$ and $Re_\infty/ft = 1{,}100{,}000$

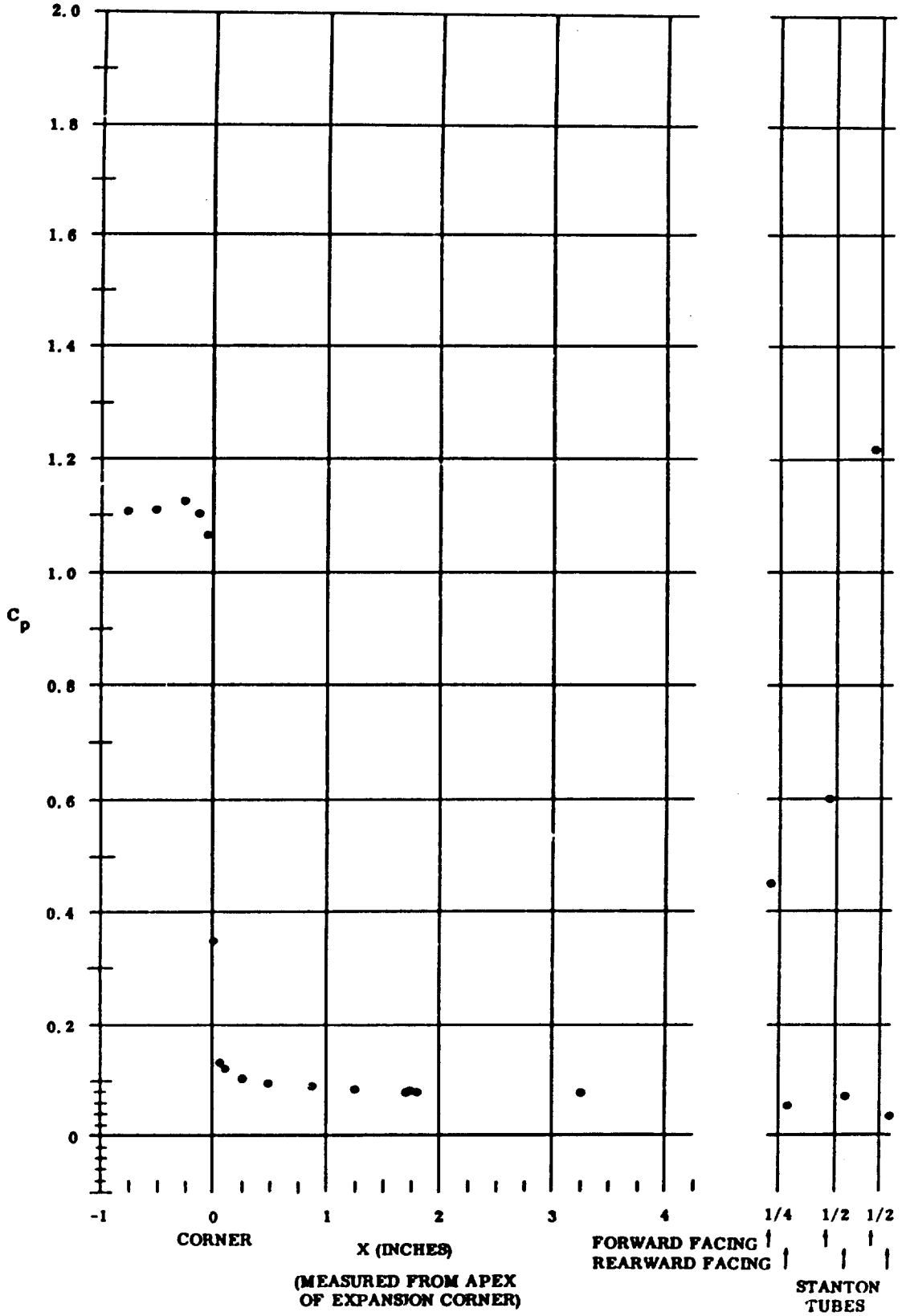

Fig. 51 Pressure Coefficient Data Plots (no coolant flow for upper surface); $\alpha = +5°$ and $Re_\infty/ft = 3,300,000$

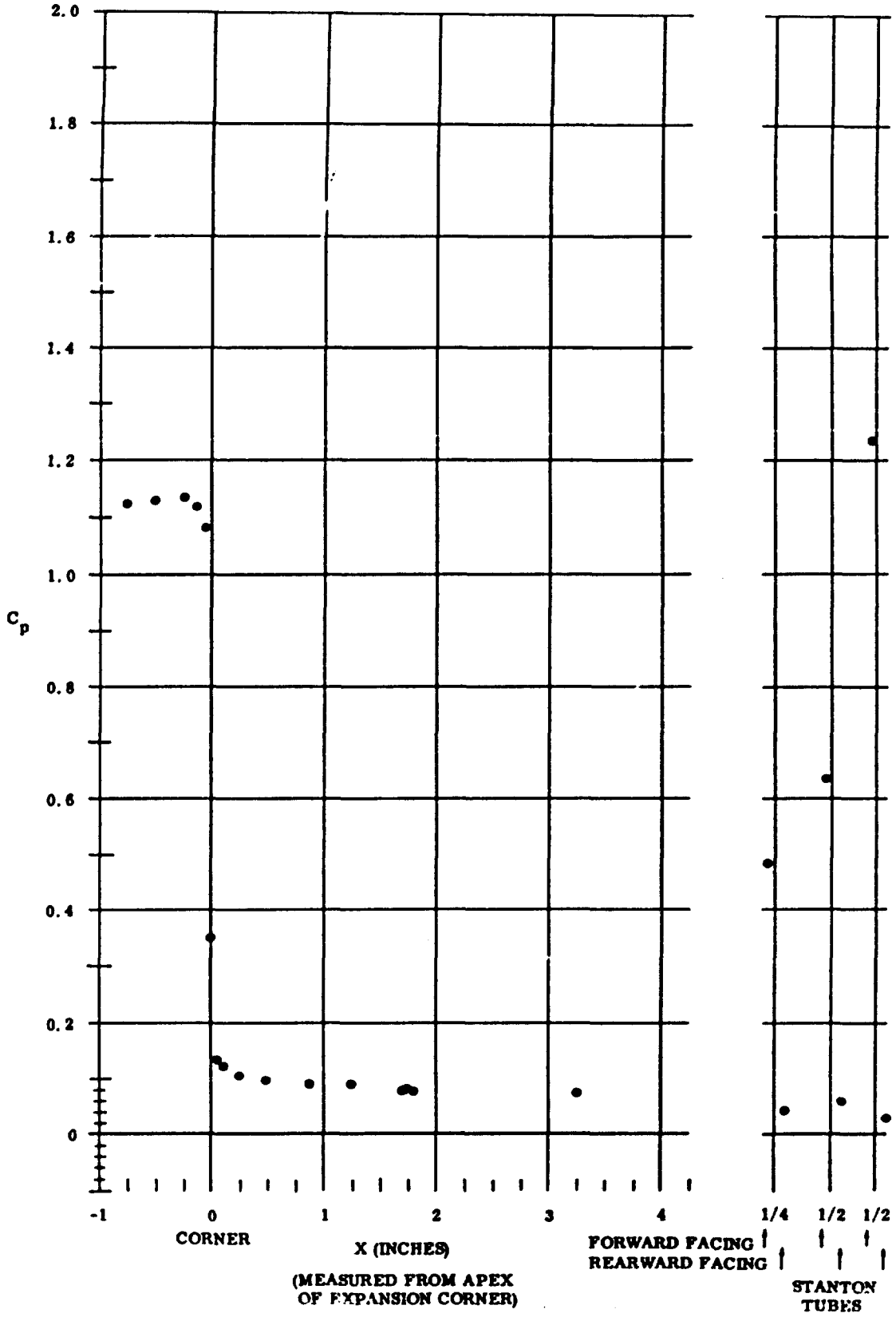

Fig. 52 Pressure Coefficient Data Plots (maximum coolant flow rate for upper surface); $\alpha = +5°$ and $Re_\infty/ft = 3{,}300{,}000$

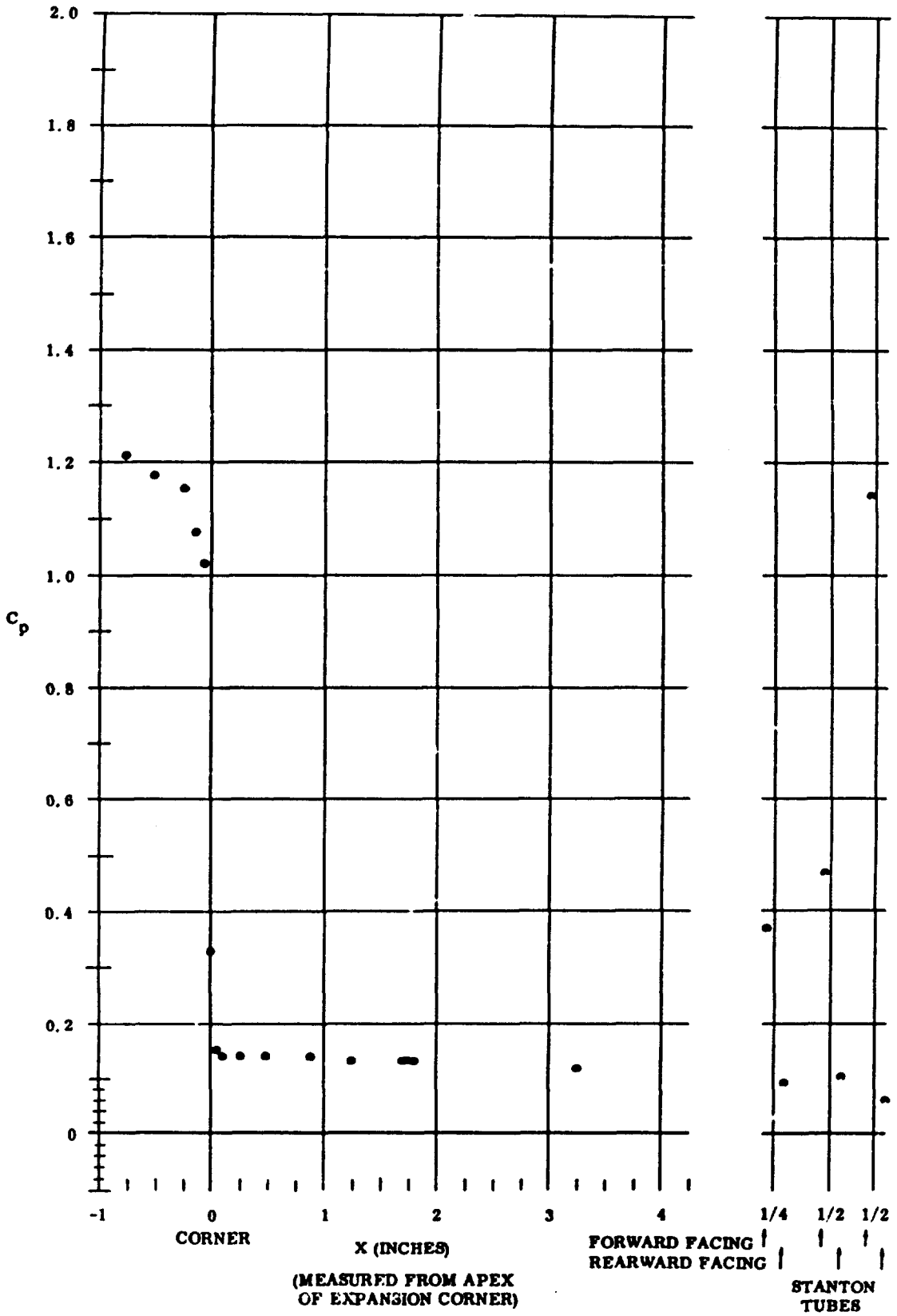

Fig. 53 Pressure Coefficient Data Plots (no coolant flow for upper surface); $\alpha = \pm 10°$ and $Re_\infty/ft = 1{,}100{,}000$

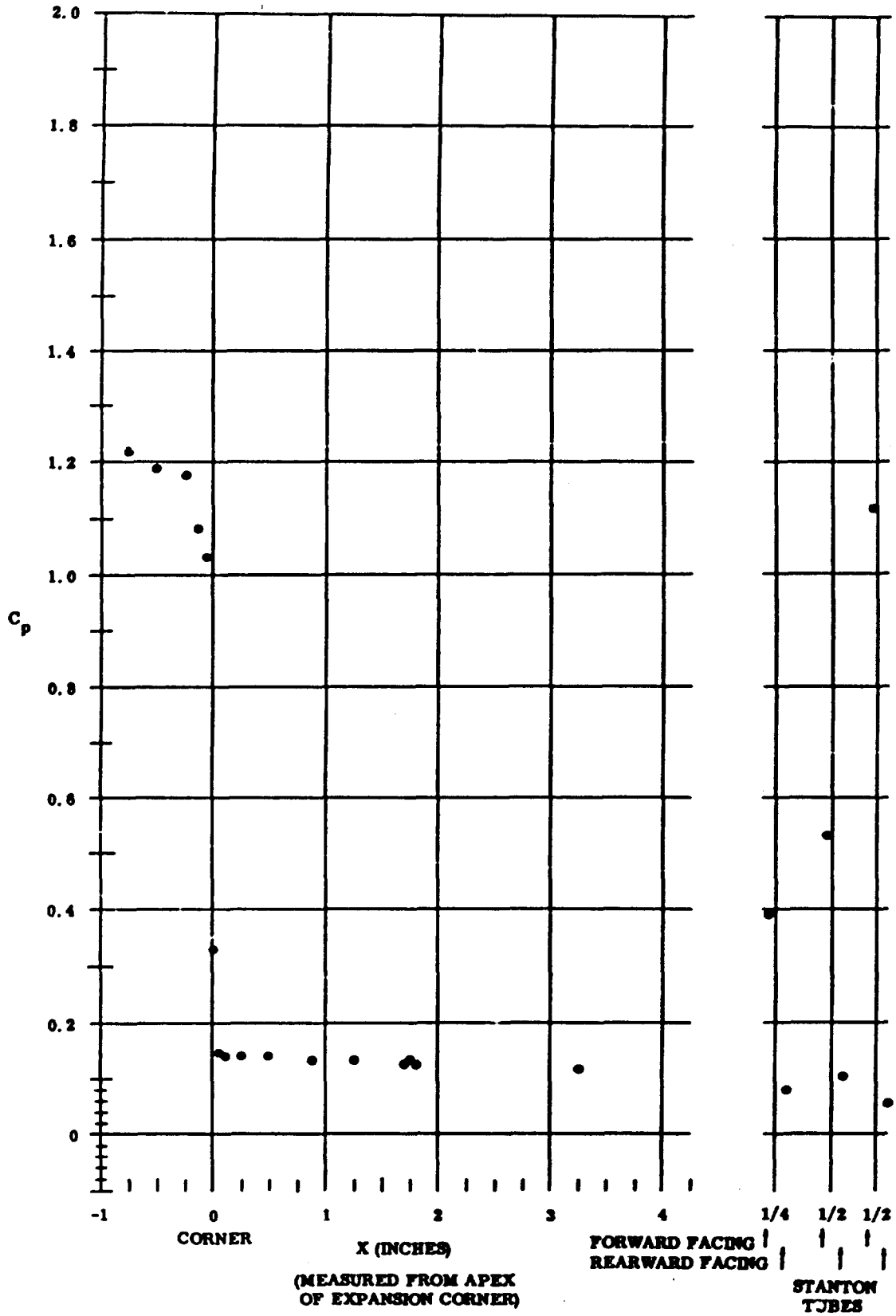

Fig. 54 Pressure Coefficient Data Plots (maximum coolant flow rate for upper surface); $\alpha = +10°$ and $Re_\infty/ft = 1{,}100{,}000$

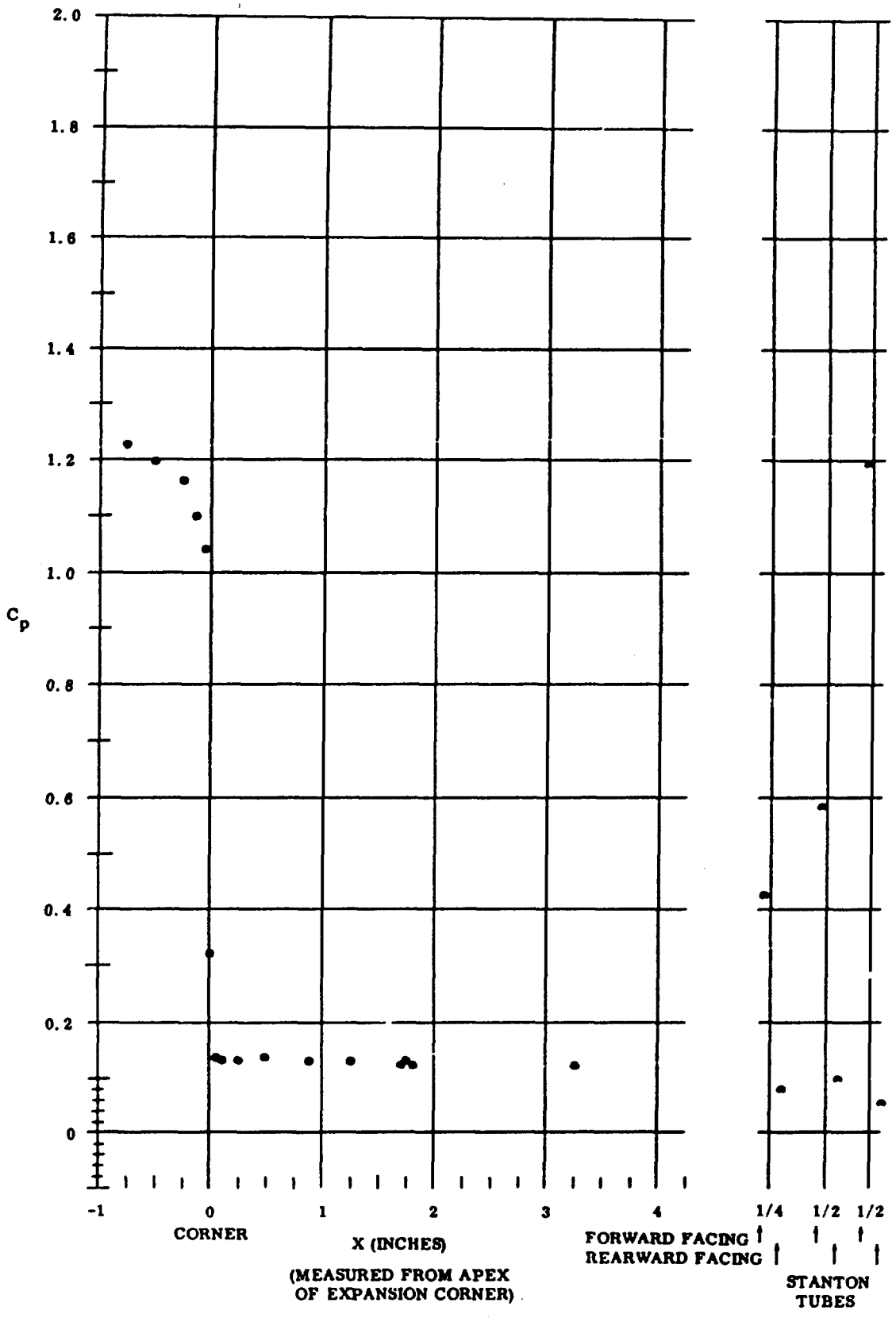

Fig. 55 Pressure Coefficient Data Plots (no coolant flow for upper surface); $\alpha = +10°$ and $Re_\infty/ft = 2{,}200{,}000$

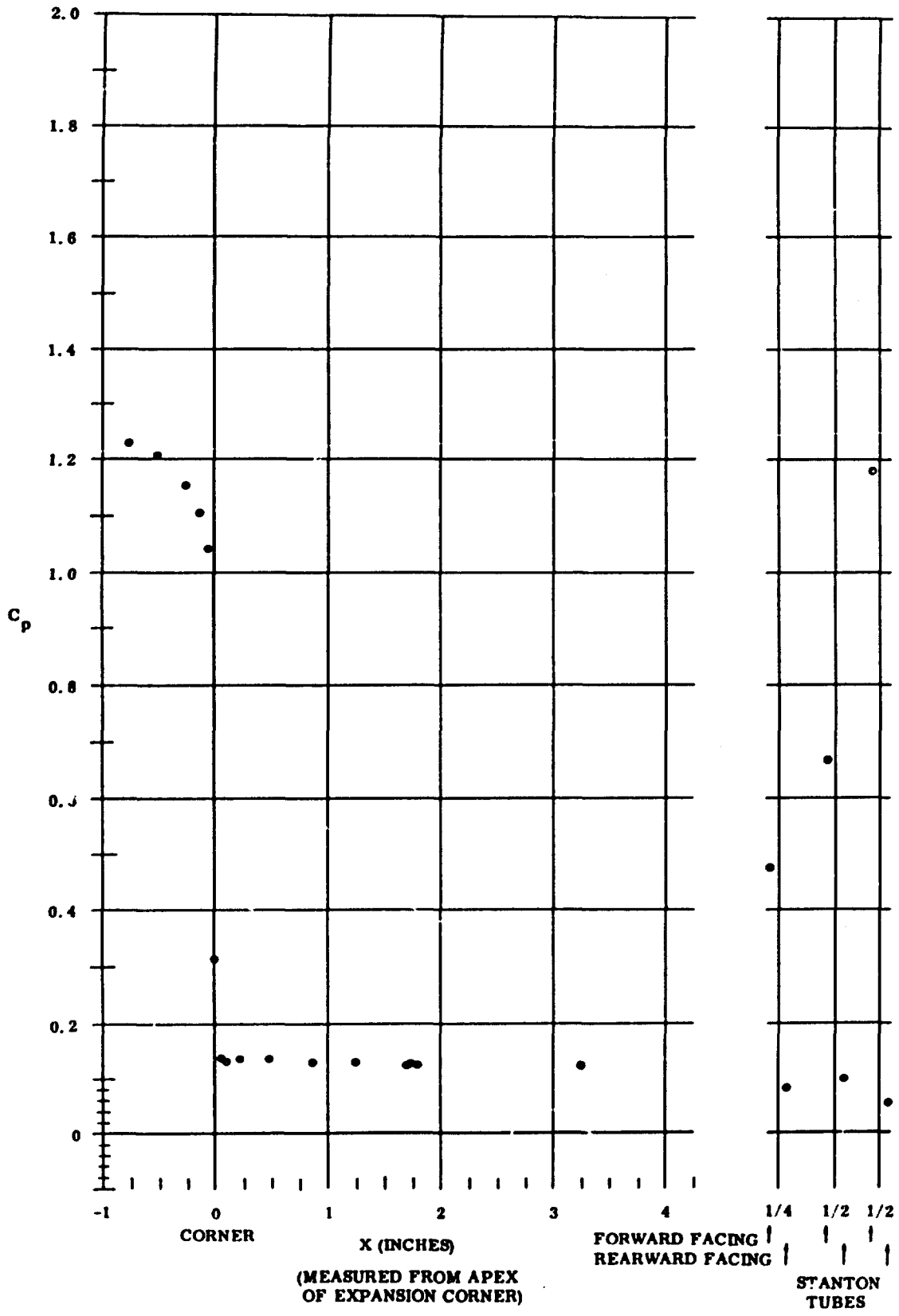

Fig. 56 Pressure Coefficient Data Plots (no coolant flow for upper surface); $\alpha = +10°$ and $Re_\infty/ft = 3,300,000$

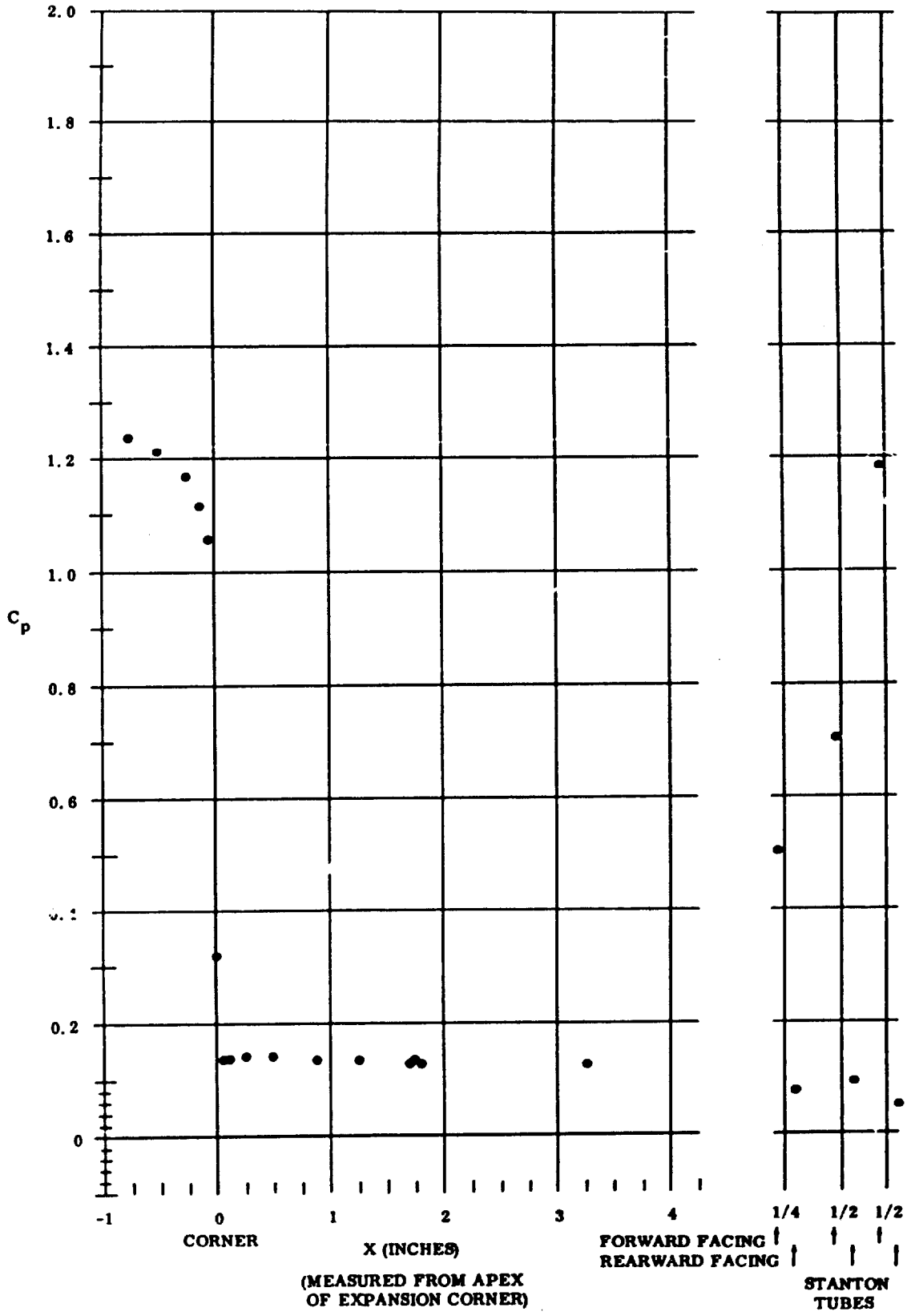

Fig. 57 Pressure Coefficient Data Plots (medium coolant flow rate for upper surface); $\alpha = +10°$ and $Re_\infty/ft = 3,300,000$

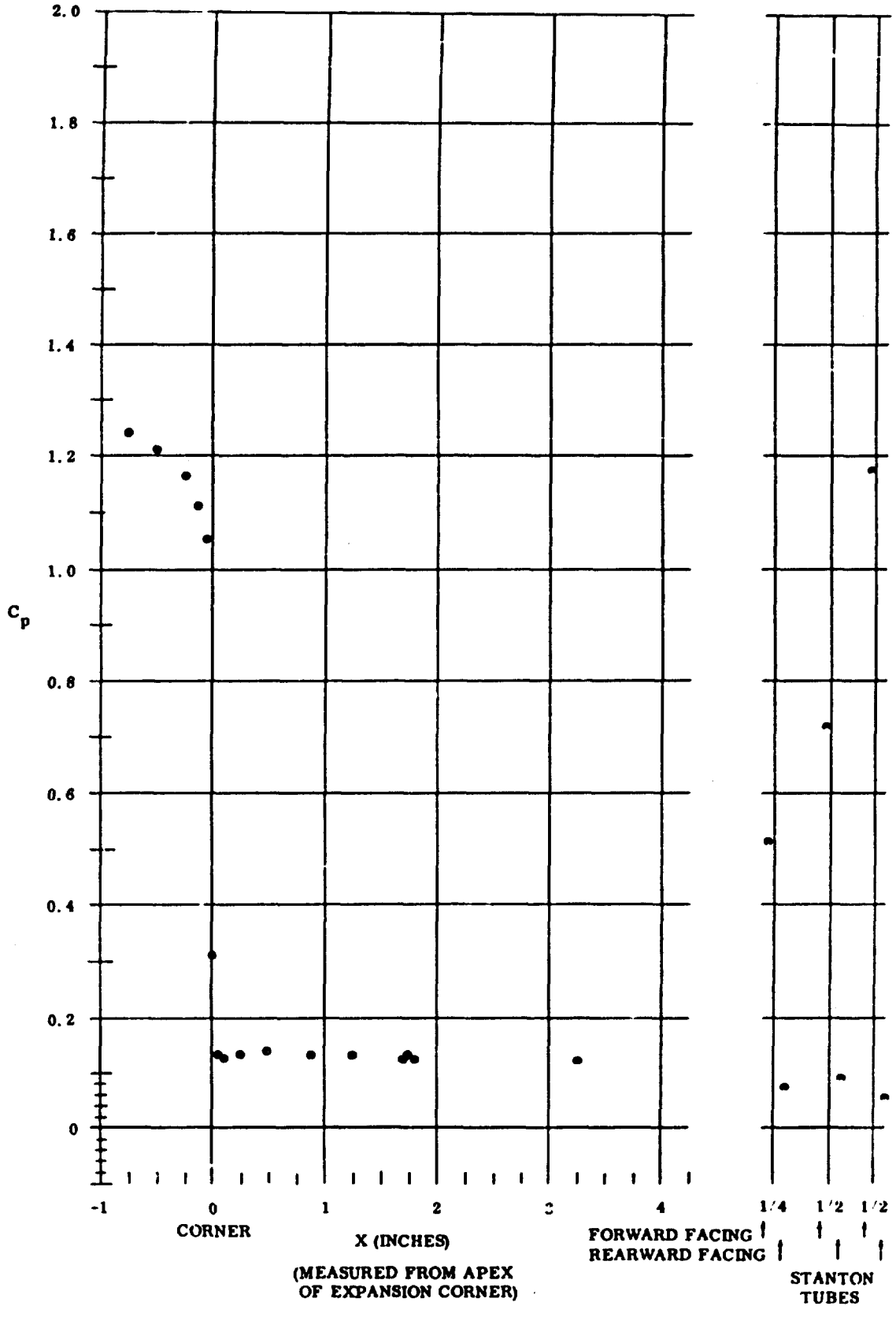

Fig. 53 Pressure Coefficient Data Plots (maximum coolant flow rate for upper surface); $\alpha = +10°$ and $Re_\infty/ft = 3{,}300{,}000$